2017

Wall Tension Regulates the Abundance of miR-133a in the Thoracic Aorta

Adam William Akerman
Medical University of South Carolina

Wall Tension Regulates the Abundance of miR-133a in the Thoracic Aorta

Adam William Akerman

A dissertation submitted to the faculty of the Medical University of South Carolina in partial fulfillment of the requirements for the degree of Doctor of Philosophy in the College of Graduate Studies.

Department of Molecular and Cellular Biology and Pathobiology
2017

Approved by:
Chairman, Advisory Committee

[Jeffery A. Jones]

[Victoria J. Findlay]

[Amanda C. LaRue]

[Paul J. McDermott]

[Michael R. Zile]

Acknowledgments

I would like to thank all of the individuals who have made an impact on my life and research career. My training at The Medical University of South Carolina has been a wonderful experience that I will cherish throughout my life. It has been an honor to train with my mentor Dr. Jeffery A. Jones and I have been privileged to have such an amazing dissertation committee. Furthermore, I would like to specifically acknowledge Robert Stroud for his significant role in the development of my laboratory skills; he has been an outstanding teacher and friend. I would like to thank Dr. Rupak Mukherjee for always making time to teach me new views and to discuss ideas. The faculty and staff of the department of surgery and the college of graduate studies have created an outstanding learning environment allowing for the successful development of my foundation in research. Thank you to all. Progression onto the next stage of my life will be bittersweet as I have cherished the time we have spent together; however, I am well prepared, and for that I cannot thank you enough.

Respectfully,

Adam W. Akerman

This work was supported by grants from: The National Institutes of Health (NHLBI) R01HL102121 (Ikonomidis), 1R01HL123478 (Zile), and the Department of Veterans Affairs (VA-ORD BLR&D) I01BX000904 (Jones)

Table of Contents

List of Tables

List of Figures

ADAM WILLIAM AKERMAN. Wall Tension Regulates the Abundance of miR-133a in the Thoracic Aorta. (Under the direction of JEFFERY A. JONES, PhD)

ABSTRACT

A reduction in microRNA (miR)-133a is associated with dilation of the thoracic aorta (TA). Since wall tension increases with vessel diameter, this study tested the hypothesis that elevated mechanical tension induces the loss of miR-133a in the TA. Elevated tension (1.5g, 3hrs) applied to murine TA *ex vivo* reduced miR-133a (0.31±0.17 vs 1.00±0.25 fold; $p<0.05$ vs normotension (0.7g)). Cyclic stretch (12%, 1Hz, 3hrs) reduced miR-133a in TA fibroblasts (0.21±0.02 vs 1.00±0.27 fold; $p<0.05$ vs static control), with no change in smooth muscle cells. Neither transcription of miR-133a nor mRNA/protein levels of three microRNA-specific exoribonucleases were altered with stretching of the fibroblasts. However, stretch induced exosome secretion of miR-133a. Two *in vivo* models of hypertension were utilized to determine the effect of elevated wall tension on miR-133a in the TA: Angiotensin-II infusion (1.44mg/kg/day, 28 days) and a spontaneous hypertensive mouse line (BPH2). In both models, blood pressures were elevated and miR-133a was decreased in the TA compared to normotensive mice (0.69±0.06 and 0.52±0.04 vs 1.00±0.13 fold respectively; $p<0.05$ for both). Plasma miR-133a was elevated in the BPH2 mice (3.39±0.77 vs 1.00±0.41 fold; $p<0.05$ vs normotensive). Plasma miR-133a was also elevated in hypertensive human subjects (1.55±0.26 vs 1.00±0.18 fold, $p<0.05$ vs normotensive). These findings demonstrate that the reduction in miR-133a levels that occurred with increased mechanical stretch of the TA was likely driven by exosome secretion from TA fibroblasts, and may provide a novel target for detrimental remodeling of the vasculature in the setting of hypertension.

CHAPTER 1: Introduction

The Aorta

The aorta is the largest artery within the body and functions to carry oxygenated blood from the left ventricle to the systemic circulatory system. The aorta is separated from the left ventricle by the aortic valve and may be divided into seven regions: the aortic root, ascending aorta, ascending arch, the vessel bearing arch, aortic isthmus, descending aorta and abdominal aorta.(1) The abdominal aorta may be further divided into the paravisceral and infrarenal segments. The characteristics of each region affect both clinical manifestation of disease as well as selection of treatment strategies. Embryologically, the thoracic and abdominal portions of the descending aorta develop from distinct sources of mesenchymal cells, and regional heterogeneity is becoming increasingly evident.(2) Conventionally, the aorta has been considered as a conduit, carrying blood from the heart with uniform cellular and extracellular

structure and function; however, it is becoming increasingly evident that the aorta is a highly complex tissue system that is dynamically regulated.

The ability of the aorta to stretch radially is referred to as vessel compliance, and this property serves to maintain continuous flow of the pulsatile exiting of blood from the heart. During systole, blood is ejected from the left ventricle causing the proximal aorta to distend approximately 4%, and during diastole the aorta will recoil, continuing to propel blood forward toward the capillary beds.(1, 3) This allows for cardiac output to be delivered steadily throughout the cardiac cycle.(4) The radial stretch of the aorta caused by the blood ejected from the aortic valve initiates a pressure wave which is propagated along the aorta as it moves peripherally. This pressure wave travels much faster than the blood, at a rate of 4 m/second in the proximal aorta, 6 m/second in the abdominal aorta and approximately 12 m/second in the peripheral arteries,(5) and is the pulse that can be detected by palpation.

The velocity of the pressure wave is inversely proportional to the compliance of the aorta and arterial wall stiffness may be measured non-invasively by the measuring pulse wave velocity.(6) The portion of the aorta that is proximal to the heart is more compliant than the distal regions, such as, the abdominal aorta.(7) Aortic compliance reduces the workload of the heart. If compliance is lost and the vessel wall becomes ridged, pulse pressure rises dramatically, requiring the heart to pump against a large afterload. With increased blood pressure, the aorta will become stiffer, as it is already distended.

Furthermore, regardless of alterations in pressure, if the aortic wall becomes more ridged as a result of alterations in vessel composition, this will allow pressure to reflect back from peripheral vascular system to the heart, while the aortic valve is still open, increasing the afterload on the heart.(8) Therefore, a less compliant aorta places more stress on the heart through elevated myocardial work and a less efficient cardiac ejection.

Aortic wall tension is directly proportional with vessel diameter and wall thickness. The law of Laplace illustrates the relationship between transmural pressures pushing outward against the constricting forces of the elastic components in the aortic wall. This relationship yields wall tension, which is equal to pressure multiplied by the radius of the vessel then divided by vessel thickness. Therefore, either an increase in pressure or an increase in aortic diameter results in elevated wall tension, and loss of aortic compliance.

The Aortic Wall

The human aorta is composed of a trilaminar wall approximately 4mm in thickness. The three layers are referred to as the intima, media, and adventitia. Each consists of distinct structural and cellular components that coordinate the primary function of maintaining aortic compliance. The proper function of the aortic wall is governed by the ongoing homeostatic balance between deposition

and degradation of the extracellular matrix (ECM) components in the microstructure by the endogenous cells within each layer.

The extracellular matrix (ECM) refers to the composite of multiple proteins that form structures connecting cells within a network. Two major components of the ECM include collagen and elastin, which comprise a cytoskeleton surrounding the cells and further contain sequestered growth factors and cytokines. This high amount of elastic and collagen fibers, allow the vessel to be distensible and compliant. Fibrillins, a class of microfibers, are closely associated with elastin, forming elastic lamella.(9) Elastin is a matrix protein which is composed of nonpolar hydrophobic amino acids, such as, glycine, alanine, valine, and proline. After being secreted by the endogenous fibroblasts and smooth muscle cells of the aorta, the elastin molecules remain in a random coil configuration in the extracellular space. They are covalently cross-linked between lysine residues and assemble into a highly elastic network of fibers, capable of stretching more than 100% under physiological conditions.(10) Fibronectin plays a key role in cellular attachment to the ECM through interaction with integrins, and has been demonstrated to effect major aspects of cellular phenotype, such as proliferation and migration.(11) Proteoglycans are also found in the aortic wall and function to interact with hyaluronic acid, a component of the ECM which contributes to tissue hydrodynamics, cellular signaling, and interaction with collagen.(12) Collagens function to provide structural support of the vessel wall. Much less elastic than elastin, collagen can only be stretched

approximately three to four percent under normal physiological conditions. The basic units of collagen fiber secreted by the endogenous aortic cells are type I and type III collagen.(13) These are two of the fibrillar collagens that once secreted assemble into fibrils that aggregate forming collagen fibers. Compliance of the aorta is largely determined by elastin and collagen content, two components of the ECM which have gained a significant interest and thus have been well studied.

The ratio of elastin to collagen is greater in the proximal aorta, and approximately equivalent in the distal portions.(1) This histologic structure results in the ability of the proximal aorta to accommodate the stroke volume delivered by the heart at physiologic pressures. Energy is stored as the aorta distends, and then is released to passively continue the flow of blood to the capillaries. These components, as well as the cells that produce and maintain them, are organized into three distinct layers that coordinate the primary function of maintaining aortic compliance.

The intima is the thin, innermost layer of the aorta, composed of an endothelium, a monolayer of simple squamous epithelial cells, fixed to a connective tissue matrix. In the normal aorta, the endothelial cell layer functions to regulate diffusion of nutrients and water from the blood, and also to transduce adrenergic stimulation. Marking the border of the intima is a perforated layer consisting of an elastic fiber network principally organized in a longitudinal direction, known as the fenestrated membrane. If exposed to vascular disease

risk factors, such as, hypertension, smoking, dyslipidemia or diabetes for example, the intima is prone to development of atherosclerotic plaques, ulcers, and thrombi. Interestingly, presence of atherosclerotic lesions may be predicted by blood flow simulation, identifying that location is related to hemodynamics.(14, 15) At these points, the endothelium is exposed to the influence of low shear stress, identified as atherogenic, or oscillatory shear stress, which has been attributed to increased risk for the formation of calcified plaques, a condition leading to the deposition of calcium salts leading to increased stiffness of the vessel.(16)

The tunica media comprises the middle layer and is the thickest portion of the aortic wall. This layer is composed of lamellae sheets of elastic fibrils and collagen (in humans, approximately 50 in the thoracic and 28 in the abdominal), smooth muscle cells, fibroblasts, and other extracellular matrix proteins.(17) The composition and organization of the media give the aorta elastic properties allowing for distention while providing strength.

The outer most layer of the aortic wall is the adventitia. This layer is a complex heterogeneous portion of the vessel wall, containing largely collagen acting as an ECM scaffold with fibroblasts, blood and lymphatic vessels, nerves, progenitor and immune cells.(18) The adventitia provides metabolic support to the aorta and functions as a fibroblasts and stem cell progenitor reservoir.(19) The adventitia allows for these cell types to rapidly migrate into the media in response to injury. It is these cellular components that interact with the

extracellular components of the aortic wall to mediate normal function. The adventitia has been demonstrated to respond to elevations in wall tension. It has been described as the principal “injury-sensing tissue” of the vessel wall.(20)

The three endogenous cell types residing in the aortic wall are fibroblasts, smooth muscle cells, and endothelial cells. Each is capable of altering the structure of the aorta, contributing to the maintenance of vascular homeostasis. First, the layer of endothelial cells functions in the regulation of diffusion and migration of circulating components from the blood and is responsible for signal transmission and vascular tone. Second, the smooth muscle cells make up the largest percentage of cells in the healthy aorta and are arranged circumferentially within the elastic lamellae. The major function of the smooth muscle cells consists mainly of regulation of medial strength and vessel contraction. Finally, the fibroblasts are considered the critical cell type functioning to maintain homeostasis of the aortic wall. The homeostasis-maintaining function is fulfilled through an outside-in regulation of vascular structure and functions by vascular adventital fibroblasts in response to stress, injuries, cytokines, and hormones.(18, 21, 22)

Aortic Aneurysms

Aortic disease in general are a significant source of mortality for the population, causing as many as 15,000 deaths annually in America, consistently

placing aortic disease among the top 20 causes of death. The most recent data available from the Centers of Disease Control and Prevention (2014) indicate that aneurysm disease is the 18th most common cause of death in all individuals and the 15th most common cause of death in individuals older than 65 years of age, accounting for 13,843 and 11,147 deaths in these 2 groups respectively.(23-25) An aortic aneurysm is defined as a localized dilation of the aorta with a cross-sectional diameter greater than fifty percent larger than the normal range for a given age and body size. Locations of aortic aneurysms vary. Believed to be due to regional heterogeneity of the aorta, abdominal aortic aneurysms (AAAs) occur below the diaphragm and appear to be strongly associated with atherosclerosis and inflammation.(26) Conversely, thoracic aortic aneurysms (TAAs) are consequence of degenerative or hypertension associated aortic remodeling or based on genetic mutations in rare disorders; however the underlying mechanisms responsible for pathology are unclear.(27)

It is expected that approximately 25 percent of aortic aneurysms occur in the supradiaphragmatic portion. It has further been estimated that 60 percent of the thoracic aortic aneurysms involve the aortic root or ascending aorta, 10 percent involve the arch, 40 percent the descending thoracic aorta, and 10 percent involve the thoracoabdominal portion of the aorta.(28) Within the spectrum of cardiovascular diseases, these thoracic aortic aneurysms (TAAs) are considered to be of the most dangerous and difficult to treat problems in cardiothoracic surgery. Thoracic aortic aneurysms are often asymptomatic and

results in a weakened aortic wall and can progress to rupture if left untreated.(29) Etiologies include those of genetic and non-genetic origin. Hereditary disorders predisposing the aorta to dilation include, presence of a bicuspid aortic valve, Marfan syndrome, Ehlers-Danlos syndrome. Pathological conditions from an acquired disorder also affect aortic dilation. For example, hypertension and atherosclerosis leave the aorta prone to distention and stiffening. This results in the lack of ability of the aorta to receive the stroke volume, resulting in further systolic hypertension, and acceleration of the pulse wave velocity. There remains a paucity in information with regards to the underlying molecular mechanisms leading to the development of TAA. Further studies in the pathways leading to the development of TAA are essential and will provide novel, less invasive therapeutic strategies.

Genetic and Non-genetic factors leading to TAA Formation

Numerous etiologies can contribute to the development of TAA; however, most commonly idiopathic non-genetic degeneration of the aortic vascular extracellular matrix occurs. While a number of factors have been identified that increase the risk of developing an aortic aneurysm, such as, hypertension, atherosclerosis, smoking, increased age, and the male gender, the molecular mechanisms involved with theses associations require further understanding.

Inherited connective tissue disorders have been attributed to a high incidence of TAA. Marfan syndrome, for example, is one of the major heritable disorders of connective tissue with a prevalence of between 1 in 5-10,000.(30) The primary cause of morbidity and mortality in Marfan syndrome relates to the common development of cardiovascular complications including dilation of the aortic root leading to the formation of ascending aneurysm and increased incidence of aortic dissection.(31) Marfan syndrome has been attributed to multiple identified mutations within the coding sequence of the Fibrillin-1 (FBN1) gene.(32-34) Fibrillin-1 is exported from cells, where it functions as a key component of microfibrils in the extracellular matrix. These microfibrils compose elastic fibers, which provide elasticity to the aorta,(35) and also function to store latent cytokines and growth factors, such as, the transforming growth factor β (TGF-β). Motifs within FBN1 interacts with the proteins which target and sequester latent growth factors to the ECM allowing for their release.(36) Therefore, it has been suggested that abnormalities in the FBN1 gene may lead to impaired sequestration of latent TGF-β complexes, making more available for activation, leading to enhanced signaling.(37, 38)

Other syndromic aortic aneurysms occur in patients with Loeys-Dietz syndrome, and Ehlers-Danlos syndrome. Loeys-Dietz syndrome is result of a heterozygous mutation in the transforming growth factor beta receptors 1 and 2 (most commonly TGFBR2).(39) Mutations in the TGF-β receptors are believed to result in the overall up-regulation of TGF-β signaling. The classical TGF-β

signaling pathway has been demonstrated to induce extracellular matrix deposition and degradation, and this has been described as the predominant mechanism in Loeys-Dietz aneurysm formation.(40) In Ehlers-Danlos syndrome, an autosomal dominant mutation in the collagen 3a1 (COL3A1) gene results in highly fragile vessels, and effected individuals at a high risk of developing aneurysm.(41)

Non-syndromic aneurysms are also a significant occurrence, and are divided into two categories: Familial Thoracic Aortic Aneurysms, where more than one individuals in a family are affected, and sporadic TAAs, where only a single person in the family is known to have an aneurysm.(42) Increasing numbers of genetic loci linked to nonsyndromic TAAs are being identified, such as, individuals with mutations in genes encoding contractile proteins appear to be susceptible to TAA. Mutations in the smooth muscle cell α-actin (ACTA2) gene, as well as, the beta-myosin heavy chain (MYH11) were identified in families with increased incidence of TAA.(43-45) Mutations of the vascular isoforms of actin and myosin are thought to trigger profound remodeling of the vessel wall followed by an increase in aortic stiffness and, ultimately, aortic dilation.

Other factors that have been attributed to the formation and progression of TAA include developmental malformation of the aortic valve. Typically the aortic valve consists of three leaflets. However, congenitally two of these three leaflets may become fused throughout development resulting in a bicuspid aortic valve (BAV) anatomy. This is the most common genetic cardiovascular malformation,

occurring in approximately 2% of the population.(46) From an etiological standpoint, the vast majority of BAV patients have an increase in aortic dimensions and approximately 20% of these individuals have overt TAA, most commonly in the aortic root, requiring surgical repair.(47-49) While there is a clear association between the BAV phenotype and the occurrence of TAA, the nature and extent of this relationship remains unclear.

Nevertheless, patients with genetic TAAs generally present at an earlier age (56.8 years) than patients with idiopathic TAAs. This is likely due to the close observation of aortic diameter in these individuals. The diagnosis of idiopathic TAA typically occurs serendipitously in individuals over the age of 65 (64.3 years on average) undergoing non-related cardiovascular imaging studies indicated for diagnostic purposes.(50) Normal aortic diameter is determined based on gender, age, and body size; however, generally speaking the non-remarkable ascending aorta is <2.1 cm/m^2 and the descending aorta is <1.6 cm/m^2.(51)

Following identification of aortic dilation, it is usually recommended that a transthoracic echocardiography is performed after six months following the recognition of increased aortic diameter to ensure the absence of a rapid evolution of dilation.(52) Echocardiography however, does not allow for visualization of the entire aorta, therefore, computed tomography (CT) and magnetic resonance imaging (MRI) are the most widely used imaging examinations to evaluate the thoracic aorta.(53) This is due to high spatial and

temporal resolutions, large fields of view, and multiplanar imaging reconstruction capabilities, allowing for the assessment and calculation of aortic diameter. Therefore, CT and MRI play an important role not only in the diagnosis of thoracic aortic aneurysm, but also in the preoperative assessment and follow up after treatment. Accurate measurement of aortic diameter is vital in monitoring the progression of TAA. Aortic measurements are made in true short axis projection acquired from double oblique views, from one blood-wall boundary to the other. Furthermore, with CT, gating is performed based on ECG analysis to insure accurate measurement of aortic diameter in accordance with the cardiac output, particularly in the ascending aorta.(53)

As aortic diameter is tracked over time, medical therapies are initiated until the risk of rupture outweighs the risk of surgical repair. The aneurysmal thoracic aorta grows at an average rate of about 0.1 cm per year in the ascending portion and a bit faster at 0.3 cm per year in the descending portion.(54) An analysis of aortic diameter and increased risk of complication revealed sharp hinge points at which aortic rupture or dissection is likely to occur. These hinge points occur at 6 cm in the ascending aorta and 7 cm in the descending aorta.(54) Thus, it is important to intervene before aortic diameter reaches these dimensions.

The consideration for medical treatment is a result of a balance between risk and benefit. While the risk of current pharmacotherapies is generally low, tolerance of therapy may not be seamless. The current aim of medical treatment

is to limit the hemodynamic stress imposed on the aortic wall. To lower wall stress, medical therapy has been directed at the reduction of shear stress on the aneurysmal segment of the aorta by reducing blood pressure and vessel contractility. With the understanding that aortic dilation is increased by intraluminal pressure, both the distention of the aortic wall with cardiac ejection during systole and blood pressure have been the target of therapies. However, it is unclear whether the biochemical alterations driving aortic remodeling may be attenuated through current pharmacologic antihypertensive treatment.

First line therapy for TAA patients is usually blockade of the beta-adrenergic receptor. Beta-adrenergic receptors are classified as beta-1, beta-2, and beta-3 adrenoceptors. These receptors are members of the G-protein coupled receptor family and consist of seven membrane spanning domains.(55) The beta-1 receptors of the myocardium, play an important role in the regulation of cardiac function. Beta-Blockers were initially proposed as medical therapy for TAAs based on their ability to reduce blood pressure, cardiac contractility, and shear stress on the aorta.(56) Initially proposed by Wheat and colleagues, examination of flow in artificial aortas constructed from Tygon tubing coated internally with rubber cement revealed that a flattened pressure curve, as that which occurs with the use of beta-blockers, lessened the separation of rubber cement when a small tear was introduced, and thus demonstrated a reduction in shear stress.(57) While it is clear beta-blockers do reduce wall stress, the clinical

benefit in reference to the reduction of aneurysm growth rate and eventual rupture remains under debate.

The main work cited advocating the use of beta-blockers in the aneurysm patient was demonstrated in the study of Marfan Patients.(58) In the study performed by Shores and colleagues, 70 predominantly young patients with Marfan syndrome were randomized to treatment with or without a beta-blocker, then followed over time. The main outcome of this study was that with beta-blocker treatment, aortic root dilation rate was attenuated. Other beneficial findings were that beta-blocker treatment improved the rates of death, congestive heart failure, aortic regurgitation, and dissection. Interestingly, other studies have demonstrated contradictory results. In fact several studies found contradictory results and demonstrate no benefit of beta-blocker treatment in the aortic growth rate in pediatric (59) or adult (60, 61) Marfan patients. Furthermore, no studies to date have been able to confirm demonstrate a reduction in the rate of aortic dilation in non-Marfan TAA patients, which make up the majority of individuals suffering from aortic aneurysm. In fact, one study suggests that beta-blocker therapy does not protect against TAA growth in non-Marfan patients.(62)

While beta-blockers continue to be the leading pharmacotherapy for patients with TAA, toleration may be low and another strategy is indicated. Statins were initially proposed as treatment for abdominal aortic aneurysms based on their lipid-lowering and antioxidative effects, and are an established

therapeutic option for patients with TAA. However, no study to date has demonstrated that statins reduce the rate of thoracic aortic dilation in humans. A retrospective analysis from the Aortic Institute at Yale-New Haven Hospital of 1,561 patients with TAA indicated that statin therapy was associated with a delay in time to surgery and complications, including aortic dissection, rupture or death.(63) While, retrospective analyses suggest a possible therapeutic benefit, direct proof is lacking.

Nevertheless, current pharmacotherapy available for the treatment of TAA remains extremely limited, and were derived from studies conducted in select populations, such as, in patients with Marfan syndrome. In short, even with current treatment options, the majority of thoracic aortic aneurysms will continue to increase in diameter over time until the hinge point diameter is reached, and the risk of rupture outweighs the risk of surgical repair; however, current surgical options are also limited and include open-chest aneurysm repair or endovascular intervention.

Surgical Management

The present standard surgical treatment for thoracic aortic aneurysms is open-chest aneurysm repair. The goal of the open-chest approach is to replace the weakened, dilated portion of the aorta with a graft. This approach to repair requires a highly experienced thoracic surgical team and presents the surgeon

with a multitude of technical and cognitive challenges that extend through the perioperative and postoperative period. Replacement of the dilated aorta carries acceptable risk in regard to operative death and postoperative quality of life.(64) Early reports indicated a perioperative mortality rate ranging between 12% and 44% depending on the extent of comorbidity and urgency of the repair.(65, 66) However, more recent reports indicate significant improvements in mortality rate of between 4-9% (67) and an incidence of paraplegia at 3% (68) for descending thoracic aortic resections of TAAs performed in high-volume aortic centers. Despite these vast improvements in operative complications and mortality rate, long-term survival (5-year all-cause mortality) remains poor following open-chest aneurysm repair and adverse cardiovascular events are more common in these individuals relative to the general population.(69) Nonetheless, a minimally invasive approach is appealing, especially in older TAA patients, or individuals with significant comorbidities rendering them unsuitable candidates for the open surgical repair.

Endovascular repair of thoracic aneurysms is a novel technology that allows for a less invasive approach for the treatment of thoracic aortic aneurysms. This is achieved by transluminal placement of one or more stent-graft devices across the longitudinal extent of the aneurysm. Thoracotomy, aortic cross-clamping, left-heart bypass, and single-lung ventilation are all avoided with an endovascular aortic procedure. While prospective randomized studies comparing open repair and endovascular treatment of descending

thoracic aortic disease are limited, it does appear that endovascular stent-grafting decreases early mortality and operative complications associated with open surgical repair.(70) A multicenter, comparative, phase II, nonrandomized report on the results of open repair versus stent grafting for the treatment of descending TAAs yielded promising results. In this study, the Gore TAG thoracic endograft was evaluated against an open-surgery control cohort of patients with descending TAAs.(71) Operative mortality and occurrence of paraplegia were significantly lower in the group receiving the TAG stent when compared with the open surgical group, 2.1% versus 12% ($p<0.001$) and 3% versus 14% ($p<0.003$) respectively. While perioperative mortality appears to be lower with endovascular stent grafting, this technique is not without limitations. The 2-year follow-up in this study was limited; however, it was determined that there was no difference in 2-year survival between the two groups. In a prospective, comparative, nonrandomized trial of stent grafting versus open surgery of the descending thoracic aorta, the rate of operative death was halved with stent grafting, despite the overall higher-risk population of patients being treated, but unfortunately, there was similar late survival for both cohorts.(72) In several more recent studies, it was determined that, while peri-operative mortality is lower with endovascular stent repair, patients selected for this procedure have worse long-term (4 year) survival than patients selected for open repair.(73, 74) The results of these observational studies suggest that higher risk patients are being offered endovascular stenting, and that some do not benefit based on long-

term survival, highlighting the need for future work to identify candidates who are less likely to benefit from endovascular stent repair.

Importantly, neither open surgical repair, nor endovascular intervention address the underlying mechanisms responsible for disease and are only directed at preventing complications from end stage pathology. Furthermore, the current pharmacotherapy utilized for the TAA patient remains limited, and it is unclear whether the biochemical alterations driving aortic remodeling may be attenuated through current antihypertensive treatment. Therefore identifying significant need for further studies directed toward determination of the underlying mechanisms responsible for pathology. To further understand mechanisms involved in the development and progression of aneurysm disease, research efforts have been placed on the development and characterization of several different animal models.

Animal Models of Aortic Aneurysm

Animal models have become an important pillar for examining mechanisms that contribute to the development and progression of human disease, and the study of aortic aneurysm is certainly no exception. Accordingly, several methods are commonly utilized to study aneurysm development, primarily in rodents.(75, 76) The three methods routinely used in mice and rats include, intraluminal elastase perfusion,(77, 78) infusion of angiotensin II (AngII),(79, 80) and

application of periadventitial calcium chloride.(81, 82) It must be recognized, that no singular animal model perfectly replicates human aneurysm on a temporal and molecular scale; however, each of these methods, initiate abnormal remodeling of the vascular ECM resulting in vessel weakening, loss of compliance, and increased diameter.

Intraluminal Elastase Perfusion

The intraluminal elastase perfusion model of aneurysm induction was developed in 1990 by Anidjar and colleagues for the specific purpose of induction of aneurysm in the abdominal portion of the rat aorta.(77) Since then, these methods have been successfully applied to the abdominal aorta of mice.(78, 83) This method includes, exposing the abdominal aorta via laparotomy, then dissecting the inferior vena cava free from the aorta and ligating the collateral arteries. This is followed by insertion of a catheter into the femoral artery and advancing it until the tip is visually confirmed via microscopy to have reached the infrarenal abdominal aorta. The aorta is then clamped at the level of the left renal artery and ligated distally around the inserted catheter. A balloon catheter is then inflated and the vessel is mechanically expanded as the aorta is perfused with porcine elastase under supra-physiologic pressures for a desired amount of time. This method, while relatively straightforward in the abdomen, requires circumferential access to the vessel and temporary vessel occlusion. Reproducible dilation is achieved immediately following the procedure, and

progresses rapidly over a relatively short period of time (>100% dilation in 2 weeks).(78) While efficient in the abdominal aorta, this method would be extremely difficult to perform in the thoracic portion of the aorta due to the anatomy of the vessel. Since development of this model, application of periadventitial porcine pancreatic elastase has been attempted.(61) This model results in a rapid dilation of the abdominal aorta, or approximatly 82% from baseline measurments in two weeks. While highly reproducible, and less invasive as the infusion model, the rapid vessel wall injury and progression of dilation limits the ability to study the initiation and progression phase of aortic aneurysm. It is believed these models applied to the thoracic portion of the aorta would cause excessive mortality and/or paralysis and therefore, is more suited for the study of abdominal aortic aneurysms.

Angiotensin II Infusion

Angiotensin II (AngII) has been shown to have a number of biological effects on the cardiovascular system. Effects of AngII include, increased peripheral vascular resistance through vasoconstriction leading to elevated vascular wall tension,(84) vascular hypertrophy, cellular proliferation, production of extracellular matrix, and inflammation in the vessel wall.(85) Increased plasma levels have been implicated in human atherogenesis (86) and studies in murine models have demonstrated that prolonged infusion of AngII increases the development of atherosclerotic lesions in hypercholesterolemic mice driven by macrophage

infiltration leading to the formation of aortic aneurysm.(79, 87) This model is achieved in a relatively non-invasive manner through the implantation of an osmotic pup which delivers AngII over a 4 week period. When AngII is delivered to the apolipoprotein E knock out mouse, abdominal aortic aneurysm (87) and ascending aortic aneurysm(88) is induced, and in the low density lipoprotein knock out mouse, induction of abdominal aortic aneurysm occurs(79). While this method of aneurysm induction is relatively straightforward and highly reproducible when performed in the hypercholesteolemic mouse, the occurrence of aneurysm in wild type C57BL/6 mice is significantly diminished (<50% of that in the low density lipoprotein knock-out mouse).(89, 90) Therefore, the use of this model becomes limited due to the requirement of specific transgenic strains.

Periadventitial Calcium Chloride Exposure

First introduced in 1988, Gertz and colleagues developed methodology to induce progressive aneurysmal dilation accompanied with disruption of the elastic network within the media of the rabbit common carotid artery.(91) This process involved bathing the periadventitial surface of the vessel with 0.5 Molar calcium chloride for fifteen minutes. Advantages of this model include the ability to apply this procedure to any mouse strain without consideration to genetic background or lipid status, such as with the AngII infusion model.(92) Subsequently, this model was applied to the rabbit abdominal aorta,(93) then in 2001, Chiou *et al.* adapted this procedure to be performed in the murine abdominal aorta.(81) In the

abdomen, it was described that aneurysm development was result of the disruption of the elastic network within the media accompanied by calcium precipitations and an increase in inflammatory cell infiltration associated with progressive dilation.

While this model was proven to be highly reproducible and efficient in the abdominal aorta, these studies do not address aneurysm specifically in the thoracic aorta. Evidence was accumulating that embryologically, the thoracic and abdominal portions of the aorta develop from regionally distinct rests of mesenchymal cells.(2) With the understanding that the cellular biology is different in these regions, it was inferred that the cause of aneurysm in the thoracic portion may be distinct as well. Therefore, to define the mechanisms involved in thoracic aneurysm formation, Ikonomidis and colleagues sought to adapt this method by selectively exposing the murine descending thoracic aorta to calcium chloride.(82) For this approach, following intubation and mechanical ventilation, a left-side thoracotomy is made between the 4^{th} and 5^{th} intercostal space, and the lung is carefully packed away. The descending thoracic aorta is exposed and diameter is obtained by calibrated video microscopy. A sponge soaked with 0.5 Molar calcium chloride is then applied directly to the periadventitial surface and kept in place for 15 minutes. The animal is then recovered and followed over time.

This method results in the reproducible dilation of the exposed portion of the thoracic aorta reaching maximal diameter of approximately 72% over baseline measurements at 16 weeks. Similarly to what was observed by Basalyga, the elastic lamellae thin and flatten as the aneurysm progresses. While the inciting stimulus of TAA formation remains undefined, it has become clear that TAA is not

the result of an acute chemical injury, but a process that is initiated and slowly progresses over time. Early examination of aortic tissue sections two weeks following calcium chloride exposure revealed normal wall structure and the absence of inflammatory infiltrate. Specifically, TAA tissue stained for macrophages, neutrophils, T-cells, and B-cells revealed little change from untreated control aortic sections.(94) This murine model of TAA has been proven to not only recapitulate the structural hallmarks of human TAA, but also the changes in cellular content, the modifications in biochemical mediators, and the altered intracellular signaling consistent with what is observed in clinical specimens, thereby allowing for the elevated potential to identify therapeutic targets that could influence aneurysm progression.

Alterations in the cellular composition of the aortic wall with the development of thoracic aortic aneurysm

Through studies of human tissue and animal models of aneurysm, we have only begun to unravel the complex underlying pathophysiology. In an early study performed by Jones and colleagues, it was demonstrated that the resident endogenous cellular population changes throughout the development of TAA.(94) Using the periadventitial calcium chloride exposure method, aneurysm was induced in the descending portion of the murine thoracic aorta and tracked over time. Following tissue harvest at various time points, histological analysis of

cell-type specific markers was performed, and four marker proteins were utilized to define the independent cellular populations.

In this study, fibroblasts were identified using an antibody specific for the collagen receptor, DDR2, which has been shown to be highly specific and display fibroblast restricted expression in cardiovascular tissue.(95) Smooth muscle cells were identified using antibodies targeting the intermediate filament protein, desmin, which has been demonstrated to be found specifically in muscle-derived cells, including smooth muscle cells.(96-98) To further define the SMC population, antibodies against α-Smooth muscle actin (αSMA) and the smooth muscle myosin heavy chain (MYH11) were used. The interesting results of this study revealed an increase in DDR2 positive cells at 8 and 16 weeks following the induction of TAA, suggesting an increase in fibroblasts or fibroblast derived cells. This occurred concomitantly with an increase in MYH11 positive cells, while αSMA remained unchanged throughout the 16 week time course. Combined with the observation that the number of desmin positive cells peaked at 4 weeks, then drastically decreased, this would suggest that as TAA progresses the number of smooth muscle cells decline, while the emergence of a synthetic fibroblast-like cellular population occurs. To confirm loss of SMCs, Jones and colleagues stained serial tissue sections for desmin and active Caspase-3, which is activated in the apoptotic cell by both extrinsic and intrinsic cell death pathways.(99) The results demonstrated significant overlap with

Caspse-3 staining and desmin positive cells at 8 and 16 weeks following TAA induction, confirming apoptotic loss of specifically SMCs.

Interestingly, this previous study failed to identify the presence or accumulation of monocytes or macrophages in the aortic media with the progression of TAA, a characteristic finding in AAA. Using the periadventitial calcium chloride application method in the murine abdominal aorta, Xiong *et al.* demonstrated that AAA formation is highly dependent on monocyte/macrophage infiltration in the aortic media.(100) These conflicting observations suggest that exposure of the thoracic aorta to calcium chloride initiates aortic dilation via different mechanisms as to what occurs in abdominal aneurysm formation, highlighting the differences in regional heterogeneity of the aorta.

In agreement with many other studies, it has become well described that in both mouse models and clinical specimens, an apoptotic loss of smooth muscle cells occurs with aneurysm development.(101) One theory put forth has suggested that reactive oxygen species (ROS) may play a role in this process. Increased ROS formation can be stimulated by mechanical stress,(102) and has been implicated in both AAA,(103) and TAA,(104) and results in elevated ROS production by smooth muscle cells.(105) It has been demonstrated that ROS are involved in both degradation of the ECM (106) and also trigger the apoptotic loss of smooth muscle cells of the thoracic aortic wall *in vivo*.(107) Moreover, when ROS production was inhibited in murine knockout models, a reduction in AAA and TAA formation was observed, strongly suggesting that ROS and the

apoptotic loss of smooth muscle cells are important factors leading to the development of aneurysm.(108, 109)

The emergence of a cellular population displaying DDR2/MYH11/αSMA positive staining is consistent with that of an activated and synthetic phenotype, meaning these fibroblasts possess properties of both SMCs and fibroblasts. A fibroblast derived cell type possessing characteristics of both the secretory properties of fibroblasts and the contractile properties of smooth muscle cells constitutes a unique cell type, termed myofibroblast. Studies have demonstrated that following injury, fibroblasts differentiate into myofibroblasts and play a significant role in the tissue injury response.(110, 111) It is thought that the myofibroblasts contribute to tissue repair during normal wound healing; however, their presence can lead to severe impairment of tissue function when contraction and ECM protein secretion becomes excessive.(111, 112)

Interestingly, it has been demonstrated that mechanical tension alone can directly stimulate the differentiation of fibroblasts into this activated synthetic myofibroblast phenotype.(113) Kessler and colleagues demonstrated that fibroblasts seeded into a collagen lattice that was mechanically stretched, allowed for fibroblasts to take on a similar myofibroblast phenotype.(113) The presence of activated fibroblasts has been well documented in a variety of pathologies(114), and has also been attributed to a significant role in the tissue injury response, where these fibroblasts migrate toward the site of injury and produce critical matrix proteins.(110, 111)

While cell type identification remains a challenge, particularly for fibroblasts and smooth muscle cells, Jones *et al*. were able to identify the emergence of an activated synthetic fibroblast, with a decline in smooth muscle cells.(94) While it remained to be determined whether this population of activated fibroblasts was induced secondary to aortic dilation, or its presence exacerbated pathological remodeling, it was clear that the synthetic fibroblasts became the predominant cell type within the aortic wall with aneurysm and strongly suggests that this population may be managing the process of aortic dilation.

To support this notion, Jones and colleagues further demonstrated that associated with this alteration in cellular constituents, aneurysm development was accompanied with structural changes within the aortic wall.(94) An analysis of medial elastin content and architecture was performed by histological staining of aortic tissue sections following the induction of TAA. This analysis, in agreement with previous work,(115) identified flattening and thinning of the elastic lamellae at the early stages of aneurysm development progressing to a decrease in the number of elastic lamellae from six in the control sections to four at 8 weeks following induction. This reduction in integrity of the elastic lamellae is a common feature of advanced aortic remodeling as seen in clinical TAA specimens undergoing vascular remodeling, and likely allows for aortic dilation.(101, 116, 117) Therefore, it became apparent that rather than a simple degenerative course, aneurysm development is a dynamic remodeling process

managed by the cellular population within the aortic wall as a result of adverse remodeling of the vascular extracellular matrix.

Extracellular matrix remodeling and release of harbored cytokines

While multiple factors contribute to the development of aortic aneurysm, a hallmark of TAA is abnormal remodeling of the vascular extracellular matrix (ECM). This process results in vessel weakening and loss of compliance that allows for progressive dilation and eventual rupture if left untreated. Vascular remodeling may be defined as any lasting change in the size and/or composition of an adult blood vessel. It is becoming apparent that remodeling within the aortic wall results in not only excessive deposition of matrix proteins, but also significant degradation of critical ECM components. This dynamic process thereby alters the mechanical strength and integrity of the aorta allowing for progressive dilation, and furthermore, results in the release of harbored growth factors and cytokines, progressing pathology by altering phenotype of the endogenous cellular population.

Importantly, the ECM is no longer thought to be a passive structural support, but rather a dynamic regulator of growth factor bioavailability.(118) For example, the ECM serves to sequester and concentrate transforming growth factor-β (TGF-β), a soluble cytokine secreted into the extracellular space by endogenous cells. This particular cytokine is a critical growth factor known to

effect multiple phenotypic characteristics, such as cellular proliferation, migration, differentiation, and apoptosis.

This multifaceted cytokine is stored in the ECM within a large latent complex (LLC), which is composed of a homodimer of mature TGF-β peptide, a homodimer of an inactive cleaved peptide fragment of TGF-β (the latent associated protein, LAP), and latent transforming growth factor binding protein (LTBP1).(36) Sequestered TGF-β is released in its mature form by several mechanisms, including by direct proteolysis of the ECM,(119) allowing for interaction with cell surface receptors. This process allows for the induction of signaling cascades whereby complex cellular pathways may be activated.

Best known for its role in stimulating collagen production and deposition,(120) dysregulated TGF-β signaling has been implicated in multiple vascular pathologies, including, atherosclerosis,(121) pulmonary hypertension,(122) and thoracic aortic aneurysms.(123) TGF-β signaling is highly complex, involving multiple different functional ligand subtypes, receptor types and subtypes, and downstream signaling. To simplify, the classical TGF-β pro-fibrotic signaling pathway is initiated with ligand binding to the type II TGF-β receptor (TGF-βRII), which is autophosphorylated, then recruits the type I TGF-β receptor (TGF-βRI). Upon transphosphorylation of the TGF-βRI, a common receptor-SMAD is activated. The SMADs make up a class of intracellular proteins which function to transduce extracellular signaling from the TGF-β ligands to the nucleus. Once activated, the receptor SMAD then binds a co-SMAD (SMAD 2/3) and

translocates into the nucleus, where it further interacts with transcriptional co-factors and forms an activated transcriptional complex, inducing a pro-fibrotic profile of gene expression that favors matrix deposition.(124) For example, critical pro-fibrotic genes induced in response to TGF-β are connective tissue growth factor (CTGF) (125, 126) and collagen type 1 (COL1a1)(127), which are known to play significant roles in extracellular matrix remodeling and alteration of cellular phenotype.

In addition to TGF-βRI, a second type 1 TGF-β receptor has been identified. The actavin-receptor-like kinase 1 (ALK-1) which interacts with TGF-β and plays an alternative role activating transcription of a different set of genes. Like TGF-βRI, ALK-1 is capable of interacting with TGF-βRII in response to TGF-β ligand binding.(128, 129) While activation of TGF-βRI phosphorylates SMAD 2/3, activation of ALK-1 results in SMAD 1/5/8 phosphorylation.(130, 131) Interestingly, ALK-1 mediated gene expression profiles often occur in opposition to TGF-βR1 responses, and furthermore has been identified to be an antagonistic mediator of TGF-βRI signaling.(132, 133) Nevertheless, it has been proposed that activation of ALK-1 may induce angiogenic factors that contribute to significant degradation of the vascular ECM.(123)

Interestingly, paradoxical discoveries were made by Jones and colleagues.(134) Following induction of TAA with the use of the periadventitial calcium chloride murine model, it was demonstrating that a reduction in the TGF-β receptor 1 occurs, with a concomitant increase in TGF-βRII, while ALK-1

remained unchanged throughout the progression of TAA.(134) Importantly, Jones *et al.* identified that with progression of TAA, SMAD 2/3 signaling may give way to increased SMAD 1/5/8 signaling altering the cellular response to TGF-β stimulation throughout TAA development, thus representing a significant change in signaling outcome. These findings suggest that TGF-β signaling shifts from matrix deposition in early aneurysm formation, to matrix degradation in later stage aneurysm progression.

In addition to regulation of fibrotic/degradative gene expression profiles, TGF-β has been implicated in the induction of SMC apoptosis, and modulation of fibroblast phenotype. Demonstrated in abdominal aortic aneurysms, Fukui *et al.* determined that high levels of TGF-β co-localized with markers specific for SMCs undergoing apoptosis, demonstrated by TUNEL assay, an identifying marker for DNA fragmentation.(135) In agreement with previous findings, identifying SMC apoptosis with the development of TAA in a murine model,(94) these data suggest that SMC apoptosis may be mediated in part by TGF-β, leaving the fibroblast population as the predominant cell type to manage the vascular remodeling process. Also demonstrated by Jones *et al.* the adventitial fibroblasts themselves under go phenotypic alterations in TAA by taking on synthetic characteristics,(94) and it has been proposed that TGF-β may play a significant role in this differentiation process.(136-138) Taken together, these data indicate that TGF-β is involved in the induction of SMC apoptosis and alteration of

fibroblast phenotype, both of which promote development and progression of TAA.

It is apparent that TGF-β signaling can regulate the production of critical vascular matrix proteins as well as matrix degrading enzymes, and suggests that alterations in signaling may be detrimental to normal vascular function and architecture. Therefore, further studies directed at targeting TGF-β were initiated with the goal of attenuation of aneurysm progression. Losartan, an Angiotensin I receptor blocker seems to exert beneficial effects through inhibiting TGF-β, thereby reducing matrix degradation in a Marfan syndrome mouse model.(38) In a murine model of Marfan crossed with an apolipoprotein E-deficient mouse line, in which angiotensin II is infused to induce aneurysm, losartan prevented aneurysm formation.(38, 139) However, clinical trials on the effects of losartan on aneurysm growth rates yielded interesting results. In Marfan syndrome patients treated with losartan, rate of aortic root dilation was significantly attenuated following three years of treatment. Conversely, aneurysm progression beyond the aortic root was not affected by losartan.(140) Furthermore, the efficacy of losartan on aortic dilation in non-Marfan patients remains to be determined. To confound these reports, a recent finding published by Lareyre *et al.* demonstrated that systemic inhibition of TGF-β exacerbates sustained aneurysmal dilation in an elastase induced murine model of abdominal aortic aneurysm.(141)

Alterations in TGF-β signaling are undisputedly associated with vascular remodeling and have been directly implicated in aortic aneurysm development. While, each cell type reacts differently to TGF-β stimulation, it is likely that the homeostatic balance governing ECM integrity are managed through differential cellular responses, including newly acquired cellular functions, such as, degradation of major components within the aortic wall. This process alters the mechanical strength and integrity of the aorta, thus increasing the potential for vessel dilation, and therefore increasing wall tension, as tension is directly dependent on vessel diameter (law of Laplace). Nevertheless, the many roles TGF-β signaling plays in this process highlight the need for further investigation in the upstream regulatory mechanisms of these processes.

The role of Matrix Metalloproteinases in vascular ECM remodeling

Both intracellular and extracellular mechanisms function to balance matrix deposition and degradation in order to maintain structural integrity of the aortic wall. In the aneurysmal aorta, this balance becomes disrupted in favor of enhanced proteolysis resulting in the pathological remodeling of the vascular ECM leading to progressive dilation. As, the aortic ECM provides structural and biochemical support to the resident cells, remodeling is an important process in which a critical family of proteolytic enzymes, the matrix metalloproteinases (MMPs), actively participate through the degradation of all ECM components and

subsequent release of sequestered growth factors and cytokines.(123, 142) This breakdown of normally long lasting matrix molecules, such as elastin and collagen, has placed a great deal of emphasis on research focusing on the involvement of MMPs in the ECM remodeling associated with aortic aneurysm formation and progression.

Interestingly, the first MMP described was discovered by placing a slice of tail from a tadpole undergoing metamorphosis on a collagen gel, This resulted in a clearing of a zone surrounding the tissue section, indicating collagenase activity, and emphasized a key role these enzymes play in the degradation of ECM molecules.(143) Since this initial discovery, the MMPs have become a growing class of proteolytic enzymes, with over 24 different sub-types described.(144, 145)

The MMPs are either secreted from cells, or anchored to the plasma membrane, and classification has been divided into six groups based on substrate specificity, sequence similarity, and domain organization. The collagenases are a group of MMPs with the ability to hydrolyze interstitial collagens I, II, and III at a specific site, and also retain the ability to digest a number of other ECM and non-ECM molecules. The gelatinases consist of gelatinase A and B, MMP-2 and MMP-9 respectively. This group of proteolytic enzymes has three repeats of a type II fibronectin domain inserted into the catalytic domain, allowing for binding, and subsequent hydrolysis, to gelatin, collagens, and laminin.(146) The stromelysins consist of two members with

similar substrate specificity. In addition to digestion of ECM components, stromelysin 1 (MMP-3) is capable of activating a number of other MMPs, through cleavage of the pro-domain, thereby exposing the catalytic domain.(147) The matrilysins are characterized by the lack of a hemopexin domain, and have the ability to degrade a number of ECM components. The membrane type MMPs (MT-MMPs) are a unique class of membrane bound proteolytic enzymes. These six members are anchored in the plasma membrane of cells and are capable of degrading all ECM components, releasing latent ECM bound cytokines and growth factors, and activating latent MMPs. The remainder of the MMPs not listed above constitute their own class of other MMPs.

Considering the capability of hydrolyzing all components of the vascular ECM, the physiological activity of MMPs must be tightly regulated to maintain tissue homeostasis. Indeed, in normal non-pathological tissues, levels of MMPs are very low.(148) The regulation of MMP activity is controlled at multiple levels. First, like most messenger RNAs, MMPs are transcribed from DNA by an RNA polymerase-II-dependent process.(149) Cytokines, hormones, and growth factors, may increase MMP expression, in most cases by induction of transcription and increased promoter activity.(150) Second, translation of MMPs may be regulated in multiple ways. The corresponding mechanisms are primarily targeted to the control of ribosome recruitment on the initiation codon, but can also involve modulation of the elongation or termination of protein synthesis by rapid degradation of the messenger RNA sequence.(151) In most cases,

translational regulation involves specific RNA silencing proteins to be recruited to the messenger RNA sequence, a process regulated by microRNAs.(152, 153) MicroRNAs are small non-coding RNAs which direct the RNA induced silencing complex to targeted sequences within the messenger RNA transcript, inducing degradation or, more commonly, translational repression.(154) Third, MMPs are expressed as inactive zymogens and require proteolytic processing to expose the active catalytic site. While most MMPs require extracellular activation, few are activated intracellularly by a mechanism requiring the endoprotease, furin.(155) This physiological activation occurs in multiple steps. Initially, activating factors, such as, plasmin and other MMPs disrupt the cytosine-zinc interaction resulting in a partially active intermediate. For full activation, this intermediate form requires removal of the pro-peptide region, normally achieved by further proteolytic processing by other MMPs.(156) Finally, the activity of MMPs may be regulated by the endogenous tissue inhibitors of matrix metalloproteinases (TIMPs).

The tissue inhibitors of matrix metalloproteinases (TIMPs) are specific inhibitors that bind MMPs in a 1:1 stoichiometry.(157, 158) Four TIMPs have been identified in vertebrates, and expression is tightly regulated during development and during no-pathological tissue remodeling.(148) While the TIMPs have been described to be equipotent, their capacity to bind to the MMPs differ. The conserved region of the N-terminal region of the TIMP binds to the catalytically active site of MMPs.(159) In addition to inhibition of the MMPs, it

has become clear that the TIMPs possess other essential biological functions. Under certain conditions the TIMPs may act as inhibitors of proliferation or migration,(160) while also possessing growth factor properties thereby stimulating migration and even apoptosis.(161) In ECM remodeling, as seen in aortic aneurysms, imbalances in the MMP:TIMP ratio within the aortic wall are observed, which favor net proteolysis.(162)

In a study designed to demonstrate the ability MMP inhibition by the TIMPS, adenoviral transfection of human saphenous vein organ culture with TIMP-1 and TIMP-2 was shown to inhibit MMP-2 and MMP-9 gelatinogenic activity and reduce neointimal thickening without altering the protein abundance of either MMP-2 or MMP-9.(163, 164) Furthermore, Allaire and colleagues demonstrated that overexpression of TIMP-1 by local gene delivery, inhibited aneurysmal dilation in a rat xenograph model of abdominal aortic aneurysm.(165) The significance of these findings were two fold. First, this data provides support to the notion that excessive MMP activity in the vessel wall is an important contributor to aneurysmal degeneration. Second, inhibition of MMP activity is sufficient in attenuating aortic dilatation. However, the clinical applicability of local TIMP gene transfer to the aortic wall, especially within the thoracic portion, requires significant development before becoming a plausible therapeutic approach.

A loss in control of MMP activity results in pathological vascular remodeling and promotes aortic pathology by proteolytic degradation of the

elastic lamina. Furthermore, increased MMP activity has been reported in various inflammatory, malignant, and degenerative disorders and leads to degradation of the ECM.(166) The ECM provides both structural and biochemical support to the resident aortic cells. When exposed to elevated wall tension, the adventitial layer begins early and dramatic remodeling,(167) and this disruption of vascular ECM occurs in part through activation of the MMPs and results in alterations in the content of collagen and elastin within the cytoskeleton surrounding the cells.(168)

Increased expression of multiple MMPs have been observed in aortic aneurysm tissue; however, the prominent degradation of elastin focused much work on the investigation of MMPs with elastolytic capabilities. Thus, many studies in both human specimens and animal models have identified that the gelatinase subclass (MMP-2 and MMP-9), display elevated production and activity in both abdominal and thoracic aortic aneurysm disease, suggesting these enzymes may play a significant role in aneurysm development.(92, 93, 169, 170) Moreover, Longo and colleagues demonstrated that macrophage derived MMP-9 was found to work in concert with mesenchymal cell derived MMP-2 to induce abdominal aortic dilation.(92) Interestingly, utilizing the calcium chloride aneurysm induction method, Ikonomidis and colleagues demonstrated in the thoracic aorta that elevated MMP-9 localized to cells of mesenchymal origin in the absence of inflammatory infiltrate and that TAA development was attenuated in mice devoid of the MMP-9 gene.(169) These data demonstrate

that both MMP-2 and MMP-9 appear to play a significant role in aortic aneurysm development and furthermore support the notion that there are inherent differences between the thoracic and abdominal aorta that contribute to the mechanisms driving aneurysm development. While significant, these findings do not preclude an important role of other MMPs, serine or cysteine proteases in the development of aortic aneurysm.

Interestingly, inhibition of angiotensin-converting enzyme has been shown to both stimulate and inhibit MMPs and the degradation of extracellular matrix in aortic aneurysms induced in a spontaneously hypertensive rat model.(171) Thus, the effects of angiotensin-converting enzyme (ACE) inhibitors on aortic aneurysm has been examined. Due to the contradictory role in MMP activation and inhibition, it is of little surprise that clinical studies on angiotensin-converting enzyme inhibitors have reported conflicting findings. One study demonstrates that patients who received ACE inhibitors were significantly less likely to present with a ruptured abdominal aortic aneurysm,(172) whereas the results of another study show that patients taking ACE inhibitors have a faster aneurysm growth rate.(173)

Doxycycline, a tetracycline-class antibiotic, has been demonstrated to have an inhibitory effect on a broad spectrum of MMPs. Doxycycline binds the zinc-containing active site of MMPs and non-selectively inhibits activity.(174) In several early human studies of small abdominal aortic aneurysms, doxycycline treatment was suggested to be useful in suppressing MMP 2 and 9 activity.(175-

177) Therefore, it was postulated that doxycycline may affect aneurysm progression through preventing elastic fiber degeneration. However, a larger phase II multicenter study was unable to determine a clear effect of doxycycline treatment on the rate and extent of small abdominal aneurysm expansion.(178) Efficacy of doxycycline use for the attenuation of TAA was supported in an animal study of the FBN1 mutation mouse model of Marfan syndrome. Here it was demonstrated to effect the rate of thoracic aortic dilation.(179) While promising, demonstration of the efficacy in human TAA with Marfan, as well as non-Marfan patients, requires additional studies.

Other MMP inhibitors such as *o*-phenanthroline, batimastat, marimastat, GM-6001, and PD-166793 have been developed. While these molecules have demonstrated efficacy in several animal models of pathologies associated with increased MMP abundance, such as, breast cancer metastasis (180), atherosclerosis (181), and abdominal aortic aneurysm (182), they have performed poorly in clinical trials. Due to unanticipated side effects, such as tendonitis-like fibromyalgia, these trials were halted early, failing to show expected results.(183, 184) These off target effects highlight the need for alternative therapeutic strategies targeted toward the regulation of the specific molecular pathways which are aberrantly activated throughout the development of aortic aneurysm.

The Membrane Type 1 Matrix Metalloproteinase in aortic aneurysms

More recently a membrane bound MMP, the membrane type-1 matrix metalloproteinase (MT1-MMP) has been implicated in aneurysm formation. Studies examining human and mouse aneurysm specimens from both AAA and TAA have demonstrated increased abundance of MT1-MMP, suggesting this enzyme plays an important role in mediating the pathological remodeling process.(100, 185-188) This class I transmembrane proteolytic enzyme has gained significant attention due to the several ways by which it may contribute to aneurysm development. First, MT1-MMP possesses gelatinolytic and collagenogenolytic activity that can directly degrade the structural ECM.(189) Second, when on the cell surface, MT1-MMP plays an essential role in the activation of other MMPs and when internalized, takes on a signaling role. For example, MMP-2 is secreted into the extracellular space as an inactive propeptide, there the catalytic portion of MMP-2 is exposed by the removal of the pro-domain through cleavage mediated by a complex containing MT1-MMP, TIMP2, and pro-MMP-2.(190, 191) Third, MT1-MMP is known to release ECM-sequestered cytokines and growth factors that can further act to drive ECM remodeling. When MT1-MMP is phosphorylated, it is internalized from the cell surface, and its role is shifted from MMP-2 activation to intracellular signaling through the release of theses cytokines and growth factors.(192) Both the latent TGFβ-binding protein 1 and fibrillin-1a have been identified as substrates for MT1-MMP.(193, 194) These roles of MT1-MMP identify the multifunctional contribution toward ECM remodeling and subsequent TAA formation and progression.

In a study performed by Jones and colleagues, it was demonstrated that MT1-MMP expression, abundance and activity is elevated during TAA development, suggesting a key role in aneurysm disease.(188) In this previous set of investigations, TAA was induced in murine descending thoracic aortas using the periadventitial application of calcium chloride. Development of TAA was tracked over time and aortic dilation was confirmed to be increased when compared to unoperated control mice. Two weeks following the induction of TAA, MT1-MMP mRNA levels were increased; however, expression returned to baseline at subsequent time points. Importantly, MT1-MMP protein remained unchanged at two weeks post TAA induction, then progressively increased through the 16 week time course. Combined, these findings identify that increased protein abundance of MT1-MMP was not simply a result of increased transcription, but implicate the loss of a posttranscriptional regulatory mechanism.

Interestingly, in this previous study, it was also identified that MT1-MMP co-localized to DDR2 positive fibroblasts.(188) In agreement with an earlier study performed by Jones and colleagues, when aortic fibroblasts from TAA and control mice were isolated and expanded in culture, it was determined that the fibroblasts had undergone a significant and sustained alteration in phenotype, resulting in enhanced proteolytic gene expression, including elevated MT1-MMP.(195) Combined, these results further implicate this cell type as a major mediator of TAA development. Furthermore, Jones and colleagues

demonstrated a 33% increase in the number of cells staining positive for MT1-MMP at 16 weeks following the induction of TAA. (195) However, the observed 70% increase in total MT1-MMP protein abundance observed in 16 week TAA tissue homogenates suggest that not only is there an increase in the number of cells producing MT1-MMP, but there is also an increase in the amount of MT1-MMP being produced by each cell.

In agreement with the finding that MT1-MMP is elevated during TAA formation in a murine model, Ikonomidis and colleagues recently demonstrated elevated MT1-MMP protein abundance in clinical ascending TAA samples.(192) In this investigation two cohorts of TAA specimens were selected from an aortic tissue bank, small TAAs (4.0-4.9 cm in diameter), and large TAAs (6.5-8.0 cm in diameter) and MT1-MMP abundance was compared to aortic tissue harvested from patients without aneurysm disease. This previous study identified that, similar to mouse models, MT1-MMP was elevated in both small and large TAAs, further suggesting that MT1-MMP may indeed play an important role in TAA formation and progression.

The multiple unique characteristics of MT1-MMP position it at the center of several mechanisms capable of regulating ECM remodeling; however, less is understood about the endogenous mechanisms by which this proteolytic enzyme becomes adversely produced in TAA disease. Thus, studies directed at the identification of post-transcriptional regulatory mechanisms of MT1-MMP may provide novel therapeutic strategies for the treatment of TAA.

MicroRNAs: Regulators of Translation

Increasing evidence supports a direct role for altered microRNA (miR) abundance in pathological cardiovascular remodeling and disease progression. The microRNAs constitute an endogenous class of small non-coding RNA molecules, 20-25 nucleotides in length that have been demonstrated to have important translational regulatory functions.(196) These small RNA molecules are used by eukaryotic cells to direct gene silencing.(196) Inside the nucleus, protein coding genes are transcribed by RNA polymerase II, and following processing, the messenger RNA is then exported into the cytoplasm. Here ribosomes catalyze translation of the messenger RNA to form polypeptide chains that fold into proteins. It is at this point where microRNAs have their gene silencing effects.

To date, nearly 2000 unique high confidence miRNAs have been identified in the human genome (mirbase.org). Importantly, it has been well described that a single miR can target multiple mRNAs, and that a single mRNA can contain multiple miR binding sites.(197, 198) This suggests that miRs, alone or in combination, may be able to regulate a coordinated cassette of genes that together can influence complex cellular functions, such as phenotype.

MicroRNA biogenesis begins from transcription from DNA (overview in Figure 1.1). Some microRNA sequences are identically repeated in multiple

locations within the genome, and are differentiated by referring to them as -1 and -2, and so forth.(199) Like most messenger RNAs, microRNAs are transcribed from DNA by an RNA polymerase-II-dependent process.(149) However, microRNA genes are often embedded in introns or exons of other genes.(200) The transcriptional regulatory elements of microRNAs largely overlap with that of mRNAs and include, DNA binding factors, promoter structure and histone modifications.(201, 202) Transcribed is a long primary (pri-) sequence, which can be over 1,000 nucleotides in length(203), possessing a hairpin structure where the mature sequence is embedded.(203) Following transcription, the pri-miR undergoes several steps of maturation. The nuclear ribonuclease (RNase) Drosha initiates this maturation process by cleaving the stem-loop portion to release a small hairpin-shaped RNA of approximately 65 nucleotides in length, called the precursor (pre-) miR.(204) In the precursor miR stemloop structure, the 5p strand is present in the forward position, while the 3p strand is located in the reverse position.(199) Following processing by Drosha, the protein, exportin 5 (XPO5) forms a transport complex with a GTP-binding protein and the pre-miR, allowing for translocation through the nuclear pore complex.(205) Following nuclear export, the GTP is hydrolyzed resulting in disassembly of the complex and subsequent release of the pre-miR into the cytosol.(206) Here the pre-miR is cleaved by RNase III-type endonuclease, Dicer, near the terminal loop, thus liberating the small RNA duplex.(207) This small RNA duplex is subsequently loaded onto an Argonaut (AGO) protein, which involves two steps. First, loading of the RNA duplex, then subsequent unwinding.(208). The two strands of the

small RNA duplex are cleaved and one strand, known as the passenger strand, is liberated from AGO, while the remaining strand, known as the guide strand, remains serving as a recognition sequence for targeted mRNA transcripts.(209) In the case of the following studies included in this body of work, the guide strand microRNA being quantified and studied is miR-133a-3p. The passenger strand either functions merely as a carrier strand and is degraded following ejection from AGO, or it becomes incorporated in a different AGO complex and functions as a guide strand itself.(210) Next, the AGO protein containing the guide strand miR recruits the GW182 protein to form a multimeric effector protein complex known as the RNA-induced silencing complex (RISC).(211) Silencing of translation is achieved in two distinct ways: mRNA decay by recruiting deadenylases and decapping factors, or more commonly translational repression. Repression may also occur by two mechanisms, one involving disassociation of the eIF/4E cap, or by recruitment of translational inhibitors thereby preventing ribosomal loading.(154)

It is widely accepted that miRs are key regulators of complex biological processes, and it is becoming increasingly apparent that alterations in miR abundances are associated with multiple cardiovascular diseases. For example, pathologies including left ventricular hypertrophy, ischaemic heart disease, heart failure, hypertension, arrhythmias, and more recently aortic aneurysm have all been associated with abnormal miR levels.(212-218)

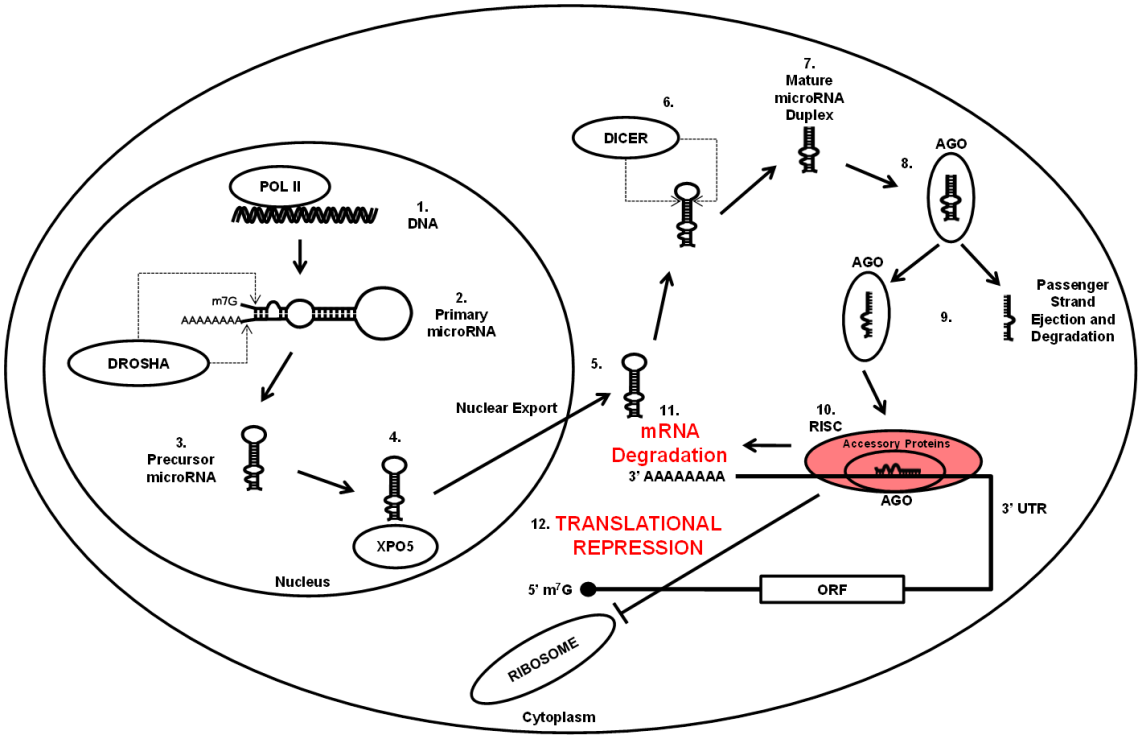

Figure 1.1 MicroRNA Biogenesis

Like all messenger RNA, microRNAs are transcribed from DNA, and this process is RNA polymerase II dependent and regulated by transcription factors.(**1**) Transcription of microRNAs generates a long primary transcript, termed the primary microRNA.(**2**) Following transcription, microRNA processing continues with hydrolysis of the transcript by the enzyme Drosha to produce a precursor microRNA,(**3**) which then interacts with Exportin-5 (XPO-5)(4) and is then exported from the nucleus to the cytoplasm (**5**) where further hydrolysis by the Dicer Ribonuclease removes the loop portion of the precursor microRNA (**6**), generating a double stranded microRNA duplex (**7**). In the cytoplasm, final processing occurs as the microRNA duplex interacts with Argonaut (AGO) protein (**8**) and is stripped of its complementary passenger strand (**9**). Incorporation of accessory protein, GW182, forms the RNA-Induced Silencing Complex (RISC), which can interact with the 3'UTR of target mRNAs (**10**) resulting in two possible outcomes. Dependent upon the level of homology between the microRNA and targeted mRNA sequences: if the homology is high, the targeted mRNA transcript is degraded (**11**); or if the homology is low, imperfect base paring between the microRNA and mRNA results in translational repression (**12**). The latter outcome occurs in 85% of interactions. In this scenario the RISC Complex functions by using the incorporated mature microRNA sequence as a target recognition component. This allows for imperfect interaction with complementary binding sites predominantly located in the 3' UTR of a targeted mRNA and results in translational repression of that particular message.

To determine if TAA development coincides with alterations in miRs, Jones and colleagues performed a microRNA microarrary analysis comparing the relative abundance of miRs in TAA and non-aneurysm control aortic tissue. This array identified 37 differentially expressed miRs between normal and TAA tissue, and furthermore identified 106 miRs that changed from detected to undetected, or undetected to detected.(212) From this list of differentially regulated miRs a comprehensive literature search was performed, identifying a focused set of miRs which appeared to be highly discussed in the cardiovascular literature. This previous study then confirmed by PCR analysis, that several microRNAs, including miR-1, -21, -29a, -486, -720, and miR-133a, were reduced in the ascending aortic tissue from patients with thoracic aortic aneurysm (TAA).(212) Many of these miRs, including miR-1, -21, 29a, and -133a, displayed an inverse linear correlation with aortic diameter, such that as diameter increased, the abundance of miR-133a was reduced.(212)

Upon further review of this set of microRNAs, miR-133a was identified to directly regulate multiple proteins that are highly involved in both genetic and idiopathic thoracic aortic aneurysms. Many of the targets of miR-133a play key roles in determining aspects of cellular phenotype and regulating ECM remodeling; therefore, finding miR-133a reduced in TAA tissue suggests that the loss of miR-133a may play an important role in TAA development. First, miR-133a targets TGF-β,(219) which is elevated in TAA tissue, induces CTGF expression, alters fibroblast phenotype and causes apoptosis in smooth muscle

cells. Second, miR-133a targets TGF-βRII,(219) which is elevated in TAA tissue, and with the concomitant decline in TGF-βI receptor, shifts TGF-β ligand signaling to ALK-1, activating the SMAD 1/5/8 pathway, which induces a profile of gene expression resulting in matrix degradation. Third, miR-133a targets CTGF,(220) which is elevated in TAA tissue and also alters fibroblast phenotype. Fourth, miR-133a is known to target the repression of Col1a1.(221) Finally, mir-133a targets MT1-MMP,(222) which is elevated in TAA tissue, degrades components of the ECM, activates other MMPs, such as MMP-2, and directly releases cytokines such as TGF-β. In addition to the above listed direct targets of miR-133a, it is apparent that miR-133a may have the capacity to regulate multiple pathways involved in complex pathology, increasing the significance of the loss of miR-133a observed in the development of TAA.

The importance of miR-133a in the regulation of extracellular matrix remodeling in cardiovascular tissue is becoming increasingly recognized. Carè *et al.* demonstrated in a murine model of cardiac hypertrophy, that miR-133a is reduced in the hypertrophied myocardium, and that *in vivo* knockdown of miR-133a (using anti-miR-133a) induced cardiac hypertrophy.(216) Similarly, Torella *et al.* demonstrated miR-133a was reduced in the carotid artery following balloon distension injury in a rat model. Importantly, they demonstrated that systemic overexpression of miR-133a by adenovirus, attenuated post-injury remodeling, in contrast to miR-133a knockdown (using an anti-miR-133a oligonucleotide) enhanced post-injury remodeling.(214) Data from these studies emphasize the

key role that miR-133a plays in cardiovascular remodeling and suggest that the loss of miR-133a-mediated translational control of targeted genes likely contributes to pathologic changes in the extracellular matrix.

While much effort has been directed toward understanding the role of miRs in modulating cellular targets, less is known about how miR abundance is regulated within the cell. Accordingly, understanding the mechanisms that regulate miR-133a cellular abundance is essential, and may provide insight into potential therapeutic targets.

SUMMARY

Thoracic aortic aneurysm (TAA) is a localized dilation of the supradiaphragmatic aorta. This devastating disease process is often asymptomatic and results in a weakened aortic wall and can progress to rupture if left untreated;(29) however, the underlying molecular mechanisms leading to the development of TAA are largely unknown. While there are numerous etiologies that contribute to the manifestation of TAA, abnormal remodeling of the aortic extracellular matrix (ECM) and changes in the resident cellular population universally occur. Histological examination of aortic structure and composition has demonstrated a decline in the smooth muscle cell population coinciding with an emergence of fibroblast derived myofibroblasts.(94) It is believed this population of fibroblasts is managing the remodeling process through the association with observed elastic fiber and medial degeneration.(63, 94, 168) Interestingly, it has been demonstrated that isolated primary aortic fibroblasts from TAA tissue sustain a stable alteration in gene expression profile.(195) Under normotensive conditions, a physiologically relevant level of wall tension is essential for maintaining normal vessel structure.(223) According to Laplace's law (vessel wall tension = pressure X radius), wall tension is directly related to the radius of the vessel and intra-arterial pressure, thus, even when blood pressure is constant and vessel dilation occurs, wall tension rises. Alterations in the amount of tension placed on fibroblasts have been demonstrated to modulate complex cellular phenotypes (224-228); however, the regulatory mechanisms remain unknown. MicroRNAs are powerful regulators of protein abundance and

cellular phenotypes. Protein translation is regulated by microRNAs through interaction with the 3'-untranslated region of targeted mRNAs.(229) Importantly, it has been well described that a single miR can target multiple mRNAs, and that a single mRNA can contain multiple miR binding sites.(197, 198) Alterations in microRNA abundance have been associated with a multitude of pathologies.(230, 231) Previous results from this laboratory determined in clinical specimens: miR-133a displays an inverse relationship with aortic diameter. As the aorta dilates, the abundance of miR-133a decreases.(212) The importance of miR-133a in maintaining tissue homeostasis is becoming increasingly recognized and these findings suggests that loss of miR133a-mediated translational control of specific gene targets may contribute to pathological aortic remodeling. However, the exact mechanism by which miR-133a may be reduced in thoracic aortic tissue has yet to be defined.

SPECIFIC AIMS

Therefore, the following studies tested the hypothesis that **increased thoracic aortic wall tension reduces miR-133a.** Accordingly, a stepwise approach will be utilized to test the following specific aims:

1) **Demonstrate miR-133a is mechanosensitive.** Utilizing murine aortic rings in an *ex vivo* tissue myograph, and in vitro with isolated primary aortic cells (fibroblasts and smooth muscle cells): demonstrate increased tension alters the abundance of mature miR-133a.
2) **Determine the mechanism of miR-133a reduction**. In isolated aortic fibroblasts: investigate the mechanism by which miR-133a is reduced (transcriptional regulation, degradation, or regulated cellular export).
3) **Demonstrate the effects of hypertension on miR-133a levels.** Utilizing two distinct *in vivo* murine models of hypertension (AngII induced pretension and a spontaneously hypertensive mouse line), demonstrate that hypertension is sufficient in alteration of miR-133a levels in thoracic aortic tissue and plasma.

CHAPTER 2: MicroRNA-133a is Mechanosensitive

INTRODUCTION

Mechanical factors play a significant role in the maintenance of vessel homeostasis. Under normotensive conditions, a physiologically relevant level of wall tension is essential for preserving normal vessel structure and function.(223) However, conditions of increased vascular wall tension, for example, hypertension, precipitates structural changes in the thoracic aorta (TA) as a result of remodeling of the vessel wall leading to increased stiffness and often dilation.(63, 232, 233) In this process, alterations in the expression and abundance of multiple proteases involved in remodeling occurs, and this process has been attributed to increased wall tension in the thoracic aorta.(234-236)

While alterations in microRNA levels have been associated with aortic pathologies, the role of wall tension in this process remains unclear. The microRNAs target short nucleotide sequences (seed regions) within the 3' untranslated region (UTR) of specific messenger RNAs (mRNAs), and function to

induce message degradation, destabilization, or more typically, translational repression. Moreover, a single microRNA is capable of targeting multiple mRNAs, and a single mRNA may contain multiple microRNA binding sites.(197, 237, 238). Therefore, alterations in microRNA levels may profoundly affect cellular function.

A particular microRNA, miR-133a, has been demonstrated to regulate adverse vascular remodeling *in vivo* (discussed in Chapter 1).(214) Previous results from this laboratory determined in clinical specimens, miR-133a displays an inverse linear correlation with aortic diameter, such that, as diameter increased, the abundance of miR-133a was reduced.(212) Based on the fundamentals of the Law of Laplace, we know that vessel wall tension is dependent upon the relationship between pressure and diameter (wall tension = pressure X diameter). Accordingly, during aneurysm formation wall tension increases as the aorta dilates, and this may play a role in determining miR levels in the thoracic aortic wall. Therefore, the objective of these studies was to demonstrate mature miR-133a levels may be reduced with increased tension.

RESULTS

Increased mechanical tension reduces mature miR-133a in thoracic aortic tissue.

To determine the effects of elevated applied tension on miR-133a levels, intact murine TA segments (rings) harvested from wild-type, normotensive mice

were hung on parallel wires in an *ex vivo* tissue myograph. Control thoracic aortic segments were held at a previously determined level of tension (0.7 g) that approximates *in vivo* normotension (mean arterial pressure (MAP), ~70 mmHg) (234, 235) To simulate elevated wall tension (hypertension), an increased amount of tension (1.5g, MAP ~150 mmHg) was applied directly to the aortic segments for 3 hours. The abundance of mature miR-133a was reduced in response to increased applied tension as compared to control segments (0.31±0.08 vs 1.0±0.25 fold; $p<0.05$ vs control; n=7) (Figure 2.1).

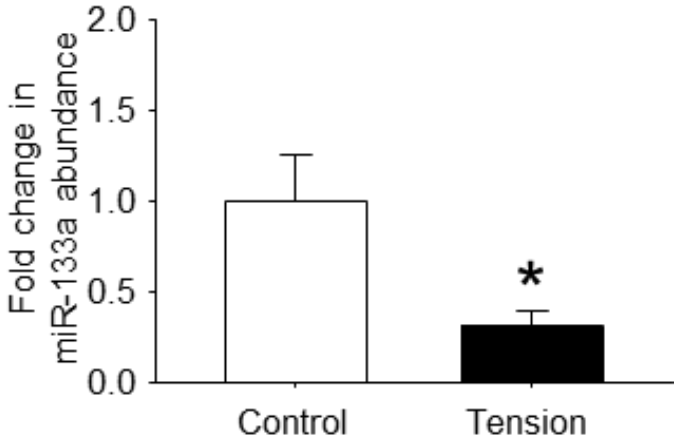

Figure 2.1 Effects of applied *ex vivo* mechanical tension on miR-133a levels in thoracic aortic rings. Descending aortae from wild-type C57BL/6 mice were transversely cut into 3 mm rings and suspended in a tissue myograph on parallel wires in oxygenated Krebs-Henseleit solution. Displayed is the fold change in mature miR-133a abundance in aortic rings held at 0.7 g (Normotension, Control, n=7) or with 1.5 g applied tension (Tension, n=7) for three hours. Data are represented as mean ± SEM. Comparisons were made using a two-sample t-test (unpaired, two-tailed). * $p<0.05$ vs. control.

Angiotensin II (AngII) is known to modulate adhesion molecules, chemokines, cytokines, and growth factors that control cellular proliferation, hypertrophy, fibrosis, and inflammation in the vessel wall.(85) Furthermore, it is well described that AngII causes increased vascular resistance through vasoconstriction which leads to elevated vascular wall tension.(84) Therefore, we sought to determine the effects of developed tension in response to AngII on the abundance of miR-133a.

Thoracic aortic rings from normotensive wild-type mice were hung on parallel wires in an *ex vivo* tissue myograph and held at 0.7g tension, then were exposed to 100nM AngII for three hours in an *ex vivo* tissue myograph. Angiotensin II-dependent vessel contraction resulted in increased developed wall tension compared to rings treated with vehicle (1.51±0.15 vs. 0.73±0.03g; $p<0.05$ vs control; n=8) (Figure 2.2 **A**). Following 3 hours of AngII-induced contraction, miR-133a abundance was reduced compared to non-contracting rings treated with vehicle (0.42±0.09 vs 1.0±0.22 fold; $p<0.05$ vs control; n=8) (Figure 2.2 **B**).

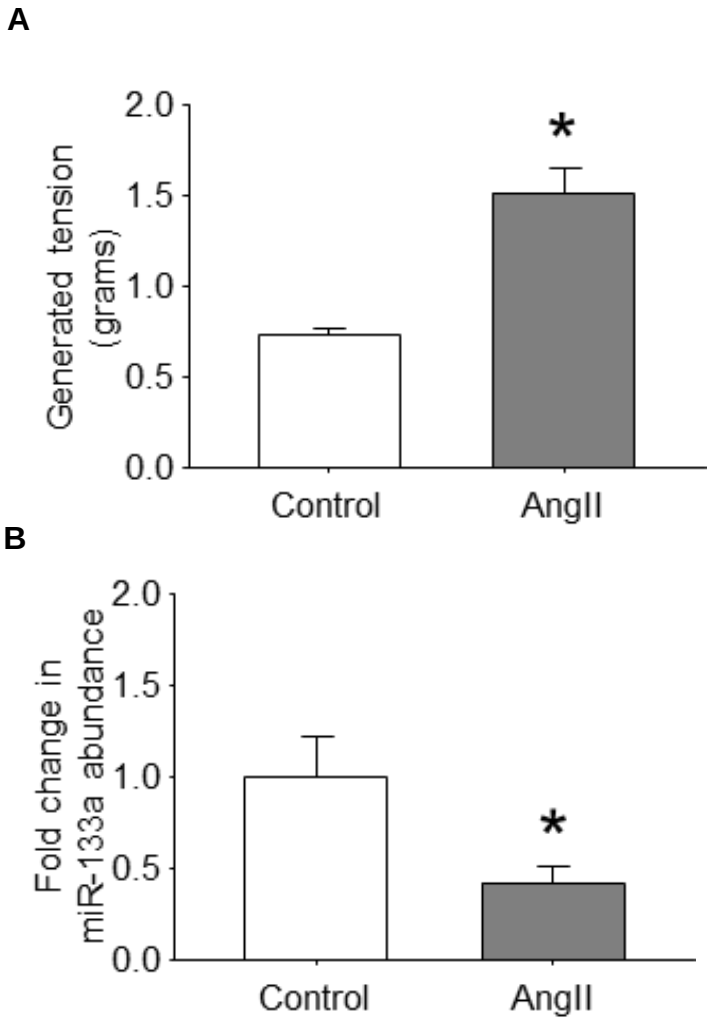

Figure 2.2 Effects of generated *ex vivo* mechanical tension on miR-133a levels in thoracic aortic rings. Descending aortae from wild-type C57BL/6 mice were transversely cut into 3 mm rings and suspended in a tissue myograph on parallel wires in oxygenated Krebs-Henseleit solution. (**A**) Peak generated tension (grams) in aortic rings held at normotension (0.7 g) in the absence (Control, n=8) or presence of 100nM AngII (AngII, n=8) for three hours. (**B**) Effect of generated tension on miR-133a abundance in aortic rings held at normotension (0.7 g) in the absence (Control, n=8) or presence of 100nM AngII (AngII, n=8). Data are represented as mean ± SEM. Comparisons were made using a two-sample t-test (unpaired, two-tailed). * $p<0.05$ vs. control.

Increased mechanical tension results in reduced miR-133a abundance in isolated thoracic aortic fibroblasts.

When isolated aortic fibroblasts and smooth muscle cells (SMCs) where exposed to mechanical tension by biaxial cyclic stretch, mature miR-133a was reduced in stretched fibroblasts as compared to static fibroblast controls (0.21±0.02 vs 1.0±0.27 fold; $p<0.05$ vs control; n=8) (Figure 2.3). Interestingly, no change in miR-133a abundance was observed in stretched SMCs (0.98±0.43 vs 1.0±0.12 fold; $p=0.46$ vs control; n=7) (Figure 2.4). These findings suggested that the reduction in mature miR-133a observed in aortic tissue segments exposed to elevated tension (Figure 2.1) may have been due to a corresponding reduction of miR-133a in aortic fibroblasts.

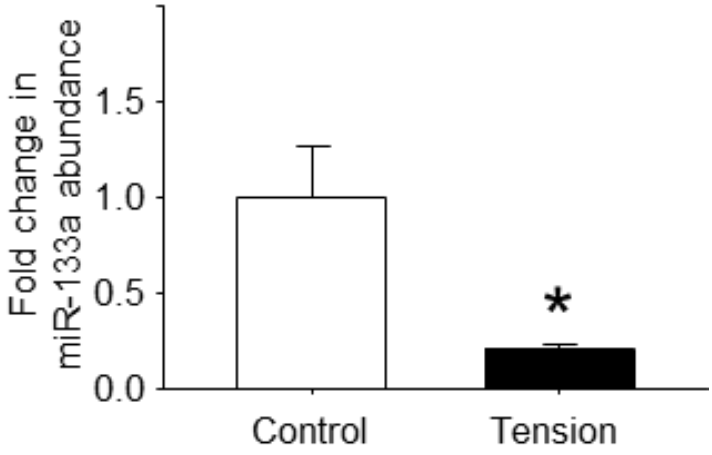

Figure 2.3 Effects of mechanical tension on miR-133a levels in isolated thoracic aortic fibroblasts. Aortic fibroblasts were isolated from the descending aortae from C57BL/6 mice. Displayed is the fold change in mature miR-133a abundance measured in aortic fibroblast lines following exposure to 3 hours of 12% biaxial cyclic stretch (Tension, n=8) or held static (Control, n=8). Data are represented as mean ± SEM. Comparisons were made using a two-sample t-test (unpaired, two-tailed). * $p<0.05$ vs. control.

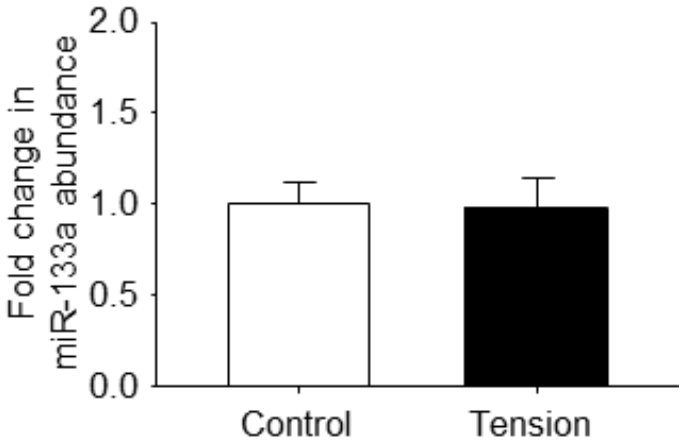

Figure 2.4 Effects of mechanical tension on miR-133a levels in isolated thoracic aortic smooth muscle cells. Aortic smooth muscle cells were isolated from the descending aortae from C57BL/6 mice. Displayed is the fold change in mature miR-133a abundance measured in aortic SMC lines following exposure to 3 hours of 12% biaxial cyclic stretch (Tension, n=7) or held static (Control, n=7). Data are represented as mean ± SEM. Comparisons were made using a two-sample t-test (unpaired, two-tailed). No significant differences were observed vs. control.

To determine whether AngII receptor signaling was contributing to the loss of mature miR-133a, isolated primary aortic fibroblasts and SMCs were exposed to 100 nM AngII for 3 hours. No change in miR-133a was observed in fibroblasts (1.20±0.52 vs 1.0±0.27 fold; p=0.62 vs control, n=8) (Figure 2.5 **A**) or SMCs (1.14±0.26 vs 1.0±0.11 fold; p=0.69 vs control; n=7) (Figure 2.5 **B**). These findings suggested the alterations in miR-133a observed in the aortic ring segments was likely due to the direct effects of mechanical tension on the fibroblasts within the aortic wall, with no contribution of AngII-mediated receptor signaling.

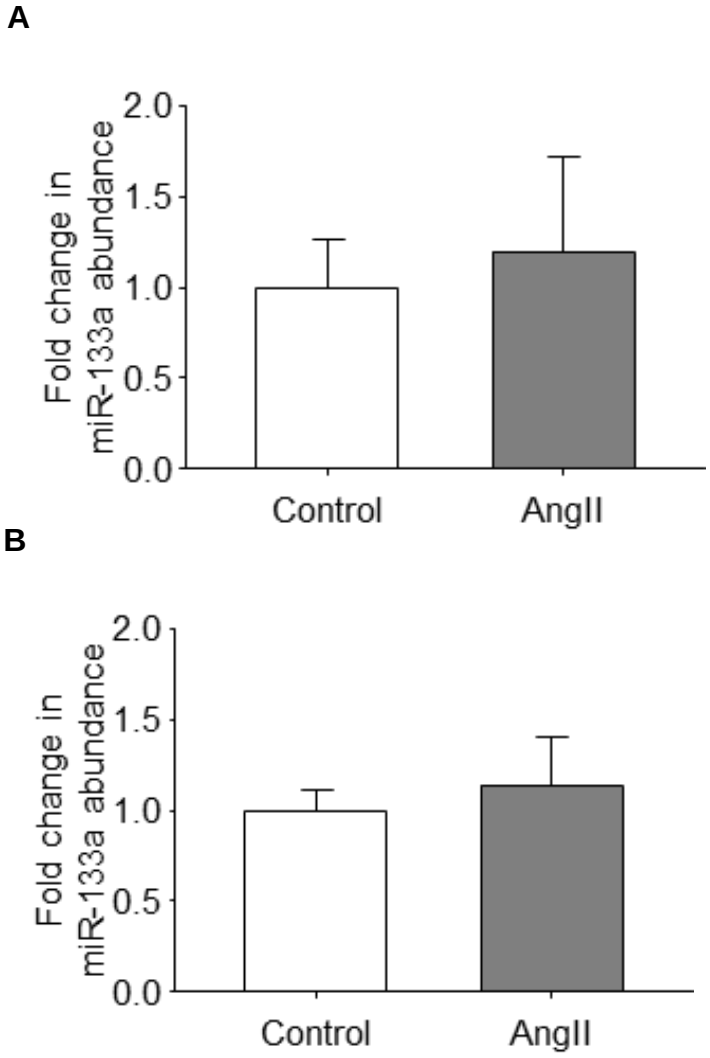

Figure 2.5 Effects of angiotensin-II on miR-133a levels in isolated thoracic aortic fibroblasts and smooth muscle cells. Aortic fibroblasts and smooth muscle cells were isolated from the descending aortae from C57BL/6 mice. (**A**) MiR-133a abundance was measured in aortic fibroblasts lines treated without (Control, n=8) or with 100nM AngII (AngII, n=8) for three hours. (**B**) MiR-133a abundance was measured in aortic SMC lines treated without (Control, n=7) or with 100nM AngII (AngII, n=7) for three hours. Data are represented as mean ± SEM. Comparisons were made using a two-sample t-test (unpaired, two-tailed). No significant differences were observed vs. control.

SUMMARY

These results demonstrate elevated tension applied to the murine thoracic aorta *ex vivo* reduced miR-133a and biaxial cyclic stretch reduced miR-133a in murine thoracic aortic fibroblasts, while no change was observed in smooth muscle cells. Furthermore, AngII induced aortic contraction and reduced aortic tissue miR-133a abundance; however, this effect was likely a result of the mechanical tension, as AngII had no effect on miR-133a levels in isolated thoracic aortic fibroblasts or SMCs.

The unique findings of this investigation were two-fold. First, it was determined that *ex vivo* tension applied to intact thoracic aortic rings resulted in an acute reduction in tissue miR-133a abundance. Second, mechanical tension in the form of biaxial cyclic stretch applied to isolated primary aortic cells (fibroblasts and smooth muscle cells) revealed that fibroblasts preferentially responded to mechanical tension, resulting in the acute reduction of miR-133a.

DISCUSSION

MicroRNAs constitute a novel class of 20-25 nucleotide small non-coding RNA molecules that target short sequences within the 3'-untranslated region of specific messenger RNAs, and function to fine-tune protein abundance by inducing message destabilization, degradation, or more commonly, translational repression.(237) To date, nearly 2000 unique high confidence miRNAs have been identified in the human genome (mirbase.org). Importantly, it has been well described that a single miR can target multiple mRNAs, and that a single mRNA

can contain multiple miR binding sites.(197, 198) This suggests that miRs, alone or in combination, may be able to regulate a coordinated cassette of genes that together can influence specific cellular functions. Previous work from this laboratory demonstrated that the abundance of miR-133a was decreased in aortic tissue from patients with TAA, and was inversely proportional to aortic diameter.(212) We hypothesized, based on the Law of Laplace, that the elevated wall tension, as experienced with increased aortic diameter, may play a role in regulating miR-133a cellular abundance.

It is well described that mechanical tension applied to a tissue is transmitted through constituents of the extracellular matrix (ECM) to the resident cells, and that this is a mechanism by which cellular and tissue homeostasis may be regulated.(239) This process, known as mechanotransduction, affords cells the ability to convert mechanical cues from the physical environment into biochemical or transcriptional changes at the cellular level.(240, 241) The association between increased wall tension and vascular remodeling, as observed in intimal hyperplasia,(242) or aortic aneurysm disease,(63) is well described. In previous results from this laboratory, mechanical tension applied to intact murine thoracic aortic rings was sufficient to alter the gene expression of several key matrix metalloproteinases (MMPs) active in ECM remodeling, such as, MMP-2 and the membrane type-1 MMP (MT1-MMP).(234, 235) Combined with previous findings demonstrating that miR-133a has the capacity to regulate the abundance MT1-MMP,(222, 243) these prior studies provided foundational

evidence that justified investigation into the effects of mechanical tension on the levels of miR-133a. In the present report, a similar approach was taken by directly applying tension to intact aortic rings *ex vivo* in order to identify the effects of acute elevated tension on the tissue levels of mature miR-133a. The results demonstrated that, in as little as 3 hours of applied tension (roughly equivalent to a MAP of ~150 mmHg), tissue levels were reduced by approximately 70%. This is in agreement with a recent study by Mohamed and colleagues whom performed a genome wide analysis on the dysregulation of miR abundance in the diaphragm of mice following *ex vivo* application of transverse mechanical tension.(244) In this study using microRNA microarray analysis, the authors demonstrated that multiple miRs were affected by the application of mechanical tension relative to control; applied tension increased the abundance of some microRNAs and also decreased the abundance of others, including miR-133a.(244) The present study added to these findings by confirming miR-133a is a mechanically sensitive miR and levels are subject to an acute reduction through the application of tension.

While the use of *ex vivo* mechanical tension has allowed for the ability to isolate the effects of wall tension alone on miR-133a levels, multiple factors influence wall tension *in vivo.* It is well known that Angiotensin-II (AngII) causes increased peripheral vascular resistance through vasoconstriction which leads to elevated vascular wall tension,(84) and it has long since been recognized that circulating levels of AngII are elevated in patients with essential

hypertension.(245, 246) Furthermore, AngII is known to modulate adhesion molecules, chemokines, cytokines, and growth factors that control cellular proliferation, hypertrophy, fibrosis, and inflammation in the vessel wall.(85) Therefore, with the use of AngII, we sought to determine the effects of a physiologically relevant form of developed tension on the abundance of miR-133a. Interestingly, this developed tension had a similar effect to the direct application of tension, acutely reducing the abundance of miR-133a, highlighting the physiological relevance of this observation in conditions of elevated wall tension, such as with hypertension.

Further exploration into the effects of tension on miR-133a abundance in two major cell types of the aorta identified that biaxial cyclic stretch also led to the acute reduction of miR-133a in fibroblasts while SMCs were not responsive. This finding identified an unexpected differential response in these two aortic cell types. Previous studies have suggested that fibroblasts are sensitive to changes in mechanical tension and can respond by altering their phenotypic characteristics, taking on a more “synthetic” or mobile role when exposed to increased tension.(239, 247) In pathological vascular remodeling, these synthetic fibroblasts become activated in the adventitia, and migrate inward remodeling the extracellular matrix and enhance vessel stiffness.(167) Previous results from this laboratory have defined changes in the cellular makeup within the aortic wall during TAA formation, revealing that aortic dilation occurs simultaneously with vessel wall remodeling and the emergence of a population of

active fibroblasts.(94) When combined with previous studies demonstrating that aortic dilation is accompanied by the apoptotic loss of SMCs,(248) it is believed that the fibroblasts may be the key cellular mediator of aortic remodeling in aneurysm development.(195) As a single microRNA may regulate translation of multiple targets, the present results, identifying an acute reduction of miR-133a in aortic fibroblasts as a result of increased mechanical tension, may provide insight in the phenotypic alterations observed in these activated fibroblasts and are studies warranting future investigation. Interestingly, when the isolated fibroblasts and SMCs were exposed to AngII, no change in miR-133a levels were observed. This finding suggests the alterations in miR-133a earlier observed in the aortic ring segments were not a direct result of AngII-mediated receptor signaling in the aortic fibroblasts or SMCs, but were likely due to the direct effects of mechanical tension on the fibroblasts within the aortic wall.

LIMITATIONS

The present study is not without limitations. First, the use of *ex vivo* aortic tissue segments raised the concern of tissue viability throughout the duration of the three-hour study. To address this, parallel studies have been performed in which aortic rings were hung for three hours on the tissue myograph, then stimulated to contract with potassium chloride (KCl). The ability of the tissue to mount a contractile response suggests preservation of tissue viability.(234)

CONCLUTIONS

Regulation of genes by mechanical force is a well describe occurrence.(234, 235) More recently, focus has shifted toward tension induced alterations in microRNA levels due to the profound effect on translation. The focus on miR-133a is of particular importance due to the strong association between reduced levels and cardiovascular disease.

Importantly, fibroblasts have been identified as a cell type that is sensitive to mechanical tension and subject to undergo changes, taking on “synthetic” or mobile characteristics. In pathological vascular remodeling, these synthetic fibroblasts become activated in the adventitia, and migrate inward disrupting the extracellular matrix and increase vessel stiffness.(167)

Combined with previous studies which have demonstrated aortic dilation is accompanied by the apoptotic loss of SMCs,(248) it is believed that the fibroblasts may be the key cellular mediator of aortic remodeling.(195) These changes in functional and structural behavior of the fibroblasts exposed to tension may be, in part, due to the early and rapid reduction of miR-133a. Therefore, identification of the mechanisms involved in the reduction of miR-133a may have potential therapeutic application.

CHAPTER 3: A mechanism for tension induced reduction of miR-133a

INTRODUCTION

The vast role microRNAs play in the regulation of translation suggests that microRNAs must themselves be regulated. There are three basic cellular functions that can contribute to the regulation of miR-133a cellular abundance: transcriptional regulation, microRNA degradation, and regulated cellular export.

Currently, the majority of literature on microRNA regulation suggests that expression is largely controlled on the transcriptional level. Like all messenger RNAs (mRNAs), microRNAs are transcribed from DNA by an RNA polymerase-II-dependent process.(149) However, microRNA genes are often embedded in introns or exons (on the reverse DNA strand) of other genes. MicroRNA-133a and miR-1 are included in the same bicistronic unit and are encoded in two locations within the genome; miR-133a-1/miR-1-2 (embedded in an intron of the Mib-1 gene, located on chr18 in mice and humans) and miR-133a-2/miR-1 (located on chr20 in humans and chr2 in mice).(249) The transcriptional regulatory elements of microRNAs, such as DNA binding factors, promoter

structure and histone modifications, largely overlap with that of mRNAs.(201, 202) MiR-133a, has been demonstrated to be regulated by transcription factors, such as, MyoD, Mef2, and SRF.(218, 250) Furthermore, an association of histone deacetylate 1 and 2 has been identified with the miR-133a enhancer region, suggesting the possibility for epigenetic regulation.(218) Independent of the specific mechanism, altered microRNA transcription affects the cellular level of primary microRNA (pri-microRNA), and ultimately the abundance of the mature form.(218)

Mature microRNA abundance may be regulated post-transcriptionally via regulated degradation.(251) MicroRNAs have been demonstrated to be highly stable in circulating plasma (252) and in cells, having a prolonged half-life roughly 2- to 20 times longer than that of typical mRNAs.(253, 254) Recent studies have shown that individual microRNAs may be subject to accelerated decay under certain conditions,(255) and this has been attributed to active degradation by microRNA specific exoribonucleases.(256-258) Three microRNA specific exoribonucleases have been identified in mammalian cells (XRN-1, XRN-2, and ExoSC4), and knockdown of these exoribonucleases have resulted in the accumulation of multiple mature microRNAs.(255-258) Chatterjee *et. al* demonstrated in *C. elegans*, that siRNA mediated knockdown of XRN-1 led to the accumulation of let-7 microRNA, while levels of primary and precursor let-7 microRNA remained unchanged;(258) however, in another study, siRNA against XRN-2 led to a greater than 2 fold increase in only 7 of the twelve microRNAs tested.(257) Interestingly, another study examining the effects of

exoribonuclease degradation on miR-382 levels, demonstrated that knockdown of ExoSC4 by shRNA affected miR-382 abundance, while knockdown of XRN-2 had no measurable differences.(256) These interesting and differing effects lead one to conclude that different microRNAs are likely targeted by distinct nucleases for decay.

Mature microRNA abundance may also be reduced at the post-transcriptional level by regulated cellular export.(259, 260) Exosomes are small lipid vesicles, with bilayer membranes, that encapsulate many different RNAs, proteins, lipids, and microRNAs. Exosomes are derived from the endo-lysosomal pathway, and are actively secreted from a wide variety of cell types. Formation of exosomes begins with the incorporation of endosomes into multivesicular bodies and this process is dependent on the activity of neutral sphingomyelinase 2 (nSMase2).(261, 262) Cellular secretion of exosomes occurs following fusion of the multivesicular body with the plasma membrane.(263)

Accordingly, this set of investigations will seek to determine a mechanism responsible for the tension induced reduction of miR-133a in aortic fibroblasts by focusing on three major pathways of microRNA regulation, transcriptional regulation, degradation, or regulated cellular export.

RESULTS

Mechanical tension does not reduce transcription of miR-133a in thoracic aortic fibroblasts.

To determine the mechanism of tension-induced loss of mature miR-133a, primary (pri-) miR-133a transcript levels (pri-miR-133a-1 and pri-miR-133a-2) were measured in isolated aortic fibroblasts following biaxial cyclic stretch. The expression of pri-miR-133a-1 did not change in response to mechanical stretch (1.14±0.33 vs 1.0±0.26 fold; p=0.62 vs control; n=8) (Figure 3.1 **A**), while the expression of pri-miR-133a-2 increased in response to stretch (2.0±0.44 vs 1.0±0.21 fold; $p<0.05$ vs control; n=8) (Figure 3.1 **B**). The results suggested that the tension-induced loss of mature miR-133a occurred post-transcriptionally.

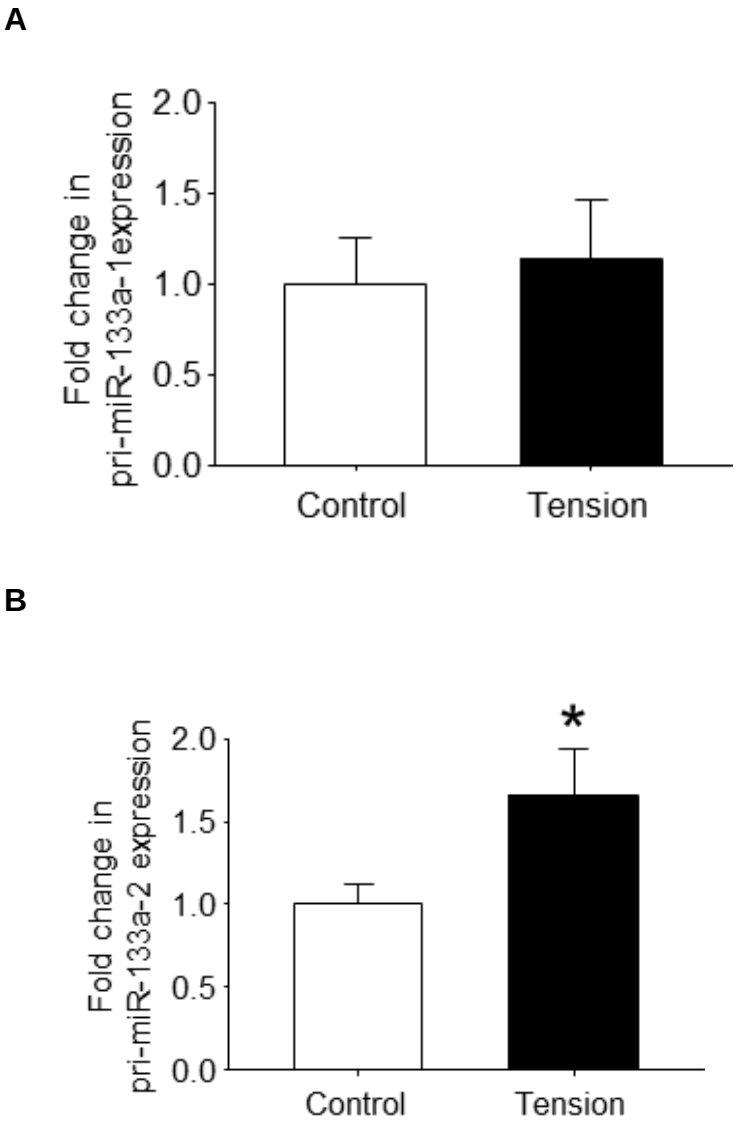

Figure 3.1. Mechanical tension and transcription of pri-miR-133a-1 and pri-miR-133a-2. Total RNA was isolated from each individual cell line, and primary-miR-133a levels were determined by real-time PCR. (**A**) Pri-miR-133a-1 expression levels in aortic fibroblasts exposed to 12% biaxial cyclic stretch (Tension, n=8) or held static (Control, n=8) for three hours. (**B**) Pri-miR-133a-2 expression levels in aortic fibroblasts exposed to 12% biaxial cyclic stretch (Tension, n=8) or held static (Control, n=8) for three hours. Data are represented as mean ± SEM. Comparisons were made using a two-sample t-test (unpaired, two-tailed). * $p<0.05$ vs. control.

Increased mechanical tension does not alter the expression or abundance of microRNA specific exoribonucleases in thoracic aortic fibroblasts.

While mature microRNAs are not likely substrates for most endoribonucleases, (255, 264) they do possess unprotected 5' and 3' ends making them susceptible to degradation by specific exoribonucleases.(253, 256) Three exoribonucleases that are capable of degrading microRNAs have been identified, XRN-1(258), XRN-2 (257, 258), and ExoSC4 (256). To examine whether mechanical tension induced these exoribonucleases, the mRNA expression and protein levels of XRN-1, XRN-2, and ExoSC4 were measured in isolated aortic fibroblasts following biaxial cyclic stretch. Neither the mRNA expression nor protein abundance of these exoribonucleases were changed compared to static fibroblasts; XRN-1 mRNA: 1.44±0.29 vs 1.0±0.47 fold, n=9, p=0.197 (Figure 3.2 **A**); XRN-1 protein: 0.86±0.14 vs 1.0±0.17 fold, n=9, p=0.555 (Figure 3.2 **B**); XRN-2 mRNA: 0.82±0.08 vs 1.0±0.42 fold, n=9, p=0.286 (Figure 3.3 **A**); XRN-2 protein: 0.93±0.29 vs 1.0±0.18 fold, n=5, p=0.851 (Figure 3.3 **B**); ExoSC4 mRNA: 0.70±0.07 vs 1.0±0.20 fold, n=9, p=0.166 (Figure 3.4 **A**); ExoSC4 protein: 1.0±0.09 vs 1.0±0.10 fold, n=5, p=0.992 (Figure 3.4 **B**). These findings suggest that the tension-induced loss of miR-133a in fibroblasts was not mediated by the rapid degradation of mature miR-133a.

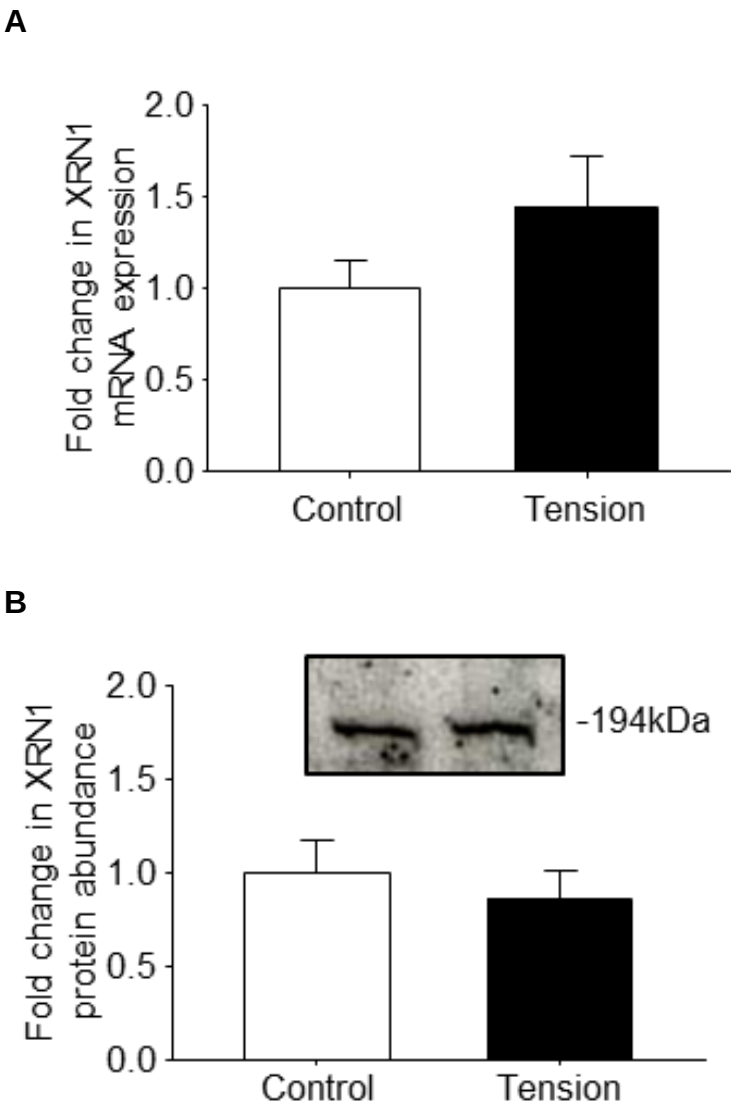

Figure 3.2. Mechanical tension and XRN1 mRNA expression and protein abundance. Total RNA or protein was isolated from each independent cell line and examined by real-time PCR or Western blotting, respectively. (A) XRN1 mRNA expression levels in aortic fibroblasts exposed to 12% biaxial cyclic stretch (Tension, n=9) or held static (Control, n=9) for three hours. (B) XRN1 protein abundance and representative immunoblot in aortic fibroblasts exposed to 12% biaxial cyclic stretch (Tension, n=5) or held static (Control, n=5) for three hours. Data are represented as mean ± SEM. Comparisons were made using a two-sample t-test (unpaired, two-tailed). No significant differences were observed vs. control.

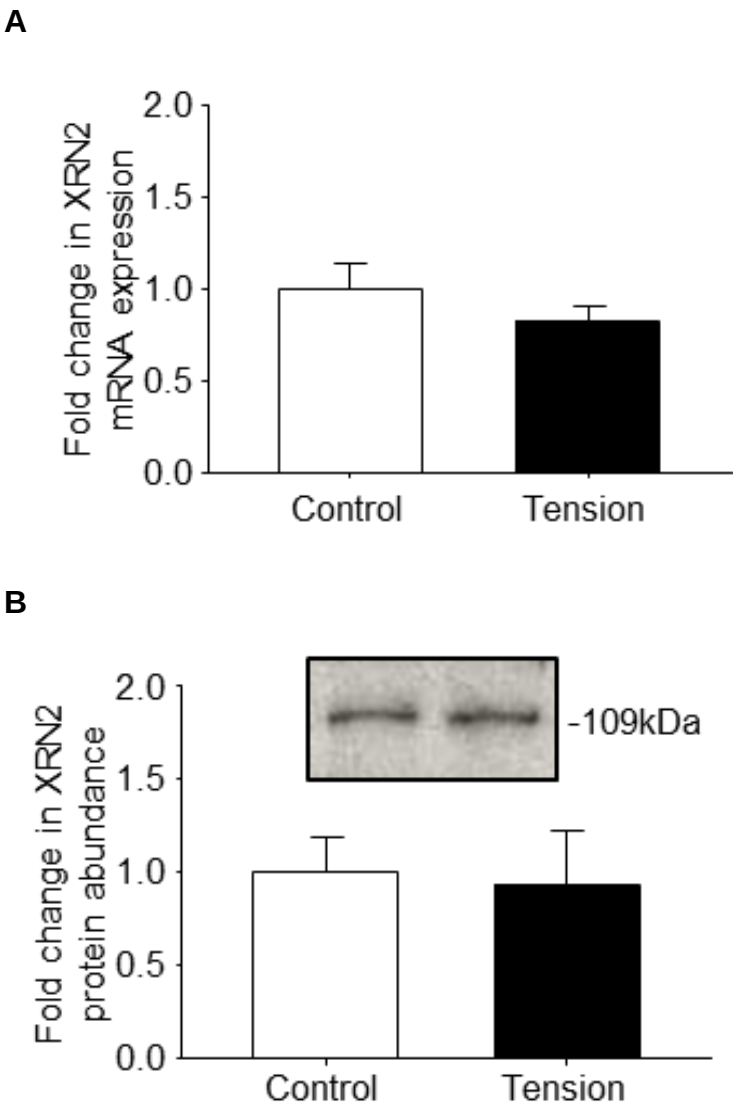

Figure 3.3. Mechanical tension and XRN2 mRNA expression and protein abundance. Total RNA or protein was isolated from each independent cell line and examined by real-time PCR or Western blotting, respectively. (A) XRN2 mRNA expression levels in aortic fibroblasts exposed to 12% biaxial cyclic stretch (Tension, n=9) or held static (Control, n=9) for three hours. (B) XRN2 protein abundance and representative immunoblot in aortic fibroblasts exposed to 12% biaxial cyclic stretch (Tension, n=5) or held static (Control, n=5) for three hours. Data are represented as mean ± SEM. Comparisons were made using a two-sample t-test (unpaired, two-tailed). No significant differences were observed vs. control.

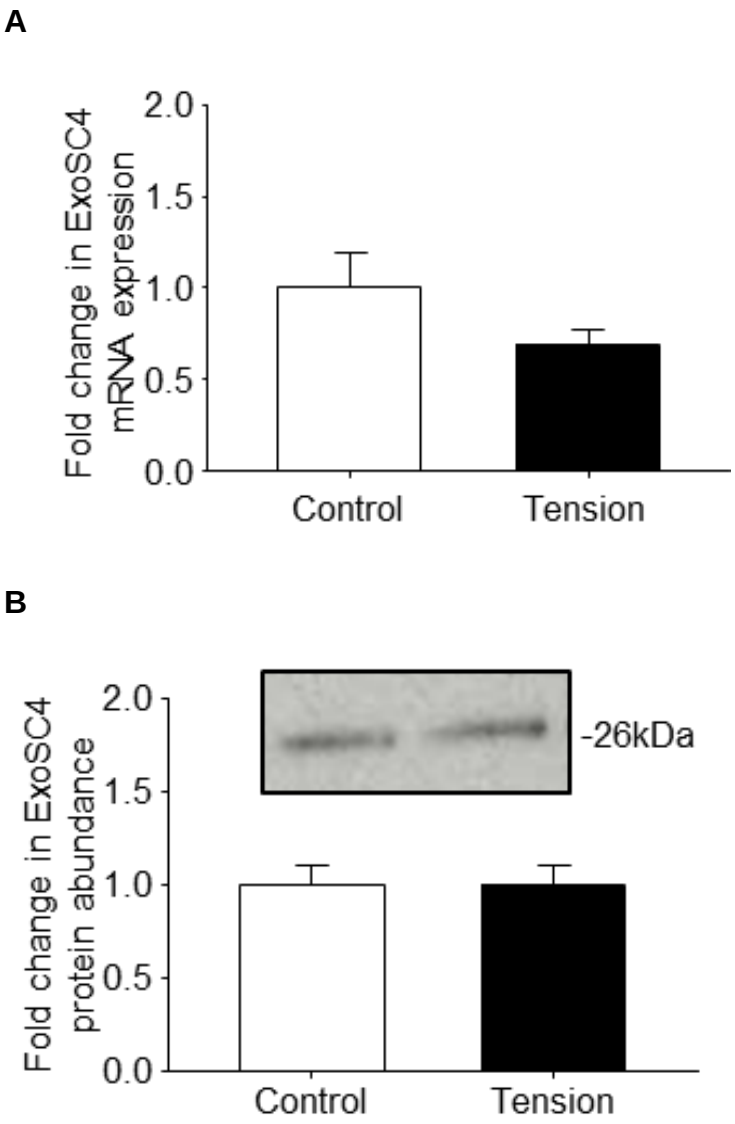

Figure 3.4. Mechanical tension and ExoSC4 mRNA expression and protein abundance. Total RNA or protein was isolated from each independent cell line and examined by real-time PCR or Western blotting, respectively. (A) ExoSC4 mRNA expression levels in aortic fibroblasts exposed to 12% biaxial cyclic stretch (Tension, n=9) or held static (Control, n=9) for three hours. (B) ExoSC4 protein abundance and representative immunoblot in aortic fibroblasts exposed to 12% biaxial cyclic stretch (Tension, n=5) or held static (Control, n=5) for three hours. Data are represented as mean ± SEM. Comparisons were made using a two-sample t-test (unpaired, two-tailed). No significant differences were observed vs. control.

A Prologue to Extracellular Vesicles

First described in 1985, extracellular vesicles have since become a topic of growing interest. Initially studied in blood cells, it was known that reticulocyte maturation into mature erythrocytes required the rapid loss (<24 hours) of the transferrin receptor; however, this receptor was not reduced by degradation, as the full, un-cleaved receptor was able to be recovered from culture media.(265-267) Pan *et al.* demonstrated that reticulocyte maturation required the shedding of the cellular component, transferrin, via vesicle secretion in order to differentiate into a mature erythrocyte.(268, 269) Since this observation, a wide variety of cellular components were discovered to be encapsulated within these vesicles and secreted from many different cell types in normal and pathological conditions. Importantly, in 2008, it was discovered extracellular vesicles contain microRNAs.(260) While the destiny of extracellular vesicles is currently under debate, it has long since been recognized that a function of vesicle secretion is to export cellular components allowing for elimination. This is an especially important mechanism during cellular transformation when relatively stable molecules must be removed to optimize new function.(270)

Two classes of extracellular vesicles have been described; microvesicles and exosomes, and each have distinct biogenesis pathways. (**Figure 3.5**) Microvesicles are lipid bilayer vesicles, approximately 100-1000nm in diameter and form by outward budding of the plasma membrane and subsequent fission resulting in release. During abscission, the molecule ARF6 facilitates the trafficking of lipid rafts in the plasma membrane, regulating contractile machinery

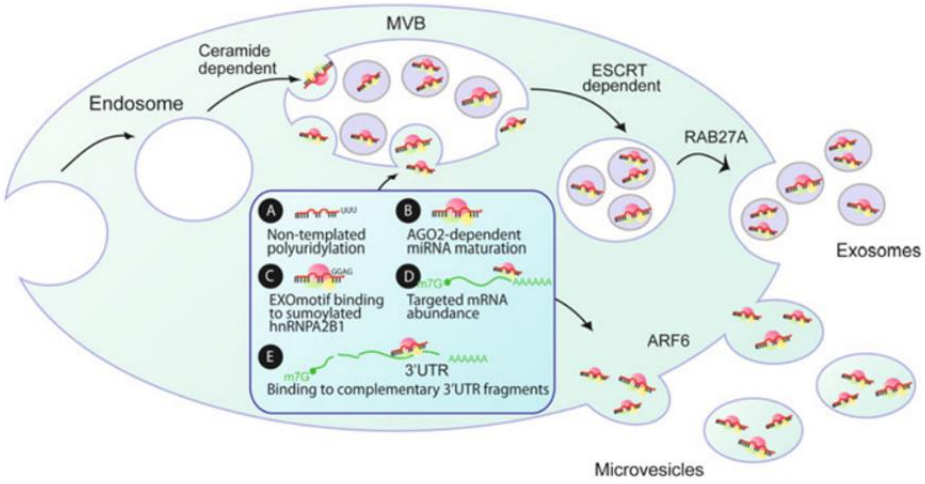

Figure 3.5. Classes of extracellular vesicles. A summary of extracellular vesicle biogenesis. While microRNAs are incorporated in both microvesicles and exosomes, production of each vesicle type by cells is distinct. Microvesicles are generated on the cell surface and are formed through the outward budding of the plasma membrane. Exosomes are formed via a regulated and ceramide dependent mechanism by incorporation of endosomes into a mutivecicular body then shuttling to the cell surface and subsequent release. A-E are the different forms in which microRNAs may be found within extracellular vesicles. Reproduced with permission from Springer. License ID: 4127100107596.

within the cleavage furrow, drawing the opposing membrane together before pinching off and shedding into the extracellular space.(271, 272) Exosomes are lipid bilayer vesicles approximately 30-100nm in diameter and originate from the endo-lysosomal pathway when multivesicular bodies fuse with the plasma membrane. Exosomes are released from cells through a ceramide-dependent secretory pathway.(273) The release of Ceramide from sphingomylinin is regulated by neutral sphingomylenase 2 (nSMase2), which regulates the formation and packaging of exosomes within the multivesicular body.(261)

Exosomes are released into the extracellular space upon fusion with the plasma membrane, which is mediated by GTPases, such as RAB27a.(274)

The ceramide dependent microRNA cargo sorting mechanism of exosomes is far better understood than that of microvesicles. Kosaka *et al.* found that overexpression of nSMase2 increased ceramide and the amount of exosomal microRNAs, while knockdown of nSMase2 by siRNA reduced exosomal microRNAs.(262) Furthermore, it is believed that exosome packaging and sorting is far more specific than that of microvesicles, which is a process that is not fully understood.(263) Therefore, this set of investigations will focus specifically on the exosome pathway as a possible mechanism for the reduction of cellular miR-133a.

Mechanical tension induces exosome secretion of miR-133a.

To determine the effects of stretch on exosome secretion, fibroblasts were exposed to biaxial cyclic stretch for 18 hours in media containing exosome depleted fetal bovine serum. Following stretch, the media was collected and the newly secreted exosomes were precipitated. Acetylcholinesterase (AChE) is enriched in the lipid bilayer membrane of exosomes,(269, 275, 276) allowing the measurement of AChE activity to be used as a surrogate for the number of exosomes present (275, 277). Acetylcholinesterase activity was higher in exosomes precipitated from the media of fibroblasts exposed to stretch as compared to static control fibroblasts (1.27±0.04 vs 1.0±0.08 fold; $p<0.05$; $n=8$)

(Figure 3.6 **A**). Furthermore, the abundance of miR-133a was increased in the exosomes collected from the fibroblasts exposed to stretch when compared to static control (1.65±0.28 vs 1.0±0.12 fold; $p<0.05$; $n=7$) (Figure 3.6 **B**). These results demonstrated that stretch induces exosome secretion of miR-133a in TA fibroblasts.

A

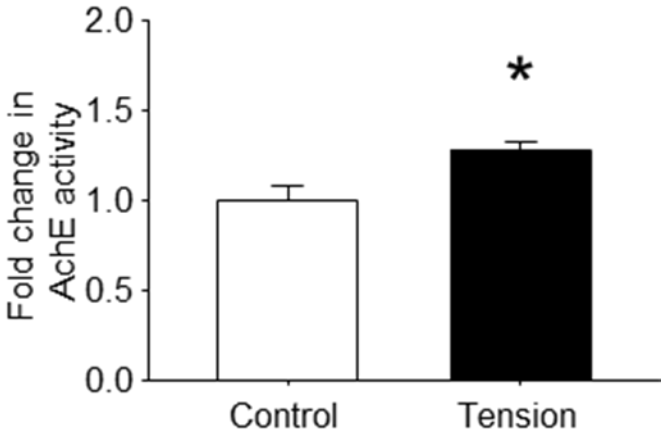

B

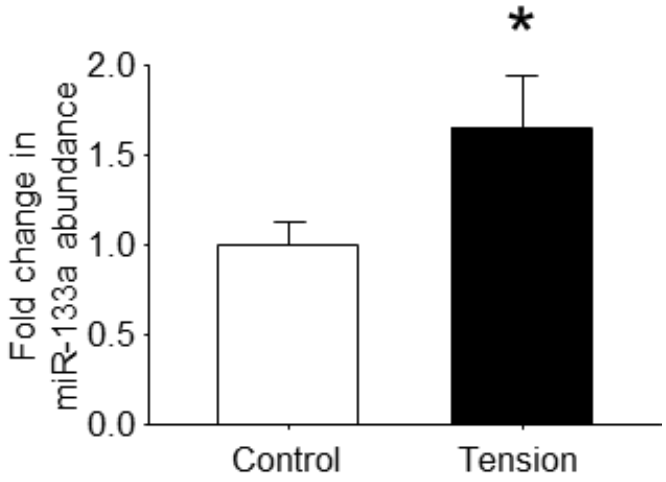

Figure 3.6 Mechanical tension and exosome secretion. Exosomes were precipitated from conditioned culture media from each fibroblast line. (**A**) Acetylcholinesterase (AChE) activity was quantitated as a measure of exosome number from each fibroblast line exposed to 12% biaxial cyclic stretch (Tension, n=8) or held static (Control, n=8) for 18 hours. (**B**) MiR-133a abundance in exosomes precipitated from the conditioned media of each fibroblast cell line exposed to 12% biaxial cyclic stretch (Tension, n=7) or held static (Control, n=7) for 18 hours. Data are represented as mean ± SEM. Comparisons were made using a two-sample t-test (unpaired, two-tailed). * $p<0.05$ vs. control.

The secretion of exosomes is dependent upon the formation of the sphingolipid ceramide.(261) Neutral sphingomyelinase 2 (nSMase2), regulates the abundance of ceramide by mediating its release from sphingomyelin.(278, 279) Inhibition of nSMase2 with the use of a well-describe non-competitive inhibitor (GW4869) has been demonstrated to prevent the secretion of exosomes.(261, 280-282) Accordingly, to demonstrate that stretch-induced secretion of miR-133a was mediated by exosome secretion, fibroblasts were exposed to stretch in the presence of GW4869. Inhibition of exosome formation prevented the stretch-induced secretion of miR-133a; no change in cellular miR-133a levels were observed with GW4869 as compared to static control (1.02±0.35 vs 1.0±0.29 fold; p=0.52, n=8) (Figure 3.7). Taken together, these studies suggest that one mechanism by which miR-133a is lost in response to elevated mechanical tension is through increased packaging and release of miR-133a in exosomes.

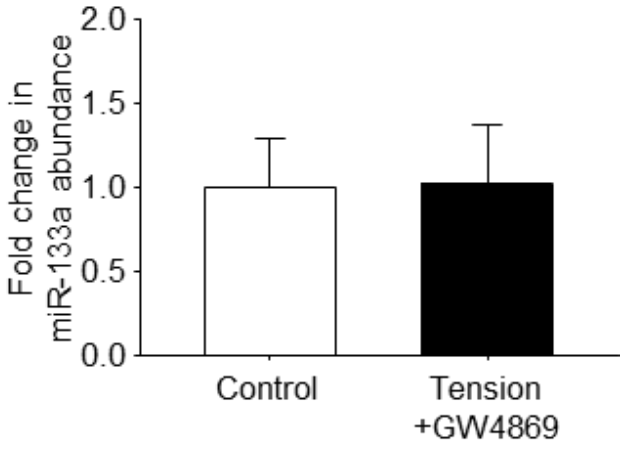

Figure 3.7 Mechanical tension and exosome secretion of miR-133a. Aortic fibroblasts were isolated from the descending aortae from C57BL/6 mice and exosome secretion was inhibited with GW4869. miR-133a abundance was quantitated in each aortic fibroblast line following exposure to 3 hours of 12% biaxial cyclic stretch in the presence of 20uM GW4869 (Tension+GW4869, n=8) or held static (control, n=8). Data are represented as mean ± SEM. Comparisons were made using a two-sample t-test (unpaired, two-tailed). No significant differences were observed vs. control.

SUMMARY

There is growing evidence focusing on the significance of microRNA export via exosomes.(283) Therefore, the effect of mechanical tension on exosome secretion of miR-133a was examined in isolated aortic fibroblasts. Acetylcholinesterase activity was demonstrated to be increased in the precipitated extracellular vesicles from the media of fibroblasts exposed to cyclic stretch. This finding may suggest either an increase in extracellular vesicle number or size. Nevertheless, more miR-133a was detected in the extracellular vesicles collected from the media of fibroblasts exposed to stretch. Increasing

evidence suggests microRNAs are not randomly incorporated into extracellular vesicles,(284-286) and several reports have indicated that microRNA abundance within extracellular vesicles is altered in pathology.(287) In agreement with these previous studies, the present results suggest miR-133a may be preferentially incorporated into these vesicles and secreted from fibroblasts exposed to stretch.

Cargo sorting mechanisms to exosomes are far better understood than that of microvesicles, and one mechanism regulating the secretion of exosomes is a nSMase2-dependent pathway.(262) The effect of inhibiting nSMAse2 with the use of GW4869 (hydrochloride hydrate) prevented stretch-induced reduction of miR-133a from fibroblasts, confirming that exosomes are responsible for mediating secretion of miR-133a.

DISCUSSION

In the present study, we examined mechanisms capable of regulating miR abundance under conditions of elevated wall tension. Accordingly, three potential mechanisms capable of regulating the cellular abundance of miRs were examined. The unique findings of this set of investigations demonstrated that tension-dependent loss of miR-133a was primarily mediated through exosome formation and release. These results identified a specific tension-sensitive mechanism by which miR-133a was reduced in a specific aortic cell-type (fibroblasts) that plays a key role in adverse vascular remodeling.

We and others have demonstrated that mechanical tension is sufficient in altering transcription.(234, 235, 288) To determine if the reduction of miR-133a in aortic fibroblasts was due to reduced transcription, primary (pri-) microRNA-133a transcript levels were quantitated following the application of mechanical tension. Production of mature microRNAs begins with the synthesis of pri-microRNAs.(203) While multiple factors regulate transcription (e.g. transcription factors, binding of RNA polymerase II to the DNA, histone methylation), a reduction in mature microRNA abundance resulting from a decrease in transcription would be observed by the detection of reduced primary microRNA transcript levels. As miR-133a is transcribed from two separate locations within the genome, both pri-miR-133a-1 and pri-miR-133a-2 were examined. Although mechanical tension had no effect on pri-miR-133a-1 levels, it did induce an increase in pri-miR-133a-2 levels. This, however, was not sufficient to overcome the loss of total mature miR-133a observed. Therefore, it was concluded, that the tension induced reduction of mature miR-133a in fibroblasts was not a result of changes in transcription, suggesting that the reduction likely occurred post-transcriptionally.

One post-transcriptional mechanism responsible for decreasing mature miR levels includes degradation by ribonucleases. Mature microRNAs have 5' and 3' unprotected ends that render them accessible to specific exoribonucleases. Three known exoribonucleases capable of degrading miRs have been identified (XRN-1, XRN-2, and ExoSC4).(253, 256) While the exact

mechanisms involved in microRNA degradation are largely unknown, it has been demonstrated that the exoribonucleases facilitate the release of microRNAs from the RISC, followed by subsequent degradation.(253, 257) Interestingly, in these previous reports it was also demonstrated that degradation of the microRNAs by exoribonuclease activity did not appear to depend on sequence context. Nevertheless, rapid decay of microRNAs is a highly efficient mechanism in regulating cellular abundance.

Therefore, the effects of mechanical tension on these 3 exoribonucleases were examined. Results demonstrated that their mRNA expression and protein abundance remained unchanged in the presence of elevated mechanical tension. It remains unclear whether other mechanisms, such as regulated activation of XRN1, XRN2 or ExoSC4, may show mechanosensitivity, however additional studies would be warranted to examine that hypothesis. Nevertheless, these results suggested that rapid degradation of miR-133a was not likely mediated by a degradation pathway in response to elevated tension.

There is growing evidence focusing on the significance of microRNA export via exosome secretion.(283) The majority of recent literature surrounding exosome secretion focuses on the trafficking of exosomes and regulation of recipient cell activity through the transport of lipids, proteins, and nucleic acids; however, exosome secretion has also been identified as an efficient mechanism for the rapid reduction of cytoplasmic nucleic acids.(11) Therefore, the effect of mechanical tension on exosome secretion of miR-133a was examined in isolated

aortic fibroblasts. Acetylcholinesterase (AChE), which is widely produced outside of the nervous system by a variety of cell types, including fibroblasts (289), is enriched in the lipid bilayer membrane of exosomes,(269, 275, 276) therefore allowing for an estimation in the relative amount of exosomes by quantitation of AChE activity (275, 277). Following application of tension, AChE activity was increased in the precipitated exosomes isolated from the media of fibroblasts exposed to cyclic stretch, suggesting either an increase in exosome size or number. Nevertheless, when normalizing for the amount of AChE activity, more miR-133a was detected in the exosomes collected from the media of fibroblasts exposed to stretch, suggesting increased packaging as well as increased export. Evidence exists suggesting that microRNAs are not just randomly incorporated into exosomes,(284-286) and reports have indicated that microRNA content within exosomes is altered in pathologic conditions, such as cancer (287) and cardiovascular disease (290). In agreement with these previous studies, the present results suggest miR-133a may be preferentially incorporated into exosomes and secreted from fibroblasts exposed to elevated tension. One mechanism regulating the secretion of exosomes is a neutral sphingomyelinase-2 (nSMase2) dependent pathway.(262) The effect of inhibiting nSMAse2 with the use of GW4869 prevented the tension-induced reduction of miR-133a in fibroblasts, suggesting that secretion of exosomes containing miR-133a is a mechanism responsible for the rapid loss of miR-133a from aortic fibroblasts in the presence of elevated mechanical tension.

A wide variety of molecules are contained in exosomes, including proteins, lipids, nucleic acids, and microRNAs.(291) Current evidence supports the notion that microRNAs are actively sorted into exosomes; however, the regulating mechanisms responsible for selective incorporation are largely unknown. Goldie and colleagues performed a total RNA analysis on exosomal RNA content released from neuroblastoma cells and determined that the microRNAs comprise the largest proportion of small RNAs.(292) Furthermore, this study determined that the percentage of microRNAs in the total small RNA pool was higher in exosomes than in the parent cells, suggesting that microRNAs may be preferentially incorporated in exosomes. In support of this finding, Guduric-Fuchs et al. analyzed microRNA expression in a variety of cell lines and their respective derived exosomes and found a subset of microRNAs that were enriched in exosomes.(286) Specifically, it was determined that miRs -451, -150, -146a, -320c, -143, -720, -125a, -486, -149, and -2110 are preferentially incorporated in exosomes, while miRs -218, -15a, -140, -148b, -378, -16, -20a, -424, -18a, and let-7f are preferentially retained within the cell. Combined, these studies demonstrate that certain microRNAs are preferentially sorted to exosomes.

More recently, it has been identified that the abundance/profile of microRNAs within exosomes is altered in several pathologies. For example, Skog and colleagues identified increased miR-21 abundance in exosomes isolated from the plasma of patients with glioblastoma.(287) However, the

mechanisms mediating this preferential incorporation as well as the functional role this characteristic plays in pathology are largely unknown.

Several recent studies have begun to unravel the complex mechanisms involved in the selective shuttling of microRNAs into exosomes(293-296). Although the underlying mechanisms remain largely unknown, two different sorting pathways have been identified thus far. These pathways include a sequence dependent mechanism, requiring the presence of a sequence motif located in the 3' end of the microRNA itself, and the second pathway is dependent on interaction with certain proteins. (296-299)

Villarroya-Beltri and colleagues determined that when the heterogenous nuclear ribonucleoproteins (hnRNP) becomes sumoylated, it binds to a GGAG motif in the 3' portion of a microRNA sequence, initiating incorporation of microRNAs containing that specific sequence into exosomes.(293) This study further identified that two other hnRNP proteins, hnRNPA1 and hnRNPC, bind to microRNAs; however, the study was unable to determine any common binding motifs among the 3' sequences of the associated microRNAs confounding the specific targeting mechanisms involved. Alternatively, Kopper-Lalic and colleagues demonstrated that microRNAs possessing a 3' uridylated tail were preferentially incorporated in exosomes derived from B cells, while microRNAs with an adenylated 3' end were mainly present within the B cells.(294) While this study identified that 3' uridylation of microRNAs results in preferential incorporation in exosomes, a mechanism mediating the actual shuttling into the

exosome was not determined. Both the hnRNP dependent sorting mechanism, and the notion that microRNAs with a 3' uridylated end are preferentially incorporated in exosomes, implicates the 3' portion of the microRNA sequence as a possible sorting signal.

Several more recent studies have identified a possible correlation between specific proteins and exosomal incorporation of microRNAs. It is known that multivesicular bodies associate with components of microRNA effector complexes and this may be key in shuttling of microRNAs to exosomes.(295) First, an RNA binding protein, the Y-box Protein 1 (YBX1) has been identified to have the ability to regulate the incorporation of miR-223 into exosomes.(296) While these studies demonstrate the function of this interaction, all experiments were performed in a cell-free biochemical assay. Whether and to what degree this interaction occurs *in vivo*, and also if it occurs with other microRNAs, remains to be determined. Second, the Argonaute 2 (Ago2) protein, which is required for microRNA-mediated repression of translation by the RNA-induced silencing complex (RISC),(297) has been demonstrated to be associated with microRNAs in exosomes.(300, 301) Activation of the KRAS oncogene, which is largely involved in the regulation of cell division,(298) was demonstrated to activate the mitogen-activated protein kinase kinase/extracellular-signal-regulated kinase (MEK-ERK) pathway, inhibiting the sorting of Ago-2 associated microRNAs -100, -320a, and Let-7a into exosomes.(299) Thus, McKenzie and colleagues

established a molecular mechanism responsible for regulating the sorting of microRNA from the cytosol into exosomes.

In summary, specific sequences present in certain microRNAs may act in the incorporation of exosomes, while a possible sequence independent mechanism involving Ago2 may control sorting into exosomes. While the present work identified that miR-133a is reduced in thoracic aortic fibroblasts via exosome secretion, it remains to be determined if miR-133a is preferentially incorporated in exosomes by a tension sensitive mechanism involving any of the above mechanisms, and studies aimed at determining underlying mechanism responsible warrant future investigation.

LIMITATIONS

The present study is not without limitations. This study was limited to the investigation of the effects of tension on miR-133a only. While increasing evidence highlights the role miR-133a plays in maintaining tissue homeostasis, it is anticipated that the abundance of other microRNAs may also be altered with elevated tension, and therefore may have an overall effect on the phenotypic characteristics of resident cells or the development of pathology. Accordingly, we are unable to conclude whether tension-induced secretion of miR-133a in exosomes is limited to miR-133a, or is a characteristic of a specific group of miRs. Studies focused on the identification of tension-sensitive miRs may reveal

further insight as to overall effects of elevated tension. Furthermore, whether and to what degree the observed reduction in mature miR-133a has on the abundance of specific gene targets, as well as, the overall effect of miR-133a reduction on cellular phenotype are studies that warrant future investigation.

CONCLUSIONS

Alterations in microRNA (miR) abundance have been associated with multiple cardiovascular diseases, and while much effort has been directed toward understanding their role in modulating key cellular targets, less is known about how miR abundance is regulated within the cell.(212-218) Previously, it was identified that elevated tension results in the acute reduction of miR-133a in thoracic aortic fibroblasts (discussed in Chapter 2). Accordingly, three potential mechanisms capable of regulating the cellular abundance of miRs were examined. The unique results of this set of investigations have identified a specific tension-sensitive mechanism by which miR-133a was reduced in aortic fibroblasts through the packaging and secretion of exosomes. While the direct effects of *in vivo* wall tension on miR-133a abundance remains to be defined, these current findings may lead to the development of novel pharmacotherapies directed at inhibiting the secretion of miR-133a from aortic fibroblasts.

CHAPTER 4: Effects of hypertension on miR-133a levels

INTRODUCTION

Reduced miR-133a is associated with thoracic aortic (TA) dilation as seen in aneurysm disease. Since wall tension increases with vessel diameter (Law of Laplace), this study tested the hypothesis that hypertension results in the reduction of miR-133a in the TA. While, hypertension has been epidemiologically associated with aortic pathologies, such as thoracic aortic aneurysm(302), a biochemical relationship between increased wall tension and aortic remodeling has yet to be identified.

The previous *in vitro* studies have identified that mechanical tension is a stimulus driving the reduction of miR-133a in thoracic aortic fibroblasts via exosome secretion. While these data provided insights into a mechanism involved in this process, it remained to be determined whether these results could be recapitulated *in vivo.* Accordingly, the following studies utilize distinct murine models of hypertension for the further analysis of the effect of a physiologically relevant level of increased aortic wall tension on miR-133a levels.

Of significant relevance, detectable levels of circulating microRNAs are becoming a topic of increased interest.(303) Since the initial observation of circulating microRNAs in 2008, it has been suggested that their presence may serve as a possible biomarker for prognostic and diagnostic purposes related to the presence of cardiovascular disease. Furthermore, various pathological conditions have been shown to be associated with altered microRNA profiles in plasma. Importantly, this laboratory reported elevated plasma miR-133a levels associated with thoracic aortic aneurysm.(213) This study demonstrated that it was indeed possible to measure an analyte directly relevant to vascular remodeling in the plasma. While other analyte signatures were combined to most accurately predict the presence of an aortic aneurysm, miR-133a alone had significant specificity. It remained to be determined if elevated vessel wall tension was sufficient in altering circulating miR-133a levels.

In the following studies, increased vessel wall tension will be simulated *in vivo* utilizing two unique murine models of hypertension. As a potent vasoactive peptide, Angiotensin II (AngII) contributes to vasoconstriction to increase vascular wall tension (Discussed in Chapter 2); therefore, the first model of hypertension was induced *in vivo* utilizing a well-established AngII infusion model.(80, 236, 304) The second murine model of hypertension, is a commercially available hypertensive mouse that has been genetically selected (BPH2). In this mouse model, it has been demonstrated that hypertension is not the result of increased circulating levels of angiotensin, allowing for the comparison of two distinctly different causes of elevated tension. Accordingly,

the effects of tension will be examined on the TA tissue and plasma levels of miR-133a.

RESULTS

Increased vessel wall tension *in vivo* results in a reduction of thoracic aortic tissue miR-133a abundance.

Murine Blood Pressure

Two distinct murine models of hypertension were utilized to examine the effects of elevated aortic wall tension on miR-133a abundance *in vivo*. To demonstrate relative changes in mean arterial pressures (MAP), murine blood pressure measurements were obtained by tail-cuff using the CODA hemodynamic monitoring system from Kent Scientific. Mean arterial pressure in wild-type normotensive mice was determined to be 121.16±2.59 mmHg (normotensive, n=12). Normotensive mice were treated with Angiotensin-II (AngII, 1.44mg/kg/day) delivered by subcutaneous osmotic pump for 28 days.(305) This resulted in an increased MAP to 169.94±3.50 mmHg (AngII, n=12) ($p<0.05$ vs. normotensive) (Figure 4.1, and Table 4.1). Second, the effects of elevated wall tension on miR-133a abundance were examined in a spontaneously hypertensive mouse line (BPH2, genetically selected, angiotensin II-independent),(306) which displayed an elevated MAP of 159.67±2.97 mmHg (BPH2; $p<0.05$ vs normotensive, n=12) (Table 4.1 and Figure 4.1).

BLOOD PRESSURE	Systolic		Diastolic		MAP	
(mmHg)	Mean	Standard Deviation	Mean	Standard Deviation	Mean	Standard Deviation
Control (n=12)	148	9.76	108	9.08	121	8.97
AngII (n=12)	199	14.05	155	11.36	170	12.11
BPH2 (n=12)	187	9.38	146	11.06	160	10.30

Table 4.1. Murine blood pressure. Data are presented as mean and standard deviation of the systolic, diastolic and calculated mean arterial pressure (MAP) as determined by non-invasive tail cuff measurements in the three groups of mice utilized in these studies.

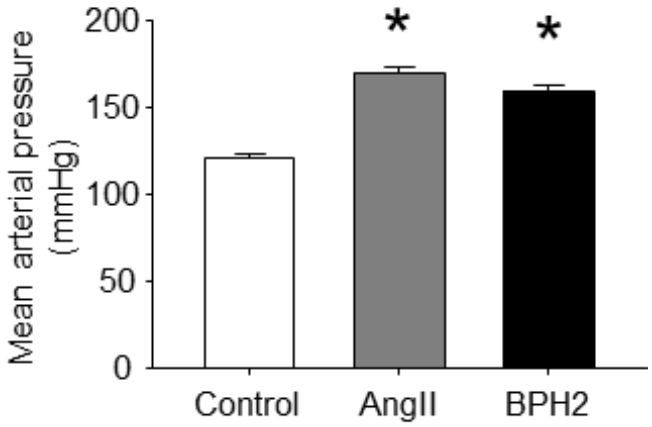

Figure 4.1. Mean arterial blood pressure and miR-133a levels in thoracic aortic tissue and plasma from two murine models of hypertension. Mean arterial blood pressure assessed by non-invasive tail cuff, in control mice (Control, n=12), Ang II-induced hypertensive mice (AngII, n=12), and spontaneously hypertensive mice (BPH2, n=12). Data are represented as mean ± SEM. Comparisons were made using a one-way ANOVA followed by pairwise comparison of means by Tukey's wholly significant difference (*wsd*) method. * $p < 0.05$ vs control.

Murine tissue and plasma miR-133a levels

The thoracic aortic tissue abundance of miR-133a was reduced in both the AngII-treated and the BPH2 mice when compared to normotensive controls (AngII: 0.69±0.06 fold, n=12, $p<0.05$ vs control; BPH2: 0.52±0.04 fold, n=16, $p<0.05$ vs control; control: 1.00±0.13, n=12) (Figure 6B). Plasma levels of miR-133a were assessed in both hypertensive mouse models. While miR-133a abundance was elevated in the plasma of the AngII-induced mice, they failed to reach statistical significance (1.80±0.64 fold, n=6, p=ns). However, miR-133a levels were significantly increased in the plasma of BPH2 mice (3.39±0.77 fold, n=8, $p<0.05$) as compared to normotensive control animals (1.0±0.41, n=6) (Figure 6C). Combined, these results demonstrated that miR-133a abundance is reduced in thoracic aortic tissue in response to elevated vessel wall tension. Moreover, circulating plasma levels of miR-133a were increased.

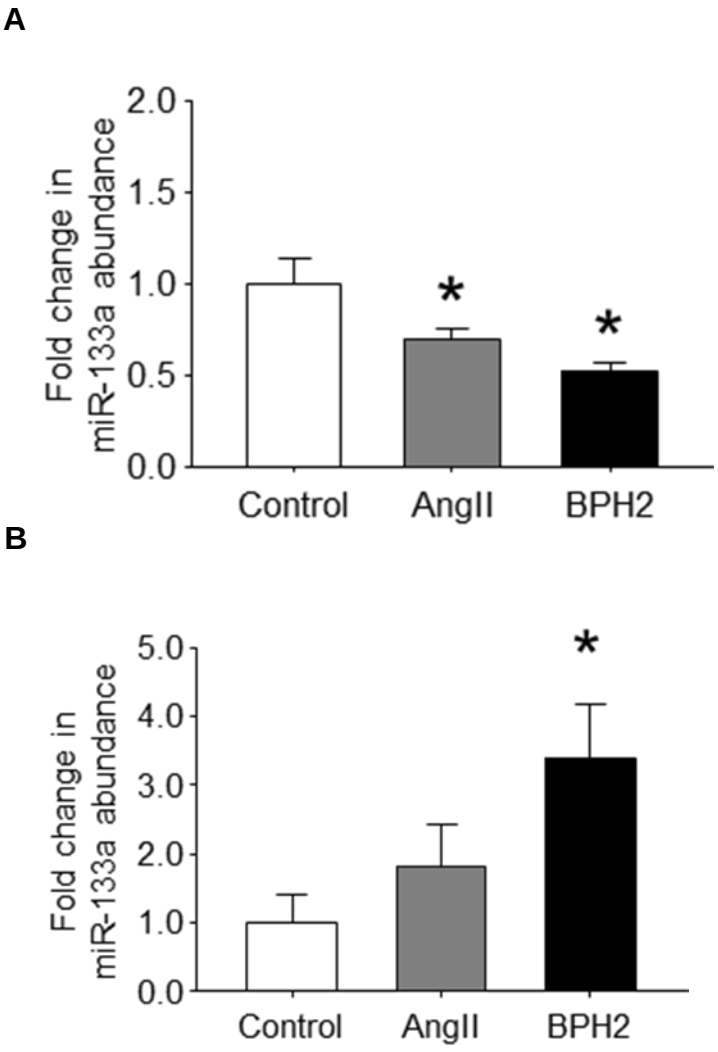

Figure 4.2 miR-133a levels in thoracic aortic tissue and plasma from two murine models of hypertension. (**A**) miR-133a abundance in thoracic aortic tissue from control mice (Control, n=12), Ang II-induced hypertensive mice (AngII, n=12), and spontaneously hypertensive mice (BPH2, n=16). (**B**) Plasma miR-133a abundance in control mice (Control, n=6), Ang II-induced hypertensive mice (AngII, n=6), and spontaneously hypertensive mice (BPH2, n=8). Data are represented as mean ± SEM. Comparisons were made using a one-way ANOVA followed by pairwise comparison of means by Tukey's wholly significant difference (*wsd*) method. * $p < 0.05$ vs control.

Circulating miR-133a abundance was increased in hypertensive patients.

The abundance of miR-133a was determined in plasma samples collected from patients previously diagnosed with hypertension and compared to normotensive controls (patient demographical information listed in Table 4.2). Blood pressure was measured at the time of blood draw, and the calculated MAP was determined to be elevated in the hypertensive patients as compared to a normotensive control group of patients never diagnosed with hypertension (97±6mmHg, n=11 vs 89±8mmHg, $p<0.05$, n=12) (Figure 4.3) (blood pressures listed in Table 4.2). Furthermore, circulating plasma levels of miR-133a were increased in the hypertensive group when compared to normotensive controls (1.55±0.26, n=11 vs 1.0±0.18 fold; $p<0.05$, n=12) (Figure 4.4). These results demonstrated that increased MAP resulted in elevated plasma levels of miR-133a.

	Normotensive (n=12)	Hypertensive (n=11)	p-value
Gender: male (%)	25	27	0.901
African American (%)	8	27	0.231
Age (years)	63±4	65±3	0.193
Heart Rate (BPM)	68±9	70±12	0.654
Body Surface Area (m^2)	1.76±0.26	2.03±0.18	0.009
Walk in 6 minutes (m)	396.8±51.4	386.6±45.3	0.620
Systolic Blood Pressure (mmHg)	122±9	131±9	0.026
Diastolic Blood Pressure (mmHg)	72±8	80±6	0.014
Mean Arterial Pressure (mmHg)	89±8	97±6	0.014

Table 4.2. Patent demographics. Demograpical information of patents included in these studies. Data are presented as a mean ± standard deviation. A Chi^2 analysis was performed on gender and ethnicities. For all other categories pairwise comparisons were made using two sample t-tests. All p-values are displayed.

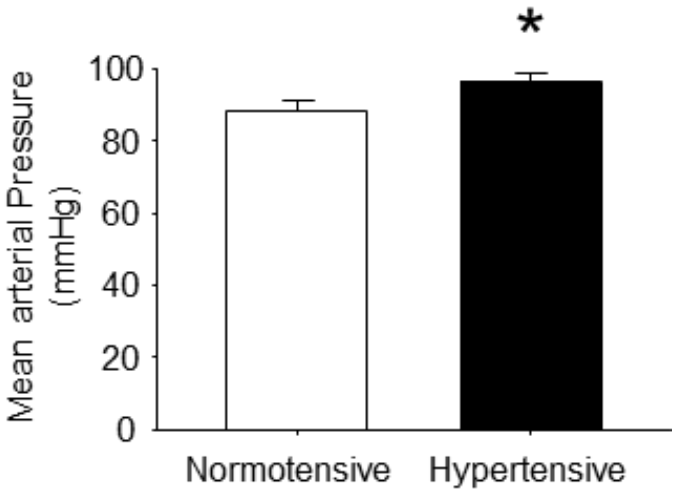

Figure 4.3. Mean arterial blood pressures. Patient mean arterial blood pressures assessed at time of plasma collection in Normotensive (n=12) and Hypertensive (n=11) patients. Data are represented as mean ± SEM. Comparisons were made using a two-sample t-test (unpaired, two-tailed). * $p<0.05$ vs. control.

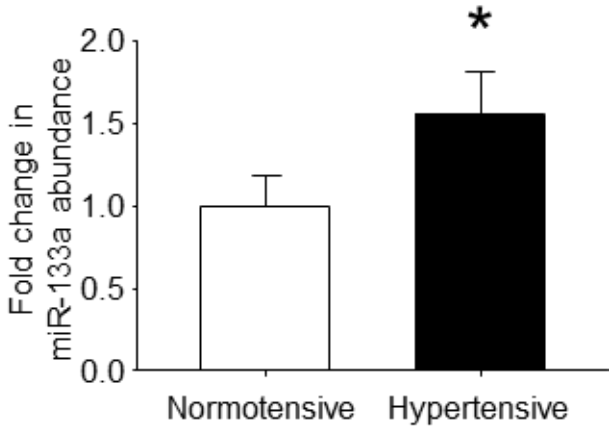

Figure 4.4. Plasma levels of miR-133a in clinical specimens. Plasma miR-133a abundance in normotensive (n=12) and hypertensive (n=11) patients. Data are represented as mean ± SEM. Comparisons were made using a two-sample t-test (unpaired, two-tailed). * $p<0.05$ vs. control.

SUMMARY

Two distinct murine models of hypertension were utilized to simulate increased aortic wall tension *in vivo*. In both murine models, elevated mean arterial blood pressures were confirmed and miR-133a was found to be reduced in thoracic aortic tissue. Circulating miR-133a was increased in the plasma of the BPH2 hypertensive mice. Finally, in clinical plasma samples from hypertensive patients, circulating miR-133a was elevated when compared to the non-hypertensive control group.

DISCUSSION

In order to examine the physiological relevance of the effects of mechanical tension on miR-133a levels, a clinically relevant form of increased vessel wall tension *in vivo* were examined on the aortic tissue levels of miR-133a. For this approach, two unique murine models of hypertension were utilized. As a potent vasoactive peptide, AngII contributes to vasoconstriction to alter vascular wall tension; accordingly in the first *in vivo* model, hypertension was induced by delivering AngII by osmotic pump infusion.(80, 236, 304) The second *in vivo* model of increased wall tension is a commercially available, hypertensive mouse line (BPH2). In this murine hypertensive model, it has been reported that hypertension is angiotensin-independent, through the observation of low circulating angiotensin-I levels in these mice.(307) In both murine models, elevated mean arterial blood pressures were confirmed compared to wild-type

mice and as anticipated, miR-133a was found to be reduced in the tissue of the descending thoracic aorta. In a similar study performed by Castoldi and colleagues, hypertension was induced in Sprague-Dawley rats by treatment with AngII via implanted osmotic pump. Following 4 weeks of induced hypertension, the levels of miR-133a were assessed in myocardial tissue and in similar fashion, miR-133a abundance was reduced. While Castoldi and colleagues were able to inhibit the loss of miR-133a with an AngII receptor blocker, irbesartan, they were unable to determine whether this effect was mediated, entirely or in part, by AngII signaling or by elevated mechanical tension.(221) Our study examined the effect of biaxial cyclic stretch on isolated aortic cells (fibroblasts and SMCs) in the absence or presence of AngII, and demonstrated that the effects of mechanical tension were fibroblast-specific and independent of AngII stimulation. Accordingly, when we examined these effects *in vivo* we were not surprised that miR-133a was reduced in the thoracic aorta of both the AngII -dependent and -independent models of hypertension. Moreover, both models of murine hypertension displayed increased plasma levels of miR-133a. While statistical significance was reached only in the BPH2 model, this may have been due to the time difference in exposure to elevated blood pressures. Whereas the AngII model of hypertension was initiated when the animals were 10 weeks of age, and allowed to continue for 4 weeks, the spontaneously hypertensive BPH2 mice were 12-14 weeks of age when examined, and had likely experienced elevated blood pressure since 5 weeks of age.(308) Nevertheless, in both murine models of hypertension, miR-133a was reduced in TA tissue, and this finding was

associated with increased circulating levels of miR-133a, demonstrating tension has a profound effect on the levels of this mechanically sensitive miR.

Taken together, these findings led us to the question of whether this effect could be observed in hypertensive patients. Accordingly, miR-133a was measured in the plasma of patients that had documented hypertension and left ventricular hypertrophy. The results of this study demonstrated that plasma levels of miR-133a were increased in hypertensive patients when compared to a normotensive group. Our results were supported by previous findings demonstrating increased circulating levels of miR-133a in patients with unstable angina pectoris, takotsubo cardiomyopathy, acute myocardial infarction,(309) and thoracic aortic aneurysm,(213) suggesting that elevated circulating levels of miR-133a are associated with the presence of cardiovascular disease. While hypertension is a known risk factor for many cardiovascular disease states, the molecular mechanisms involved in this relationship remain poorly understood, and the current findings may provide a valuable link.

Following transcription and subsequent processing, mature microRNAs are incorporated into the RNA-induced silencing complex, which directs the microRNA to the target mRNA,(310) resulting most commonly in translational repression.(237) Therefore, reduction in miR abundance would permit elevated protein translation of the targeted gene transcripts. A role of miR-133a in mediating matrix production has been demonstrated in cultured fibroblasts through the targeted repression of the TGF-β and TGF-βRII signaling cascade

that promotes production and deposition of collagens related to the development of fibrosis.(219) Furthermore, there is increasing evidence that miR-133a may play a role in the determination of cellular phenotype, such as proliferation and migration,(222, 311) and it is known that miR-133a levels alter key proteins which are highly expressed in the tissue associated with adverse aortic remodeling. For example, miR-133a directly targets and reduces the abundance of the membrane type-1 matrix metalloproteinase (MT1-MMP).(222, 243) This membrane bound proteolytic enzyme is known to contribute to both degenerative extracellular matrix remodeling, as well as matrix production through the activation of the TGF-β pathway.(192) Furthermore, using MT1-MMP overexpressor and knockout mice, Spinale and colleagues demonstrated that MT1-MMP is a direct effector of cardiac fibrosis.(312) Moreover, it has been demonstrated that MT1-MMP is elevated throughout thoracic aortic aneurysm development in both clinical specimens (186, 192) and mouse models of TAA.(188, 192) While the direct effects of tension-induced changes in miR-133a abundance, and its effect on adverse aortic remodeling remains to be defined, these current findings highlight the importance in managing elevated blood pressure, and may lead to the development of novel pharmacotherapies directed at inhibiting the secretion of miR-133a from aortic fibroblasts.

LIMITATIONS

The present study is not without limitations. First, murine blood pressures were assessed using a non-invasive tail cuff system. This system routinely

reports systolic and diastolic pressures that contribute to a normotensive MAP of approximately 120 mmHg in the untreated wild-type control mice. While a MAP of this value would typically be considered hypertensive, these results are consistent with other investigators utilizing the CODA system for measuring murine blood pressure.(313, 314) Therefore, we assessed the relative difference between the groups of mice, and were able to determine a significant increase in the blood pressure measurements in both experimental models of elevated wall tension when compared to the normotensive controls. Second, while circulating levels of miR-133a were identified to be elevated in clinical plasma samples taken from hypertensive patients, the sample size of measurements was limited therefore caution should be exercised in data interpretation. Further studies must be undertaken in a larger number of samples to determine whether there is a linear correlation between pressure and miR-133a abundance. Lastly, it is important to note that all of the hypertensive patients in this study were actively being treated with anti-hypertensive agents at the time their blood was collected. In spite of this, their blood pressures, as well as their plasma levels of miR-133a, were still significantly elevated as compared to the non-hypertensive control group. This may suggest that the amount of wall tension associated with the current suggested therapeutic blood pressure target is still sufficiently high to result in the elevated release of miR-133a. Furthermore, circulating miR-133a levels may be used to better refine therapeutic blood pressure control. Additional studies examining its use in this regard are warranted.

CONCLUTIONS

By investigating the tension-induced reduction of miR-133a, the current studies identified hypertension as a stimulus driving the loss of mature miR-133a in thoracic aortic tissue. These data lend support to the hypothesis that as blood pressure increases, tension on the aortic wall increases, and cellular miR-133a abundance is reduced in fibroblasts via exosome secretion. This may have significant implications regarding early aortic wall remodeling in response to uncontrolled hypertension. Taken together, the results of this set of investigations have identified a specific tension-sensitive mechanism by which miR-133a was reduced in thoracic aortic tissue, and elevated in plasma. These data hold significance with regard to the potential advancement in understanding the role of miR-133a in the regulation of adverse thoracic aortic remodeling.

CHAPTER 5: Conclusions and Clinical Significance

The results presented in the body of this work demonstrated that increased tension results in the loss of miR-133a from aortic fibroblasts by a mechanism involving exosome secretion. Furthermore, results demonstrate that miR-133a levels are reduced in the thoracic aortas of mice with increased vessel wall tension, and that increased circulating levels of miR-133a were detected in hypertensive mice. This observation has clinical relevance since miR-133a was also found to be elevated in the plasma of hypertensive patients. This study is the first to document increased vessel wall tension as a stimulus through which miR-133a is reduced in thoracic aortic tissue.

Following transcription and subsequent maturation, mature microRNAs are incorporated into the RNA-induced silencing complex, which directs the microRNA to the target mRNA,(310) resulting most commonly in translational repression.(237) Loss in mature microRNA abundance would allow for increased translation of targeted gene transcripts. There is increasing evidence that miR-133a plays a role in the determination of cellular phenotype, such as proliferation

and migration,(222, 311) and it is known that miR-133a levels alter key proteins which are highly expressed in the tissue associated with adverse aortic remodeling. For example, miR-133a directly targets the membrane type-1 matrix metalloproteinase (MT1-MMP).(222, 243) This proteolytic enzyme is known to contribute to degenerative extracellular matrix remodeling and is elevated throughout TAA development in clinical specimens (186) and mouse models of TAA.(188) Furthermore, miR-133a has been demonstrated to regulate vascular remodeling *in vivo,*(214) which underscores the significance in identification of regulatory mechanisms.

A previous report demonstrated vessel wall tension affects gene expression profiles of several matrix metalloproteinases in thoracic aortic tissue through the induction of promoter activity.(235) The present study built upon these previous findings by demonstrating an alternative pathway affected by mechanical tension. This report is the first to identify that increased tension alone affects the abundance of mature miR-133a in thoracic aortic tissue. Further exploration of the two major cell types of the aorta identified that biaxial cyclic stretch led to the reduction of miR-133a from fibroblasts while SMCs were not responsive. Interestingly, in another study, mechanical stretch was demonstrated to not have an effect on the level of miR-133a.(315) Combined with the results from this study, stretch induced reduction of miR-133a appears to be cell type specific.

Fibroblasts have been identified as a cell type that is sensitive to mechanical tension and subject to undergo changes, taking on “synthetic” or mobile characteristics. Once altered, these fibroblasts become known as myofibroblasts. In pathological vascular remodeling, these synthetic fibroblasts become activated in the adventitia, and migrate inward disrupting the extracellular matrix and increase vessel stiffness.(167) Combined with previous studies which have demonstrated aortic dilation is accompanied by the apoptotic loss of SMCs,(248) it is believed that the fibroblasts may be a key cellular mediator contributing to aortic remodeling.(195) Of significant relevance, a single microRNA is capable of targeting multiple mRNAs; therefore, alterations in the abundance of one microRNA may result in changes of multiple targeted proteins. Therefore, tension induced loss of miR-133a from fibroblasts may predispose patients to adverse thoracic aortic remodeling.

While hypertension is a known risk factor for aortic dilation and aneurysm formation, the molecular mechanisms involved in this relationship remain poorly understood. Not only do patients diagnosed with essential hypertension have high circulating levels of AngII,(246) it is also a known vasoconstrictor, therefore the effects of this vasoactive peptide was investigated on miR-133a levels. By mounting aortic rings on parallel wires in an *ex vivo* tissue myograph and adding AngII, it was determined that AngII induced vessel contraction resulting in elevated wall tension and a loss of miR-133a. Importantly, when investigations continued by proceeding to *in vitro* AngII stimulation of isolated fibroblasts and

SMCs, no effect on miR-133a abundance was detected. These findings led to the conclusion that the AngII effects on miR-133a in aortic tissue was not due to AngII receptor mediated signaling, but was likely the result of vessel contraction, leading to increasing tension on the endogenous fibroblasts.

To identify if transcriptional regulatory mechanisms of mature miR-133a were altered with mechanical tension, primary (pri-) miR-133a transcript levels were assessed. Production of microRNAs begins with the synthesis of pri-microRNAs.(203) A reduction in mature microRNA abundance resulting from a decrease in transcription would be observed by the detection of reduced primary microRNA transcript levels. Although mechanical tension had no effect on pri-miR-133a-1 levels, tension appeared to increase pri-miR-133a-2 levels, suggesting an increase in transcription with tension application. Combined with the observation of decreased mature miR-133a abundance, this association may suggest mechanical tension could lead to other defects in miR-133a processing, to be examined in future investigations.

Other cellular mechanisms leading to decreased mature microRNA levels include degradation by microRNA specific ribonucleases. Mature microRNAs have 5' and 3' unprotected ends that render them accessible to specific ribonucleases. Three known microRNA specific ribonucleases have been identified (XRN-1, XRN-2, and ExoSC4).(253, 256) Therefore, the effects of mechanical tension on these 3 ribonucleases were examined. While the mRNA expression and protein abundance remained unchanged for the ribonucleases,

other mechanisms of activation, for example phosphorylation, were not investigated. While it is unclear whether mechanisms of activation of XRN1, XRN2 or ExoSC4 may play a role in determining mature microRNA abundance, investigations in alternative pathways may warrant future investigations.

There is growing evidence focusing on the significance of microRNA export via extracellular vesicles.(283) Therefore, the effect of mechanical tension on extracellular vesicle secretion of miR-133a was examined in isolated aortic fibroblasts. The activity of acetylcholine esterase, which is enriched in the plasma membrane of extracellular vesicles, was demonstrated to be increased in the precipitated extracellular vesicles from the media of fibroblasts exposed to cyclic stretch. This finding may suggest either an increase in extracellular vesicle number or an increase in size. Nevertheless, more miR-133a was detected in the extracellular vesicles collected from the media of fibroblasts exposed to stretch. Increasing evidence suggests microRNAs are not randomly incorporated into extracellular vesicles,(284-286) and another report has indicated that microRNA abundance within these vesicles is altered in pathology.(287) In agreement with these previous studies, the present results suggest miR-133a may be preferentially incorporated into exosomes and secreted from fibroblasts exposed to stretch.

Cargo sorting mechanisms of exosomes are far better understood than that of microvesicles, and one mechanism regulating the secretion of exosomes is an nSMase2-dependent pathway.(262) The effect of inhibiting nSMAse2 with

the use of GW4869 (hydrochloride hydrate) prevented tension induced reduction of miR-133a from fibroblasts, confirming that the nSMase2-dependent pathway is responsible for mediating secretion of exosomes containing miR-133a.

Investigations continued by examining a clinically relevant form of increased vessel wall tension on miR-133a levels *in vivo*. For this, two unique murine models of hypertension were utilized. As a potent vasoactive peptide, AngII contributes to vasoconstriction to alter vascular wall tension; therefore, in the first model, hypertension was induced *in vivo* utilizing a well-established AngII infusion model.(80, 236, 304) The second *in vivo* model of increased wall tension is a commercially available, hypertensive mouse line (BPH2). In this murine hypertensive model, it has been reported that hypertension is angiotensin-independent, through the observation of low circulating angiotensin I levels in these mice.(14) In both murine models, elevated mean arterial blood pressures were confirmed and miR-133a was found to be reduced in the thoracic aorta. While circulating levels of miR-133a were increased in the plasma of both hypertensive mouse models, the levels in the BPH2 mice were the only to reach statistical significance by a one-way analysis of variance (ANOVA) followed by pairwise comparison using Tukey's method. This may be due to the comparison of an acute model of hypertension (AngII for 28 days) to a chronic hypertensive model (BPH2), and future studies investigating a longer delivery of AngII may provide interesting answers to the role of elevated tension on circulating levels of miR-133a.

Access to thoracic aortic tissue from hypertensive patients may provide further understanding; however, these studies were able to identify circulating miR-133a abundance in hypertensive patient plasma. While the individuals diagnosed with hypertension were being treated with anti-hypertensives at the time of blood draw, assessment of mean arterial blood pressure was identified to be significantly elevated when compared to the normotensive group. Most interestingly, patients with increased MAP had elevated plasma levels of miR-133a, supporting the notion that increased tension results in increased circulating miR-133a levels.

The risk of cardiovascular disease is higher in those with elevated blood pressures, and this could potentially be one of the many contributing factors. While the direct effects of tension induced alterations in miR-133a abundance has on adverse aortic remodeling remains to be determined; however, these findings highlight the importance in managing elevated blood pressure and may lead to the novel development of pharmacotherapies directed at inhibiting the secretion of miR-133a from aortic fibroblasts.

CHAPTER 6: Future Directions

The following chapter will provide preliminary data and rationale for future studies. This section will focus on applying the major findings presented in the previous chapters to future investigations in the regulation of thoracic aortic aneurysm (TAA) formation and progression. As demonstrated, increased mechanical tension results in the reduction of miR-133a from thoracic aortic fibroblasts, however it remains to be determined what effects this has on cellular phenotype and aortic pathologies, such as thoracic aortic aneurysm formation. Accordingly, the following studies will: 1) determine the role of miR-133a in mediating *in vitro* phenotypes, via overexpression and knockdown in primary aortic fibroblasts isolated from a murine model in which TAA has or has not been induced; and 2) explore whether viral-mediated miR-133a replacement attenuates the development of TAA in an establish murine model.

Thoracic aortic aneurysm (TAA) is a localized dilation of the supradiaphragmatic aorta. This devastating disease process is often asymptomatic and results in a weakened aortic wall and can progress to rupture

if left untreated;(29) however, the underlying molecular mechanisms leading to the development of TAA are largely unknown. While there are numerous etiologies that contribute to the manifestation of TAA, abnormal remodeling of the aortic extracellular matrix (ECM) and changes in the resident cellular population universally occur.

Histological examination of aortic structure and composition has demonstrated a decline in the smooth muscle cell population coinciding with an emergence of fibroblast derived myofibroblasts.(94) It is believed this population of fibroblasts plays a key role in managing the remodeling process through the observed association with elastic fiber and medial degeneration.(63, 94, 168) Interestingly, it has been demonstrated that isolated primary aortic fibroblasts from TAA tissue sustain a stable alteration in gene expression profile;(195) however, it remained to be determined the effects this has on cellular function.

Under normotensive conditions, a physiologically relevant level of wall tension is essential for maintaining normal vessel structure.(223) As discussed in previous chapters, wall tension is directly related to the radius of the vessel and intraluminal pressure, thus, when blood pressure is constant and vessel dilation occurs, wall tension rises. Interestingly, an alteration in the amount of tension placed on cells has been demonstrated to modulate complex phenotypes, such as proliferation, migration, and adhesion.(224-228) Previous results in this body of work have demonstrated tension reduces miR-133a in aortic fibroblasts. As, the importance of miR-133a in the regulation of ECM remodeling in

cardiovascular disease is becoming increasingly recognized, it would be highly interesting to determine if miR-133a alone has an effect on cellular phenotype.

While there are numerous etiologies contributing to the manifestation of TAA, abnormal remodeling of the vascular ECM universally occurs. ECM refers to the collagen and elastin cytoskeleton surrounding the cells which contain sequestered growth factors and cytokines. The ECM provides structural and biochemical support to the resident cells, of which remodeling is an important process in regulating the dynamic balance between degradation and deposition, in which a critical family of proteolytic enzymes, the matrix metalloproteinases (MMPs), actively participate through the degradation of all ECM components and subsequent release of sequestered growth factors and cytokines (123, 142).

Previous results determined that increased vascular wall tension results in the reduction of miR-133a in thoracic aortic fibroblasts via exosome secretion. As aortic diameter increases during the aortic dilation in TAA, wall tension rises proportionally. As discussed in Chapter 1, this laboratory has demonstrated that miR-133a is reduced in TAA tissue with increasing diameter.(212) Combined, these findings suggest that loss of miR-133a-mediated translational control of specific gene targets may contribute to TAA formation and progression.

To study the molecular mechanisms responsible for the development and progression of TAA, this laboratory has developed and validated a surgical model of TAA in mice.(82, 91, 92, 115, 134, 169, 195, 316, 317) Murine TAA may be

induced via $CaCl_2$-soaked sponge (0.5 M) placed in direct contact with the periadventitial surface of the descending thoracic aorta and kept in place for 15 minutes. This method results in the reproducible dilatation of the thoracic aorta over a prolonged period of time.(82) While the inciting stimulus of TAA formation remains undefined, it has become clear that TAA is not the result of an acute chemical injury, but a process that is initiated and slowly progresses. Importantly, early examination of aortic tissue sections following $CaCl_2$ exposure revealed normal aortic structure and the absence of inflammatory infiltrate; TAA tissue stained for macrophages, neutrophils, T-cells, and B-cells revealed little change from untreated control aortic sections.

This laboratory has now extensively characterized this mouse model of TAA and has published multiple peer-reviewed manuscripts describing mechanisms related to TAA development that not only recapitulate the structural hallmarks of human TAA, but also replicate the changes in cellular content, the modifications in biochemical mediators, and the altered intracellular signaling consistent with what is observed in human clinical specimens.

It must be recognized, there is no singular animal model, in large or small animals that perfectly replicates human aneurysms on a temporal and molecular scale; however, the similarities observed between murine and human TAAs, provide validation that this murine TAA model replicates many of the key hallmarks of human TAA pathophysiology. Therefore, this model provides a suitable test bed for the completion of the following future studies.

To confirm miR-133a is reduced in murine TAA tissue, TAA was induced as described. Following 3 weeks of aneurysm formation aortic diameter was assessed and found to be significantly increased (**Figure 6.1**) and the aortic tissue was harvested. Total RNA was isolated and miR-133a was quantitated as previously described. The aortic tissue abundance of miR-133a was reduced in TAA when compared to control (**Figure 6.2**).

Combined, the previous results from clinical specimens and this calcium chloride induced murine model of TAA demonstrate a reduction of miR-133a as a function of increased aortic diameter. Furthermore, aortic fibroblasts have been demonstrated by PCR array to undergo a stable phenotypic change in gene expression profiles during the development of TAA, (195) which is believed to drive the enhancement of extracellular matrix proteolysis in TAA development. Therefore, the directions of these investigations will aim to first define the phenotypic alterations in TAA fibroblasts, then progress these findings by determining if miR-133a is a regulator of the phonotype observed.

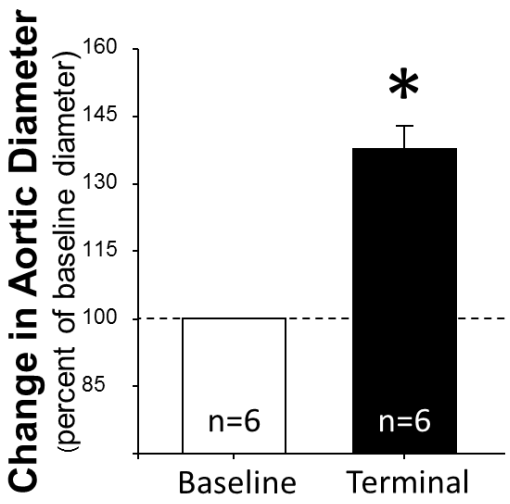

Figure 6.1 Murine model of TAA. Aortic diameter measurements obtained by calibrated video microscopy a baseline and 3 weeks following the induction of TAA (Terminal) (n=6). An unpaired comparison was made using a two sample t-test. * $p < 0.05$ vs control.

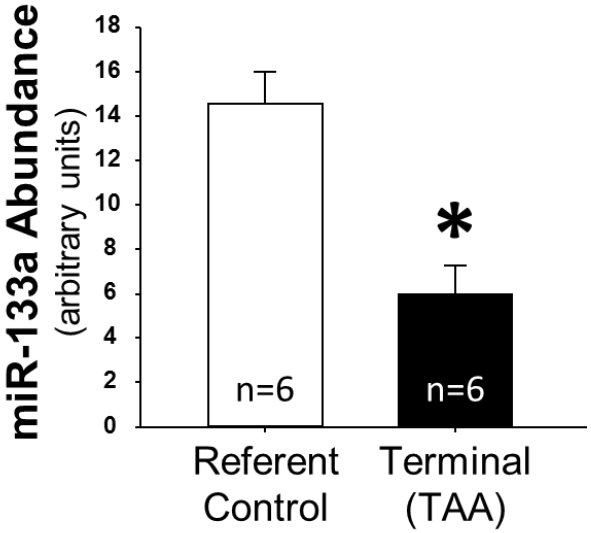

Figure 6.2 miR-133a abundance in TAA tissue. miR-133a abundance in aortic tissue from unoperated (Referent Control) and 3 weeks following induction of TAA (Terminal) (n=6). An unpaired comparison was made using a two sample t-test. * $p < 0.05$ vs control.

The role of miR-133a in mediating in vitro phenotypes

Phenotype is the composite of the observable characteristics of a cell. Many factors contribute to the determination of overall cellular phenotype. Due to the complexities of the pathways involved, multiparameter approaches allowing for the quantitation of overall effect are best suited for the observation of alterations in these phenotypes. In the following studies the parameters of proliferation, migration, and adhesion were selected to observe overall alterations in cellular phenotype. Proliferation of cells is an important process resulting in increased cell number, and can be defined as the balance between cellular division and death. Cellular migration is regulated largely by the cells ability to interact with the extracellular matrix, a process involving matrix metalloproteinase production. Furthermore, it has been demonstrated that mechanotransduction alone is sufficient in the regulation of cellular proliferation and migration.(318) Overall differences in the adhesive properties of a cell may be determined by allowing a cell to bind to a substrate, and non-bound cells are then removed by gentle washing. The remaining adherent cells are quantitated, allowing for the estimation of alterations in the ability to for interactions with the extracellular matrix, which is necessary for the ability to migrate. Therefore, assessment of overall cellular function will be described in the following sections.

Primary cultures of aortic fibroblasts were established and maintained in cell type specific media using a well-recognized outgrowth technique.(243, 319, 320) First, the cellular abundance of miR-133a was compared between control

and TAA fibroblasts (**Figure 6.3)**. As expected, these data demonstrate miR-133a abundance is significantly reduced in TAA fibroblasts as compared to control. Further alterations in phenotype *in vitro* may be quantified utilizing specific endpoints such as proliferation, migration, and adhesion. Therefore, the following studies will compare these endpoints in fibroblasts isolated from control and TAA. As a pilot study, the TAA fibroblasts were treated with 100nM of miR-133a oligo via lipofectamine transduction following manufacturer's instructions and then assayed.

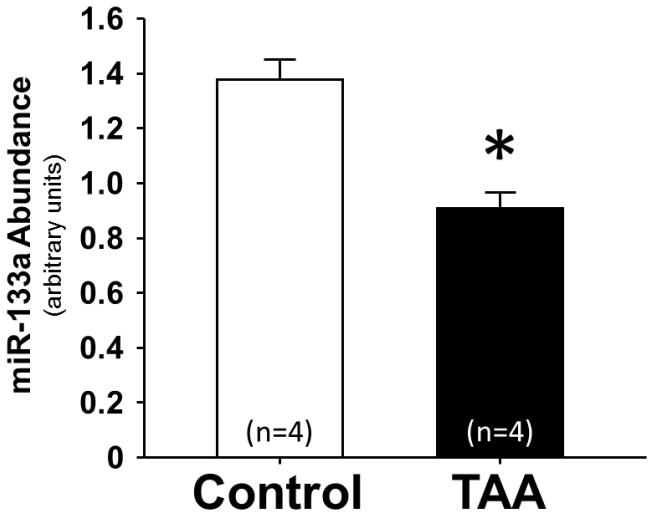

Figure 6.3 Aortic fibroblast miR-133a abundance. miR-133a abundance in cultured aortic fibroblasts isolated from unoperated (Control) and TAA mice (n=6). An unpaired comparison was made using a two sample t-test. * $p < 0.05$ vs control.

Proliferation was determined as follows. Cells were seeded at 1,000 cells per well of a 96 well clear bottom plate (Costar Flat bottom Cell bind Surface [Poly-D-Lysine] Cat# 3300, Corning, NY), and allowed to adhere overnight. The following day growth media was aspirated and replaced with fresh complete media. CyQuant Direct Cell Proliferation Assay (Cat#C35011, Molecular probes) kit was then used to determine percent change in cell number from baseline. The basis of the CyQUANT kit is the use of a green fluorescent dye, which exhibits strong fluorescence enhancement when bound to cellular nucleic acids. This kit was allowed to equilibrate to room temperature and the following will be mixed: PBS (97.5%), Cyquant Direct nucleic acid stain (0.004%), and direct

background suppressor (0.02%). 12 hours following the addition of fresh complete phenol-free fibroblast growth media, an equal volume of 2X Detection reagent was added to the cells in the culture media (assay is compatible in media with or without serum). Cells were then incubated for 1 hour at 37°C with 5% CO2. Following one hour incubation time, fluorescence was read from the bottom of the well at 480/535 Ex/Em. This was then repeated at 24, 48, and 72 hours. Proliferation results in **Figure 6.4** demonstrated that the percent change from baseline of aortic fibroblasts derived from murine TAA is increased as compared to non-TAA controls, and when TAA fibroblasts are treated with 100nM of miR-133a oligo, percent change in proliferation is significantly reduced and returned to within control range. These preliminary data demonstrate that miR-133a alone affects proliferation, and may return TAA fibroblast rate of proliferation to within normal limits.

To compare migration properties between control and TAA, fibroblasts were treated with Mytomycin C (Sigma-Aldrich; Cat# M0503) (8ug/mL) for 1 hour to inhibit proliferation, then rinsed twice with PBS and fresh complete fibroblast growth media was added and the cells were returned to standard tissue culture conditions for 24 hours. The following day the fibroblasts were lifted using a PBS-based enzyme free cell dissociation buffer. 2.5x10^4 cells were seeded in serum free medium and allowed to adhere on the top surface of an 8uM porous membrane overnight. Complete media was then added to the bottom portion of the boyden chamber and the cells were allowed to migrate through the porous

membrane for 48 hours. Results from the migration assay in **Figure 6.5** demonstrate that the motility of TAA fibroblasts was increased, and when treated with exogenous miR-133a, migration was reduced toward that of the control.

Adhesion is an important and complex cellular phenotype that involves multiple molecular interactions, including receptor to ligand binding of the cell surface and extracellular matrix, as well as modulation in the assembly of the cytoskeleton. Consequently, the adhesive properties of a cell are informative in not only the measurement of the contacts between the cell and extracellular matrix, but also the state of the cell. Therefore, aortic fibroblast phenotype was assessed by seeding 2,000 cells per well in 100 uL of complete growth media per well of a 96 well clear bottom plate (Costar Flat bottom Cell bind Surface [Poly-D-Lysine] Cat #3300, Corning, NY). Cells were then allowed to adhere by returning the plate to the incubator for 1 hour in standard tissue culture conditions. The plate was then washed five times with room temperature PBS (with Ca2+/Mg2+) using a BioPlex Pro Plate Washing Station set to “Drip Fill” to achieve consistency in washes across plates. Each well was then carefully aspirated so as to not disturb the cells, and 100 uL of complete, phenol-free fibroblast growth media was added to the cells. Cells were then fluorescently labeled, and relative fluorescence was quantitated by microplate reader. Results demonstrate that TAA fibroblasts have reduced adhesion as compared to control, and when treated with exogenous miR-133a, surpass the adhesive property of the control fibroblasts (**Figure 6.6**).

It is apparent that the phenotypic properties of TAA fibroblasts in respect to proliferation, migration, and adhesion are significantly altered and this cell population takes on classic characteristics of a more motile and proliferative myofibroblast. Most interestingly, these preliminary studies suggest miR-133a has the profound ability to regulate these aspects of cellular phenotype, shifting properties back toward normal fibroblast characteristics.

More than a simple increase in sample size is required for the resolution of these studies (Goal: n=8 as determined by power analysis, $\alpha=0.05$, $\beta=0.20$). Inclusion of proper controls in this examination is key for completion. The use of a non-mammalian targeting microRNA such as cel-miR-39 would provide valuable insight accounting for any effects of transduction by lipofectimine. Furthermore miR-1, which is included in the same two bicistronic units within the genome as miR-133a, and demonstrated by Torella *et al.* to not have the same protective capacity as miR-133a in the prevention of adverse vascular remodeling,(214) would be a highly interesting prospect for use as a control microRNA for these studies. Furthermore, knockdown of miR-133a with the use of an Anti-miR-133a would provide further evidence in the control of cellular phenotype. An Anti-microRNA is a single stranded oligo that competitively binds to a targeted microRNA, inhibiting interaction with mRNA. Therefore, treatment of control fibroblasts with the anti-miR-133a may result in a TAA fibroblast phenotype.

In addition to proper controls, I propose to strengthen the study through the inclusion of an investigation in the effects of miR-133a on several gene expression and protein markers of the fibroblast to myofibroblast transition. Fibroblasts may be identified through the expression of the discoidin domain-containing receptor 2 (DDR2). This protein is a collagen receptor that has previously been shown to display fibroblast restricted expression, and has been demonstrated in cardiovascular tissue to be a superior marker for fibroblasts than even the fibroblast specific protein-1.(95) Myofibroblasts may be identified through the positive expression for DDR2 and smooth muscle myosin heavy chain (MYH11), and α smooth muscle actin (αSMA).(94)

Based on bioinformatics analysis it does not appear that miR-133a directly targets either of these markers; however, it is our belief that reduction of miR-133a may result in the over expression of a program of genes that may influence the fibroblast to myofibroblast transition. As the myofibroblast has been identified as a critical cell type capable of modulating the ECM remodeling process, the effects of miR-133a on modulation of this phenotype would provide valuable insight in the regulation of TAA development.

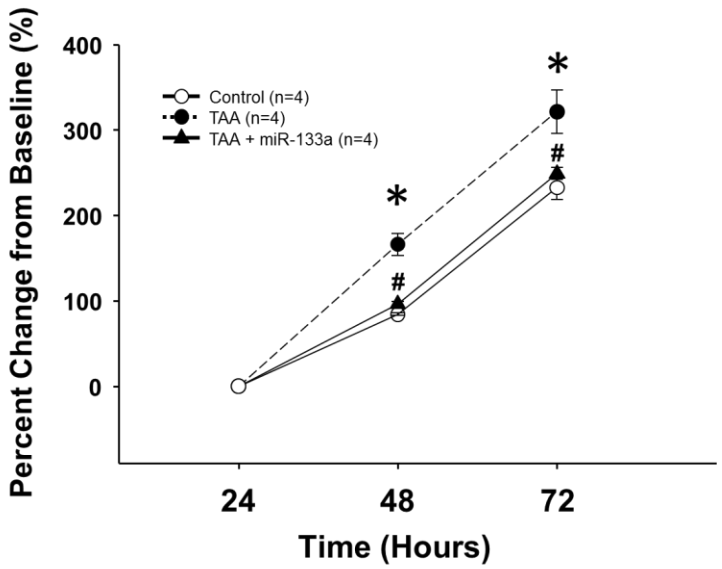

Figure 6.4 Aortic fibroblast proliferation. Percent change in cultured aortic fibroblast proliferation from Control and TAA fibroblasts. In addition, TAA fibroblasts were treated with exogenous miR-133a in culture (TAA+miR-133a) (n=4). * $p < 0.05$ vs control value at the respective time point. # $p<0.05$ vs TAA at the respective time point.

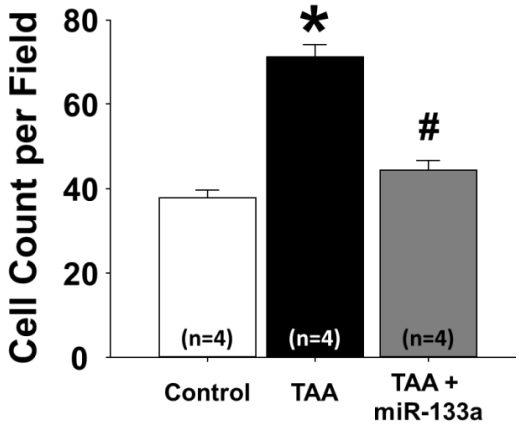

Figure 6.5 Aortic fibroblast migration. Number of migrated Control and TAA fibroblasts. In addition, TAA fibroblasts were treated with exogenous miR-133a in culture (TAA+miR-133a) then allowed to migrate (n=4). * $p < 0.05$ vs control. # $p<0.05$ vs TAA.

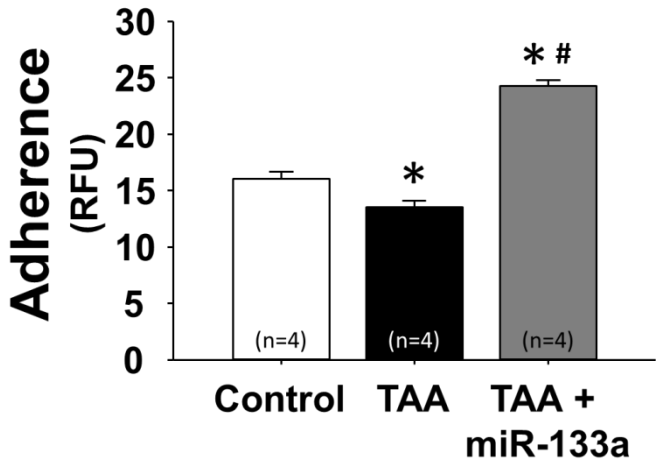

Figure 6.6 Aortic fibroblast adhesion. Fluorescently labeled Control, TAA, and TAA fibroblasts treated with exogenous miR-133a in culture (TAA+miR-133a) (n=4). * $p < 0.05$ vs control. # $p<0.05$ vs TAA.

Attenuation of thoracic aortic aneurysm by miR-133a replacement

Within the spectrum of cardiovascular diseases, TAAs are one of the most dangerous and difficult to treat problems in cardiothoracic surgery. Aortic disease in general, to which TAAs contribute, are a significant source of mortality for the population, causing as many as 13,000 deaths annually in America, consistently placing aortic disease among the top 20 causes of death (23-25). Further understanding of the molecular mechanisms involved in TAA is essential and will provide novel, less invasive therapeutic strategies.

Membrane-type 1 Matrix Metalloproteinase (MT1-MMP) has been identified as a key mediator of TAA development due to the role in activation of

other MMPs, ability to degrade all ECM components, and release/activation of latent ECM-bound growth factors.(94, 188, 195, 321, 322) Furthermore, in an earlier study performed by this laboratory, it was determined that MT1-MMP is elevated in clinical and murine TAA tissue,(186, 188) and the development of TAA was significantly attenuated in mice heterozygously deficient in MT1-MMP (**Figure 6.7**). Therefore, MT1-MMP protein abundance was compared between control and TAA fibroblasts and TAA fibroblasts with added exogenous miR-133a by methods previously described. Results demonstrated that MT1-MMP protein abundance was significantly increased in TAA fibroblasts, and addition of exogenous miR-133a reduced MT1-MMP protein abundance in the TAA fibroblasts (**Figure 6.8**). These results underscore that translational control mechanisms, such as miR-133a, has an important role in modifying aortic fibroblast MT1-MMP abundance.

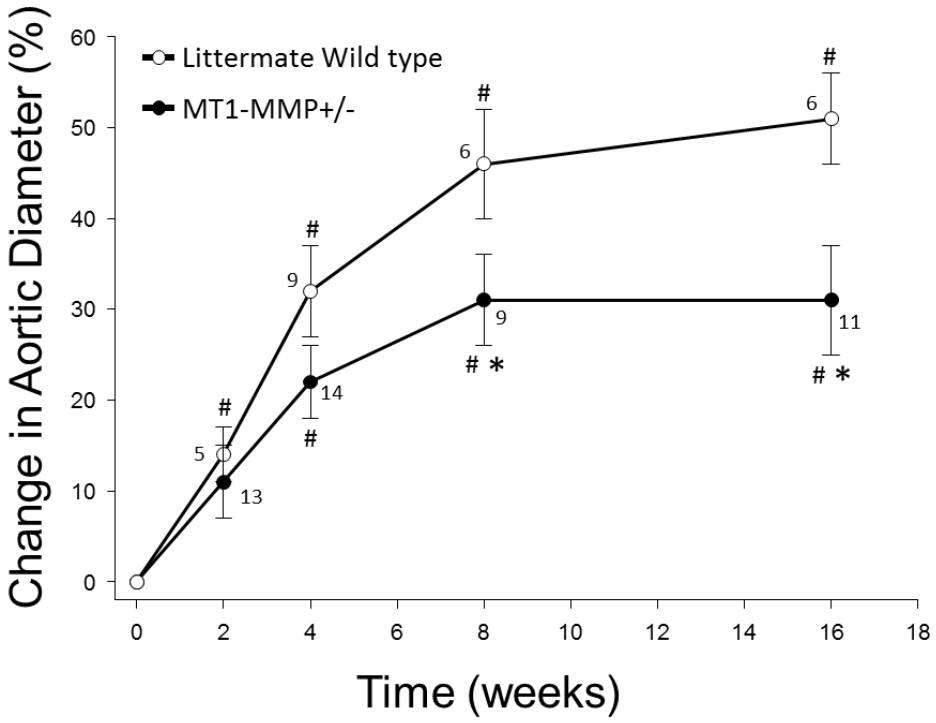

Figure 6.7 MT1-MMP is a key mediator in the development of TAA. Percent change in thoracic aortic diameter of wild type mice, and mice heterozygously deficient in MT1-MMP (MT1-MMP+/-) over time. * $p<0.05$ vs. baseline diameter (Time 0). # $p<0.05$ vs wild type littermate. Unpublished data credited to Drs. Jeffrey Jones and Rupak Mukerjee.

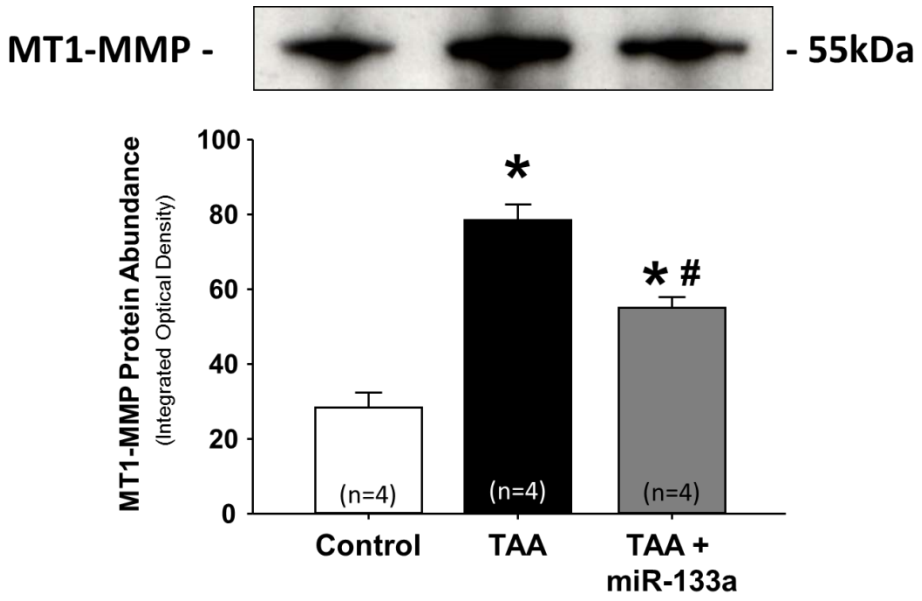

Figure 6.8 Aortic fibroblast MT1-MMP protein abundance. The abundance of MT1-MMP (IOD) determined by western blot using the antibody ab8221 in control, TAA, and TAA fibroblasts treated with exogenous miR-133a (TAA+miR-133a) (n=4). * $p < 0.05$ vs control. # $p<0.05$ vs TAA.

In agreement with the current results, this laboratory has previously published, modulation of miR-133a by lentiviral transduction modulates MT1-MMP protein abundance in myocardial fibroblasts.(243) With miR-133a overexpression MT1-MMP is reduced, and with miR-133a knockdown by anti-miR-133a, MT1-MMP is increased. To build upon this prior knowledge and preliminary results, a bioinformatics approach was utilized to identify putative miR-133a target sequences in genes known to be involved in TAA development. A TargetScan Human analysis, which is a widely used predictor of microRNA targets, identified a putative binding site in the MT1-MMP transcript and this sequence is conserved across species (human, pig, and mouse; *present in reverse orientation on 3'-DNA*

strand in mouse)(**Figure 6.9**). In addition, 5 other informatics algorithms (specifically: MicroCosm Targets Version 5; DIANA; PITA;

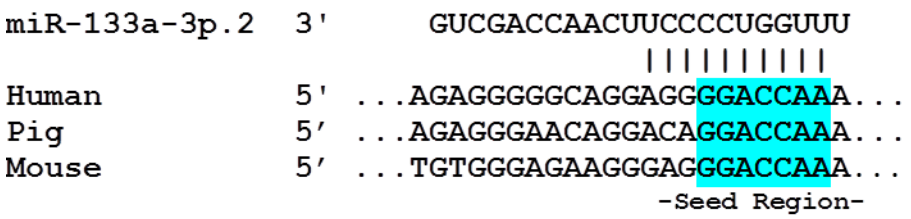

Figure 6.9 Sequence alignment of putative miR-133a seed region. Conservation of the miR-133a seed region in the MT1-MMP UTR transcripts of human, pig, and mice.

RNA22; and RNAhybrid) identified miR-133a as a strong candidate for potential interaction with the same seed region of the MT1-MMP transcript. To determine whether MT1-MMP's 3'UTR is a direct target of miR-133a, the 3'UTR of the human MT1-MMP was cloned in line (3' end) with the luciferase open reading frame in a reporter plasmid. This allowed for the quantifiable determination of luminescence dependent on whether miR-133a bound to the 3' UTR sequence. In cells co-transfected with the MT1-MMP 3' UTR and the miR-133a microRNA mimic, luminescence was reduced to 47.9±3.4% of that of cells co-transfected with the MT1-MMP 3' UTR luciferase reporter plasmid and a non-targeting microRNA mimic. Furthermore, no change in luminescence was observed in the vector devoid of a 3'UTR (empty), GAPDH 3'UTR or random sequence 3'UTR controls

co-transfected with either the miR-133a mimic or the non-targeting microRNA mimic. These findings demonstrate that the MT1-MMP 3'UTR is a direct target of miR-133a. (**Figure 6.10**).

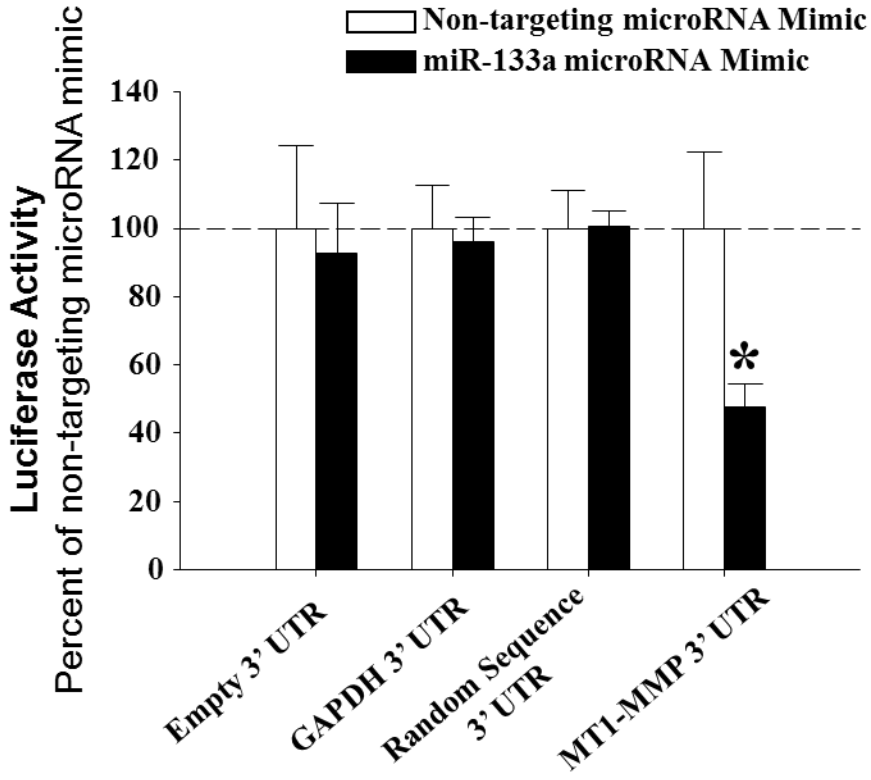

Figure 6.10 MiR-133a targets the MT1-MMP 3'UTR. HT1080 cells were transfected with luciferase reporter vector containing a vector void of a 3'UTR (Empty 3'UTR), the GAPDH 3' UTR, a random sequence3'UTR, and the MT1-MMP 3'UTR. Reporter vectors were co-transfected with a miR-133a mimic or unrelated negative control micoRNA mimic. The result of this assay was a reduction in luminescence observed in cells co-transfected with the MT1-MMP 3' UTR reporter GoClone plasmid and the miR-133a microRNA mimic, and no change in luminescence was observed in cells co-transfected with the MT1-MMP 3' UTR reporter GoClone plasmid and a non-targeting microRNA mimic. Furthermore, no change in luminescence was observed in the empty, GAPDH or random sequence 3'UTR

vector controls co-transfected with either the miR-133a mimic or the non-targeting microRNA mimic.

The importance of miR-133a in the regulation of extracellular matrix remodeling in cardiovascular tissue is becoming increasingly recognized. In addition to miR-133a targeting the repression of a key protease directly involved with the development of TAA, MT1-MMP, Carè *et al.* demonstrated in a murine model of cardiac hypertrophy, that miR-133a is reduced in the hypertrophied myocardium, and that *in vivo* knockdown of miR-133a (using anti-miR-133a) induced cardiac hypertrophy.(216) Similarly, Torella *et al.* demonstrated miR-133a was reduced in the carotid artery following balloon distension injury in a rat model. Importantly, systemic overexpression of miR-133a by adenovirus, attenuated post-injury remodeling, in contrast to miR-133a knockdown (using an anti-miR-133a oligonucleotide) which worsened the response.(214) Data from these studies emphasize the key role that miR-133a plays in cardiovascular remodeling and suggest that the loss of miR-133a-mediated translational control of targeted genes likely contributes to pathologic remodeling. Accordingly, a pilot study was performed to explore whether viral-mediated miR-133a replacement attenuates the development of TAA in calcium chloride induced murine model of TAA.

In order to increase circulating levels of miR-133a, mice were injected intravenously (by tail-vein injection) with a lentivirus that produces the murine

miR-133a precursor. In this pilot study, TAA was induced in wild type FVB mice. The following day, miR-133a lentivirus ($1x10^9$ pfu/100µl x1) was injected through the tail-vein. The mice were survived for 25 days before terminal surgery with blood and tissue harvest. Digital images were collected and aortic diameter was measured at the time of TAA induction (baseline) and terminal surgery. Plasma and aortic tissue levels of miR-133a were measured by QPCR, and MT1-MMP protein abundance in the TAA tissue was measured by immunoblotting. Results demonstrate increased plasma (**Figure 6.11**) and TAA tissue (**Figure 6.12**) levels of miR-133a, and decreased tissue levels of MT1-MMP protein (**Figure 6.13**). Importantly, the increase in aortic diameter at 3 weeks post-TAA induction was attenuated by treatment with miR-133a lentivirus (**Figure 6.14**). Using this lentiviral delivery system, we will build on this pilot data through examination of the effects of miR-133a on TAA development over time, following intravenous treatment with miR-133a lentivirus or a lentivirus expressing a scrambled non-targeting miR sequence. Key preliminary studies for this aim provide proof of feasibility of the described approach. Using this lentiviral delivery system and incorporation of non-mammalian targeting lentivirus as a vehicle control, we will increase our sample size to (n=10) as determined by power analysis (α=0.05, β=0.20).

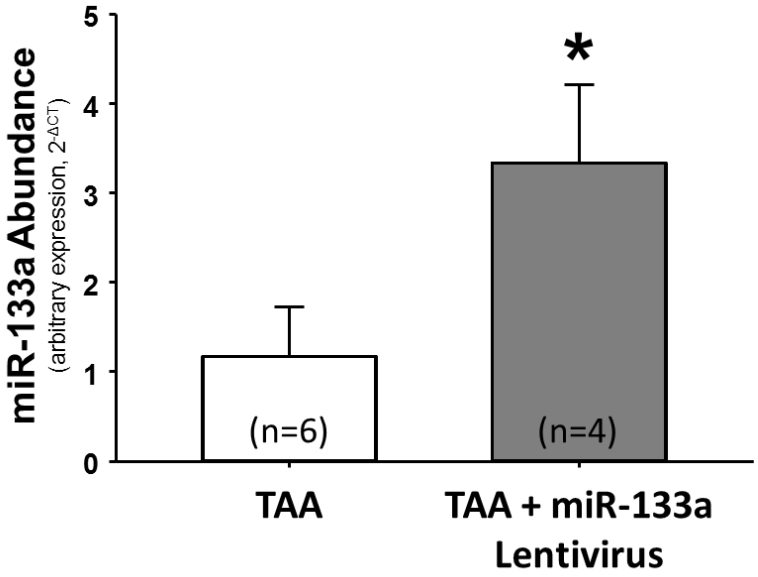

Figure 6.11 Circulating plasma levels of miR-133a. Plasma miR-133a levels 3 weeks following a single tail vein injection of the miR-133a lentivirus (TAA+miR-133a Lentivirus) (n=6) or the control saline (TAA)(n=4). An unpaired comparison was made using a two sample t-test. * $p < 0.05$ vs TAA.

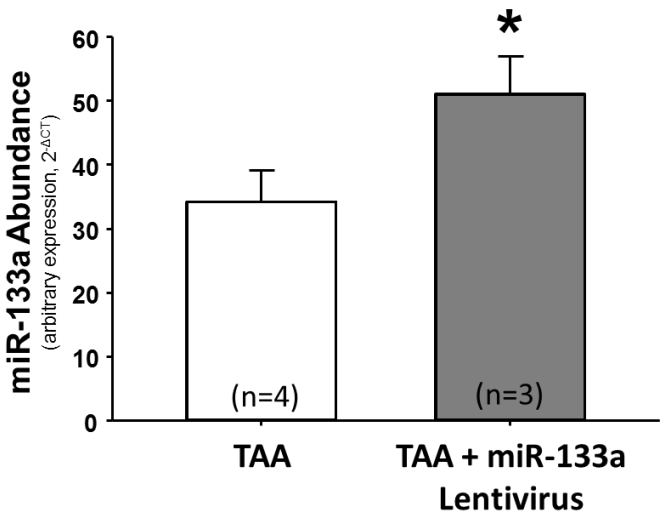

Figure 6.12 Thoracic aortic tissue miR-133a abundance. Tissue miR-133a abundance 3 weeks following a single tail vein injection of the miR-133a lentivirus (TAA+miR-133a Lentivirus) (n=4) or the control saline (TAA) (n=3). An unpaired comparison was made using a two sample t-test. * $p < 0.05$ vs TAA.

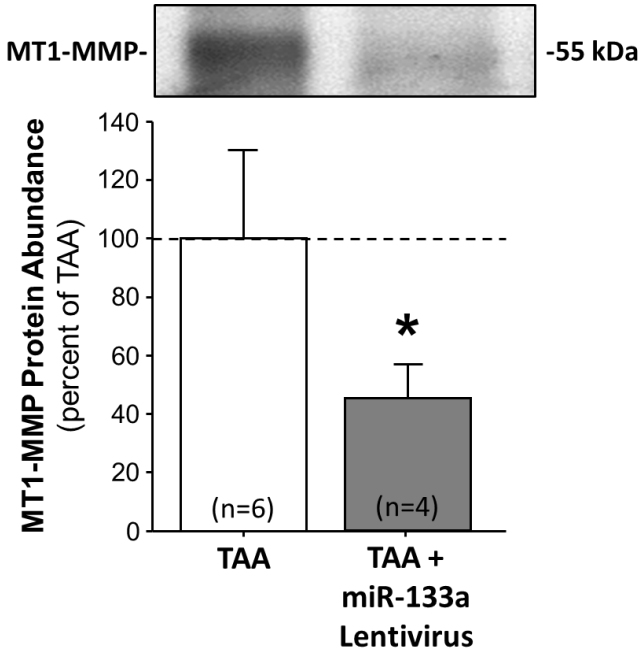

Figure 6.13 Thoracic aortic tissue MT1-MMP protein abundance. Tissue MT1-MMP abundance 3 weeks following a single tail vein injection of the miR-133a lentivirus (TAA+miR-133a Lentivirus) (n=6) or the control saline (TAA) (n=4). An unpaired comparison was made using a two sample t-test. * $p < 0.05$ vs TAA.

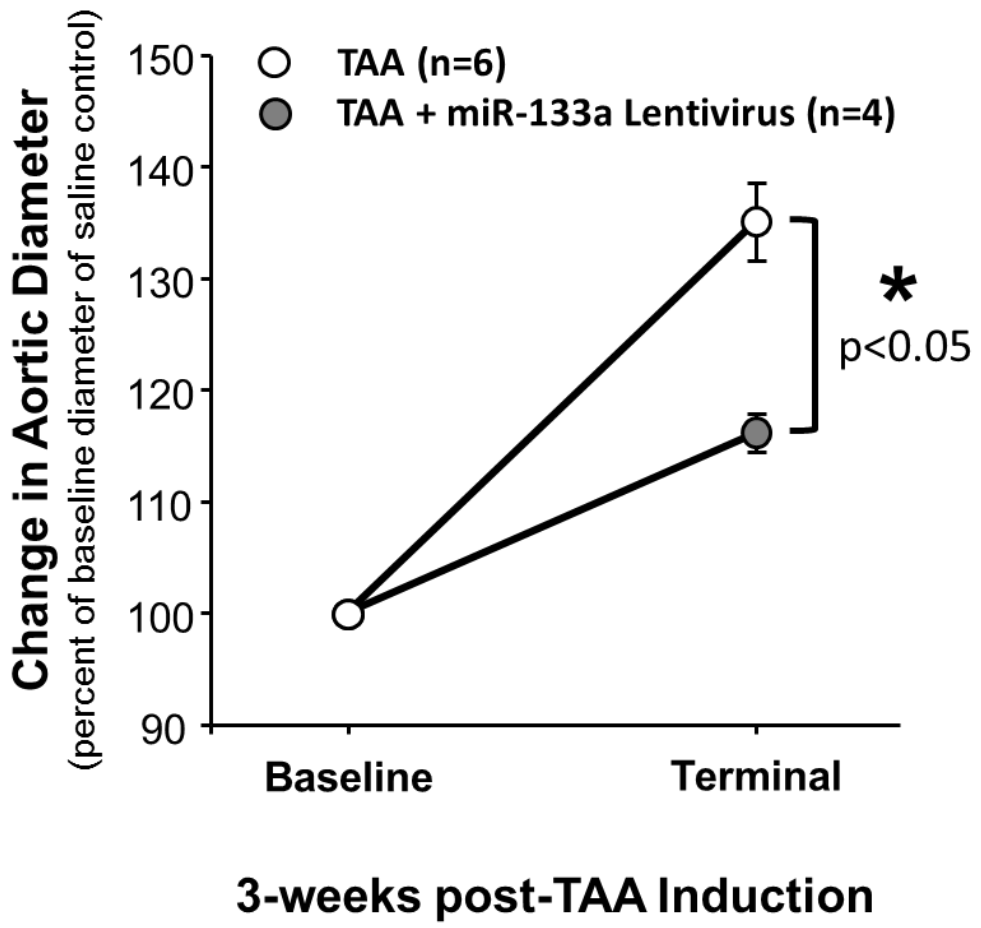

Figure 6.14 Aortic diameter measurements. Percent change in aortic diameter from baseline measurements 3 weeks following the induction of TAA. Aortic diameter was obtained by calibrated video microscopy 3 weeks following a single tail vein injection of the miR-133a lentivirus (TAA+miR-133a Lentivirus) (n=4) or the control saline (TAA) (n=6). An unpaired comparison was made using a two sample t-test. * $p < 0.05$ vs TAA.

Lentiviral transduction is not without limitations. Mammalian hosts have evolved defense mechanisms against double-stranded RNA, typically present as consequence of viral infection (interferon response). While these effects are not commonly present following microRNA delivery, careful monitoring of such a response will be maintained. An alternative approach is to utilize HDAC2 inhibition with Suberoylanilide hydroxamic acid (vorinostat), a United States-FDA approved histone deacetylase inhibitor currently indicated and prescribed orally for the treatment of patients with cutaneous T-cell lymphoma. Oral administration of vorinostat has been demonstrated to increase cellular miR-133a levels in the cardiovascular tissue of a mouse model of pressure overload induced cardiac hypertrophy.(218)

While multiple approaches exist to increase cardiovascular tissue levels of miR-133a, an additional aim of this study will be to inhibit the secretion of miR-133a from the thoracic aorta, and determine the effects on the development of TAA. As demonstrated in this body of work, tension reduces miR-133a in aortic fibroblasts via exosome secretion, and the use of GW4869, the inhibitor of nSMase2, prevents tension induced reduction of miR-133a. Most interestingly, nSMase2 has been identified to be activated in response to acute changes in vascular pressure.(323, 324) GW4869, which has been successfully delivered to mice and rats *in vivo* (325, 326), will inhibit the secretion of exosomes at a concentration of 20 uM (261, 280-282). Therefore, the use of an osmotic pump will be employed to deliver GW4869 for 4 weeks following the induction of TAA.

As an alternative method of nSMase2 inhibition, scyphostatin has been demonstrated to inhibit mechano-induced nSMase activity in a dose-dependent manner.(324) At the time of terminal surgery, aortic diameter will be obtained and the abundance of miR-133a will be assessed in the plasma and descending thoracic aorta. It is anticipated that inhibition of exosome secretion will lead to an attenuation of TAA development, an increase in thoracic aortic tissue miR-133a, and a decrease in circulating plasma miR-133a.

The significance from this body of work is through the identification that loss of miR-133a alters cellular phenotype and plays an essential role in TAA formation. Furthermore, a mechanism as to how miR-133a is reduced in thoracic aortic fibroblasts has been identified. An important translational outcome from this set of investigations is the identification of a specific molecular pathway responsible for alterations that may mediate TAA development. This will not only provide foundational evidence for the mechanistic changes that occur in thoracic aortic aneurysm formation, but may also have the potential to identify specific targets for therapeutic intervention.

CHAPTER 7: Methodology

The following section will describe in depth the methodology utilized for the studies included in this body of work.

Ex vivo Thoracic Aortic Tension Application.

All animal care and surgical procedures were approved by the Medical University of South Carolina Institutional Animal Care and Use Committee (AR3380). Following induction of anesthesia with 2% isoflurane, wild type C57BL/6 mice (10-16 weeks of age; Envigo) underwent thoracotomy and the descending thoracic aorta was harvested. Endothelial-intact aortic tissue segments were cut transversely into rings of approximately 3mm in length, which were suspended on parallel wires, and bathed in an oxygenated physiologic salt solution (Krebs-Henseleit solution) in an *ex vivo* tissue myograph. Aortic segments were maintained at an experimentally derived optimal-tension (normotension; 0.7g, ~70 mmHg equivalent) or elevated tension (1.5g, ~150 mmHg equivalent) utilizing methods previously described.(234, 235) Endothelial-intact aortic segments were also held at 0.7g then treated with or without 100nm

Angiotensin II (AngII) (A9525; Sigma) and allowed to contract against the parallel wires; the peak tension generated was recorded. Following three hours of applied tension or AngII exposure, aortic segments were homogenized in Trizol and total RNA was extracted.

Cell Culture.

The descending thoracic aorta from wild-type C57BL/6 mice (10-16 weeks of age; Envigo) was extracted and primary fibroblast cell lines were established using an outgrowth technique as described previously.(320) The isolated thoracic aortic fibroblasts were maintained in complete fibroblast-specific growth media (Fibroblast growth media 2; C-23020, PromoCell) with added 10% Fetal Bovine Serum (Gibco, Cat# 1600). Primary smooth muscle cell (SMC) lines were similarly cultured from wild-type C57BL/6 mice (10-16 weeks of age; Envigo) using a similar outgrowth procedure.(327) The isolated SMCs were maintained in SMC-specific growth media with added supplement pack (SMC Growth Medium 2; C-22062, PromoCell, Heidelberg Germany). All cell lines were treated with Amphotericin B (5 ug/mL; A2942, Sigma) and Gentamicin (0.5 mg/mL; 15710-064, Gibco) during the outgrowth phase only. All cell lines were maintained at 37^{o}C in a water-jacketed incubator, in a humidified 5% CO_2/95% air atmosphere. Primary fibroblasts and SMCs were utilized from passages 2-10.

Primary cell biaxial cyclic tension application and Angiotensin II stimulation.

Fibroblasts or smooth muscle cells were seeded at a density of 5,000 cells per cm^2 into amino coated Bioflex-6 well plates (BF-3001A; Flexcell International Corporation, Burlington NC) and allowed to adhere overnight. Culture media was then replaced with fresh complete media containing 10% exosome-depleted fetal bovine serum (EXO-FBS; System Biosciences) with or without AngII (100nM, A9525; Sigma). To inhibit exosome secretion, fibroblasts were pretreated with the inhibitor of neutral sphingomyelinase, GW4869 (20nM for 24 hours) (GW4869, Sigma, Cat# D1692). Following 24 hours, cells were rinsed with PBS and appropriate culture media was replaced. Culture plates were held static (control) or subjected to 12% biaxial cyclic stretch at a rate of 1Hz utilizing a Flexcell culture system (FX5000, Flexcell International Corporation, Burlington, NC).

QPCR.

Total RNA was extracted using TRIzol Reagent (Thermo Fisher Scientific, Cat# 15596026), and quantified by NanoDrop 2000 (Thermo Fisher Scientific). Samples were snap frozen in liquid nitrogen and stored at -80°C until use. For cellular and tissue microRNA quantitation, single-stranded cDNA was synthesized from 100 ng total RNA. Exosomal microRNA was quantified from exosomes precipitated out of 5 ml of conditioned media (exposed to cells for 18 h). Circulating

microRNA quantitation was achieved by total RNA isolation from 250uL of serum. MicroRNA cDNA synthesis and PCR quantitation was performed using the miR-133a-1-3p TaqMan microRNA Assay (Thermo Fisher, Cat# 002246-4427975) according to the manufacturer's instructions. Primary-microRNA expression was determined by reverse transcription of 1 ug total RNA using the High Capacity RNA-to-cDNA kit (Thermo Fisher Scientific, Cat# 4392339), followed by quantitation using the ThermoFisher primary-microRNA analysis kit (pri-miR-133a-1: Mm03306281_pri, and pri-miR-133a-2: Mm03307401_pri; Cat# 4427012). For ribonuclease gene expression analysis, total RNA (1 µg) was reverse transcribed with the iScript cDNA Synthesis Kit (170-8891, BioRad). Each cDNA was amplified with gene-specific TaqMan expression assays (XRN1: Mm00496326_m1, XRN2: Mm00457212_m1, ExoSC4: Mm00615045_g1, and GAPDH: Mm99999915_g1; Applied Biosystems Cat# 4331182). QPCR reactions were performed on a Bio-Rad CFX96 Real-Time System. All samples were tested in duplicate and averaged. The relative expression of each mRNA and primary microRNA was calculated and normalized to the internal control GAPDH using the comparative cycle threshold (CT) method.(328) Relative expression intensity values were calculated as $2^{-\Delta CT}$, in which ΔCT are CT values normalized to the reference control.

Immunoblot Analysis.

Relative abundance of XRN1, XRN2, ExoSC4, MT1-MMP and beta-Actin were determined by immunoblotting. Briefly, 20 µg of each aortic fibroblast

homogenate, determined by the Pierce BCA total protein assay (23225; Thermo Fisher Scientific, City, State), was fractionated on a 4% to 12% bis-tris gradient gel by electrophoresis. The proteins were transferred to nitrocellulose membranes (0.45 µm; Bio-Rad, Hercules CA) and incubated in 5% nonfat dry milk containing antisera specific for XRN1 (1ug/mL; Thermo Fisher Scientific, PA5-41888), XRN2 (1:1,000; Thermo Fisher Scientific, PA5-38789), ExoSC4 (5ug/mL; Thermo Fisher Scientific, PA5-41890), MT1-MMP (1:10,000, ABcam, AB8221), or beta-Actin (1:10,000; Biovision Inc., 3662-100). A secondary peroxidase-conjugated antibody (primary antibody species-specific) was applied (1:5000; 5% nonfat dry milk), and signals were detected with a chemiluminescent substrate (Western Lighting Chemiluminescence Reagent Plus; PerkinElmer, San Jose, CA) and recorded on film. Band intensity was quantified using Gel-Pro Analyzer version 3.1.14 (Media Cybernetics, Silver Spring, MD).

Exosome Precipitation and Quantitation.

Fibroblasts were maintained in growth media containing 10% exosome depleted FBS and exposed to 18 hours of 12% biaxial cyclic tension. Media was collected and centrifuged at 3,000 x g for 15 minutes to remove cells and cell debris. The supernatant was transferred to a separate tube and exosomes were precipitated from the culture media (5 mL) using an exosome precipitation solution (ExoQuick-TC, System Biosciences, Inc; Cat# EXOTC50A-1), following the manufacturer's instructions. Relative exosome abundance was compared using acetylcholinesterase activity as a surrogate for exosome number using standard

procedures.(275, 329) Briefly, the exosome fraction was suspended in 100uL of phosphate buffered solution and incubated with 1.25 mM acetylthiocholine iodide (Sigma, Cat# A5751) and 0.1 nM 5,5'-dithio-bis(2-nitrobenzoic acid) in a final volume of 300 uL. The incubation was carried out at 37°C for 30 minutes, and the change in absorbance was measured at 412nm on a Spectramax M3 (Molecular Devices).

Murine Models of Hypertension.

Two distinct murine models of hypertension were employed. First, a commercially available, hypertensive mouse (BPH2, Jackson Laboratories, C57BL/6 background, Cat#003005) that initiates hypertension at 5 weeks of age and peaks at 21 weeks. Low circulating levels of angiotensin-I have been recorded in these animals suggesting that their hypertension is angiotensin-II-independent.(14) The corresponding normotensive strain (BPN3, Jackson Laboratories, C57BL/6 background, Cat# 003004) was used for control as well as for the second hypertensive model consisting of the well-established angiotensin-II (AngII) model of continuous infusion for 28 days (1.46 mg/kg/day). Blood pressures were measured using a non-invasive tail-cuff system (CODA™, Kent Scientific Corporation, Torrington, CT, USA).

Human Subjects.

Approval and inclusion criteria of human subjects were previously defined.(330) Control patients fulfilled the general inclusion criteria, but did not

have a history of hypertension. Hypertensive patients fulfilled the general inclusion criteria and had a history of hypertension documented in their records and/or had been told of this diagnosis by a physician, and were receiving medication for its treatment. All hypertensive patients were diagnosed with left ventricular hypertrophy. No patients included in this study had evidence of heart failure as specified by the European Society of Cardiology and Heart Failure Society of America criteria.(331, 332)

Murine Model of Thoracic Aortic Aneurysm

Anesthesia was induced in a closed chamber containing approximately 5% isoflurane mixed with air. Following loss of consciousness each mouse was weighed, and transferred to an ECG equipped feed-back temperature controlled operating table (Indus Instruments, Houston, TX), with a modified mask assembly delivering 2–3% isoflurane in oxygen. Buprenorphine (0.05-0.1 mg/kg s.c.) was injected subcutaneously. A longitudinal incision (0.5cm) was made in the anterior midline of the neck, to expose the trachea. An 18-gauge angiocatheter was then advanced through the mouth into the trachea under direct vision using a dissecting microscope (Zeiss Opmi 6, Carl Zeiss MicroImaging, Inc., Thorwood, NY), and then connected to a rodent ventilator (Hugo-Sachs) set at a respiratory rate of 250 breaths per min with a tidal volume of 275 µl. The animal was then rotated to the right lateral decubitus position, and a 1.0 cm lateral incision was made between the left side 4th and 5th intercostal space. The muscle layers were divided sharply establishing access to the

thoracic space. Baseline aortic dimensions were obtained by video microscopy using a 3 megapixel color CCD camera (PAXcam3; MIS Inc., Villa Park, IL) linked to a computer running PAX-it image management software with the live measurement module (MIS, Inc., Villa Park, IL). Following baseline aortic diameter measurements, a 3x1x8 mm sponge soaked in 0.5 M $CaCl_2$ prepared in normal saline was placed on the distal half of the exposed descending thoracic aorta in direct contact with the periadventitial surface. After 15 min, the $CaCl_2$-soaked sponge was removed, and the thoracic cavity was irrigated liberally with normal saline. Following lung re-expansion by obstructing the outflow on the rodent ventilator for two breaths, the ribs were approximated with 7–0 suture. The muscle layers were then closed, and the animal was rotated to the prone position. Recovery was established using positive-pressure ventilation with 100% oxygen, and, following extubation the animal was monitored for spontaneous respiration then placed in a high oxygen content warmer for further recovery. The day after TAA induction, the hsa-miR-133a lentiviral construct (CS970MR-1; System Biosciences) ($1x10^9$ pfu in 100µl normal saline) was delivered via tail vein injection.

Cellular Proliferation

Thoracic aortic fibroblasts were seeded at 1,000 cells per well of a 96 well clear bottom plate (Costar Flat bottom Cell bind Surface [Poly-D-Lysine] Cat# 3300, Corning, NY), and allowed to adhere overnight. The following day growth media was aspirated and replaced with fresh complete media. CyQuant Direct

Cell Proliferation Assay (Cat#C35011, Molecular probes) kit was then used to determine cell number. The basis of the CyQUANT kit is the use of a green fluorescent dye, which exhibits strong fluorescence enhancement when bound to cellular nucleic acids. This kit will be allowed to equilibrate to room temperature and the following will be mixed: PBS (97.5%), Cyquant Direct nucleic acid stain (0.004%), and direct background suppressor (0.02%). 12 hours following the addition of fresh complete phenol-free fibroblast growth media, an equal volume of 2X Detection reagent will be added to the cells in the culture media (assay is compatible in media with or without serum). Cells were then incubated for 1 hour at 37°C with 5% CO2. Following the one hour incubation time, fluorescence was read from the bottom of the well at 480/535 Ex/Em. This was then repeated at the denoted time points. For each cell line, a standard curve was generated by preparation of a serial dilution of cell numbers ranging from 500 to 5,000. These cells were allowed to adhere overnight, and then assayed directly by CyQUANT. Fluorescence was then read from the bottom of the well at 480/535 Ex/Em. Relative fluorescence correlates linearly with cell number**.**

Cellular Migration

A Boyden chamber assay was used to determine migration of thoracic aortic fibroblasts. First, cellular proliferation was inhibited with the use of mitomycin C (8 ug/mL, 1 hour; Sigma, M4287), then media was replaced with fresh fibroblast growth media. The following day, cells were seeded ($2.5x10^5$ cells) into the upper chamber of the 8.0 µm pore polycarbonate membrane of the

Transwell (Corning; Tewksbury, MA) chamber. The cells were allowed to adhere overnight and then the media in the upper chamber was replaced with serum free fibroblast growth media, with complete media being added to the lower chamber. The cells were maintained under normal tissue culture conditions for 48 hours and then fixed by immersion of the membranes in methanol at room temperature for 30 minutes. The non-migrated cells on the top surface of the membrane were removed with a cotton swab. Membranes were stained in 0.1% crystal violet in a 20% methanol solution for 30 minutes. Stained membranes were examined by microscopy (10X) (Zeiss Axiovert 35). The number of cells which migrated through the membrane were counted in five random fields and expressed as the average number of cells per field of view.

MT1-MMP 3'UTR Target Confirmation

HT1080 cells, at a confluence of 70%, were co-transfected with DharmaFECT-Duo transfection reagent and either the miR-133a mimic or a non-mRNA targeting control (10 nM) and 100 ng of one of the following vectors: the empty 3'UTR vector, which contains only the luciferase gene and its constitutive promoter and serves as the positive control; the GAPDH 3'UTR, which contains the GAPDH 3' UTR cloned downstream of the luciferase gene; the random sequence 3'UTR, which contains non-conserved, non-genic and non-repetitive human genomic fragments cloned downstream of the luciferase gene; or the MT1-MMP 3' UTR plasmid, which contains the human MT1-MMP (NM_004995) 3'UTR cloned downstream of the luciferase gene. Reporter assays were

performed at 24 hours following transfection by the LightSwitch Luciferase Assay system (LS010, SwitchGear Genomics). Luminescence was quantitated by luminometer (VersaMax). All transfection experiments were performed four times in triplicate.

Data analysis.

All data were assessed for normality. All statistical tests utilized in data analysis for the determination of significance are listed in the corresponding figure legends. Statistical tests were performed using STATA (Intercooled STATA v8.2, College Station, TX). All data in figures were expressed as absolute value, or fold change, as indicated in the figure legends. The calculation of fold change was performed by setting the average of the control values to 1, then applying the derived coefficient to the full data set. This approach allows for sample variation to be assessed in both the control and experimental groups. Data are represented as mean ± standard error of the mean (SEM) in the text and figures. A p value of <0.05 was considered to be statistically significant.

List of References

1. Berne RM, Koeppen BM, and Stanton BA. *Berne & Levy physiology.* Philadelphia, PA: Mosby/Elsevier; 2010.
2. Ruddy JM, Jones JA, Spinale FG, and Ikonomidis JS. Regional heterogeneity within the aorta: relevance to aneurysm disease. *J Thorac Cardiovasc Surg.* 2008;136(5):1123-30.
3. Westerhof N, Lankhaar JW, and Westerhof BE. The arterial Windkessel. *Med Biol Eng Comput.* 2009;47(2):131-41.
4. Tyberg JV, Davies JE, Wang Z, Whitelaw WA, Flewitt JA, Shrive NG, et al. Wave intensity analysis and the development of the reservoir-wave approach. *Med Biol Eng Comput.* 2009;47(2):221-32.
5. Murgo JP, Westerhof N, Giolma JP, and Altobelli SA. Aortic input impedance in normal man: relationship to pressure wave forms. *Circulation.* 1980;62(1):105-16.
6. Wilkinson IB, Cockcroft JR, and Webb DJ. Pulse wave analysis and arterial stiffness. *Journal of cardiovascular pharmacology.* 1998;32 Suppl 3:S33-7.
7. Ladich E, Yahagi K, Romero ME, and Virmani R. Vascular diseases: aortitis, aortic aneurysms, and vascular calcification. *Cardiovasc Pathol.* 2016;25(5):432-41.
8. Maedeker JA, Stoka KV, Bhayani SA, Gardner WS, Bennett L, Procknow JD, et al. Hypertension and decreased aortic compliance due to reduced elastin amounts do not increase atherosclerotic plaque accumulation in Ldlr-/- mice. *Atherosclerosis.* 2016;249:22-9.
9. Wagenseil JE, and Mecham RP. Vascular extracellular matrix and arterial mechanics. *Physiol Rev.* 2009;89(3):957-89.
10. Boron WF, and Boulpaep EL. *Medical physiology : a cellular and molecular approach.* Philadelphia, PA: Saunders/Elsevier; 2009.
11. Takahashi A, Okada R, Nagao K, Kawamata Y, Hanyu A, Yoshimoto S, et al. Exosomes maintain cellular homeostasis by excreting harmful DNA from cells. *Nat Commun.* 2017;8:15287.
12. Oxlund H, and Andreassen TT. The roles of hyaluronic acid, collagen and elastin in the mechanical properties of connective tissues. *J Anat.* 1980;131(Pt 4):611-20.
13. Silver FH, Horvath I, and Foran DJ. Viscoelasticity of the vessel wall: the role of collagen and elastic fibers. *Critical reviews in biomedical engineering.* 2001;29(3):279-301.
14. Chaichana T, Sun Z, and Jewkes J. Computation of hemodynamics in the left coronary artery with variable angulations. *J Biomech.* 2011;44(10):1869-78.

15. Wasilewski J, Mirota K, Wilczek K, Glowacki J, and Polonski L. Calcific aortic valve damage as a risk factor for cardiovascular events. *Pol J Radiol.* 2012;77(4):30-4.
16. Wasilewski J, Glowacki J, and Polonski L. Not at random location of atherosclerotic lesions in thoracic aorta and their prognostic significance in relation to the risk of cardiovascular events. *Pol J Radiol.* 2013;78(2):38-42.
17. Elefteriades JA. Thoracic aortic aneurysm: reading the enemy's playbook. *Curr Probl Cardiol.* 2008;33(5):203-77.
18. Stenmark KR, Yeager ME, El Kasmi KC, Nozik-Grayck E, Gerasimovskaya EV, Li M, et al. The adventitia: essential regulator of vascular wall structure and function. *Annual review of physiology.* 2013;75:23-47.
19. Psaltis PJ, Harbuzariu A, Delacroix S, Witt TA, Holroyd EW, Spoon DB, et al. Identification of a monocyte-predisposed hierarchy of hematopoietic progenitor cells in the adventitia of postnatal murine aorta. *Circulation.* 2012;125(4):592-603.
20. Stenmark KR, Davie N, Frid M, Gerasimovskaya E, and Das M. Role of the adventitia in pulmonary vascular remodeling. *Physiology (Bethesda).* 2006;21:134-45.
21. Pagano PJ, and Gutterman DD. The adventitia: the outs and ins of vascular disease. *Cardiovascular research.* 2007;75(4):636-9.
22. Di Wang H, Ratsep MT, Chapman A, and Boyd R. Adventitial fibroblasts in vascular structure and function: the role of oxidative stress and beyond. *Canadian journal of physiology and pharmacology.* 2010;88(3):177-86.
23. Heron M. Deaths: leading causes for 2009. *National vital statistics reports : from the Centers for Disease Control and Prevention, National Center for Health Statistics, National Vital Statistics System.* 2012;61(7):1-94.
24. Heron M. Deaths: leading causes for 2010. *National vital statistics reports : from the Centers for Disease Control and Prevention, National Center for Health Statistics, National Vital Statistics System.* 2013;62(6):1-96.
25. Ziganshin BA, and Elefteriades JA. Treatment of Thoracic Aortic Aneurysm: Role of Earlier Intervention. *Seminars in thoracic and cardiovascular surgery.* 2015;27(2):135-43.
26. Forsdahl SH, Singh K, Solberg S, and Jacobsen BK. Risk factors for abdominal aortic aneurysms: a 7-year prospective study: the Tromso Study, 1994-2001. *Circulation.* 2009;119(16):2202-8.
27. El-Hamamsy I, and Yacoub MH. Cellular and molecular mechanisms of thoracic aortic aneurysms. *Nat Rev Cardiol.* 2009;6(12):771-86.
28. Kuzmik GA, Sang AX, and Elefteriades JA. Natural history of thoracic aortic aneurysms. *J Vasc Surg.* 2012;56(2):565-71.
29. Coady MA, Rizzo JA, and Elefteriades JA. Developing surgical intervention criteria for thoracic aortic aneurysms. *Cardiology clinics.* 1999;17(4):827-39.
30. Gray JR, and Davies SJ. Marfan syndrome. *J Med Genet.* 1996;33(5):403-8.
31. Hwa J, Richards JG, Huang H, McKay D, Pressley L, Hughes CF, et al. The natural history of aortic dilatation in Marfan syndrome. *Med J Aust.* 1993;158(8):558-62.
32. Halliday DJ, Hutchinson S, Lonie L, Hurst JA, Firth H, Handford PA, et al. Twelve novel FBN1 mutations in Marfan syndrome and Marfan related phenotypes test the feasibility of FBN1 mutation testing in clinical practice. *J Med Genet.* 2002;39(8):589-93.
33. Nijbroek G, Sood S, McIntosh I, Francomano CA, Bull E, Pereira L, et al. Fifteen novel FBN1 mutations causing Marfan syndrome detected by heteroduplex analysis of genomic amplicons. *Am J Hum Genet.* 1995;57(1):8-21.

34. Dietz HC, and Pyeritz RE. Mutations in the human gene for fibrillin-1 (FBN1) in the Marfan syndrome and related disorders. *Hum Mol Genet.* 1995;4 Spec No:1799-809.
35. Kielty CM, Sherratt MJ, Marson A, and Baldock C. Fibrillin microfibrils. *Adv Protein Chem.* 2005;70:405-36.
36. Isogai Z, Ono RN, Ushiro S, Keene DR, Chen Y, Mazzieri R, et al. Latent transforming growth factor beta-binding protein 1 interacts with fibrillin and is a microfibril-associated protein. *J Biol Chem.* 2003;278(4):2750-7.
37. Neptune ER, Frischmeyer PA, Arking DE, Myers L, Bunton TE, Gayraud B, et al. Dysregulation of TGF-beta activation contributes to pathogenesis in Marfan syndrome. *Nat Genet.* 2003;33(3):407-11.
38. Habashi JP, Judge DP, Holm TM, Cohn RD, Loeys BL, Cooper TK, et al. Losartan, an AT1 antagonist, prevents aortic aneurysm in a mouse model of Marfan syndrome. *Science.* 2006;312(5770):117-21.
39. Van Hemelrijk C, Renard M, and Loeys B. The Loeys-Dietz syndrome: an update for the clinician. *Curr Opin Cardiol.* 2010;25(6):546-51.
40. Loeys BL, Chen J, Neptune ER, Judge DP, Podowski M, Holm T, et al. A syndrome of altered cardiovascular, craniofacial, neurocognitive and skeletal development caused by mutations in TGFBR1 or TGFBR2. *Nat Genet.* 2005;37(3):275-81.
41. Germain DP. Ehlers-Danlos syndrome type IV. *Orphanet J Rare Dis.* 2007;2:32.
42. Pomianowski P, and Elefteriades JA. The genetics and genomics of thoracic aortic disease. *Ann Cardiothorac Surg.* 2013;2(3):271-9.
43. Guo DC, Pannu H, Tran-Fadulu V, Papke CL, Yu RK, Avidan N, et al. Mutations in smooth muscle alpha-actin (ACTA2) lead to thoracic aortic aneurysms and dissections. *Nat Genet.* 2007;39(12):1488-93.
44. Zhu L, Vranckx R, Khau Van Kien P, Lalande A, Boisset N, Mathieu F, et al. Mutations in myosin heavy chain 11 cause a syndrome associating thoracic aortic aneurysm/aortic dissection and patent ductus arteriosus. *Nat Genet.* 2006;38(3):343-9.
45. Pannu H, Tran-Fadulu V, Papke CL, Scherer S, Liu Y, Presley C, et al. MYH11 mutations result in a distinct vascular pathology driven by insulin-like growth factor 1 and angiotensin II. *Hum Mol Genet.* 2007;16(20):2453-62.
46. Hoffman JI, and Kaplan S. The incidence of congenital heart disease. *J Am Coll Cardiol.* 2002;39(12):1890-900.
47. Hahn RT, Roman MJ, Mogtader AH, and Devereux RB. Association of aortic dilation with regurgitant, stenotic and functionally normal bicuspid aortic valves. *J Am Coll Cardiol.* 1992;19(2):283-8.
48. Svensson LG, Blackstone EH, and Cosgrove DM, 3rd. Surgical options in young adults with aortic valve disease. *Curr Probl Cardiol.* 2003;28(7):417-80.
49. Svensson LG. Aortic valve stenosis and regurgitation: an overview of management. *J Cardiovasc Surg (Torino).* 2008;49(2):297-303.
50. Booher AM, and Eagle KA. Diagnosis and management issues in thoracic aortic aneurysm. *Am Heart J.* 2011;162(1):38-46 e1.
51. Erbel R, Alfonso F, Boileau C, Dirsch O, Eber B, Haverich A, et al. Diagnosis and management of aortic dissection. *Eur Heart J.* 2001;22(18):1642-81.
52. Hiratzka LF, Bakris GL, Beckman JA, Bersin RM, Carr VF, Casey DE, Jr., et al. 2010 ACCF/AHA/AATS/ACR/ASA/SCA/SCAI/SIR/STS/SVM Guidelines for the diagnosis and management of patients with thoracic aortic disease: Executive summary: A report of

the American College of Cardiology Foundation/American Heart Association Task Force on Practice Guidelines, American Association for Thoracic Surgery, American College of Radiology, American Stroke Association, Society of Cardiovascular Anesthesiologists, Society for Cardiovascular Angiography and Interventions, Society of Interventional Radiology, Society of Thoracic Surgeons, and Society for Vascular Medicine. *Anesth Analg.* 2010;111(2):279-315.

53. Rajiah P. CT and MRI in the Evaluation of Thoracic Aortic Diseases. *Int J Vasc Med.* 2013;2013:797189.
54. Elefteriades JA. Thoracic aortic aneurysm: reading the enemy's playbook. *Yale J Biol Med.* 2008;81(4):175-86.
55. Wallukat G. The beta-adrenergic receptors. *Herz.* 2002;27(7):683-90.
56. Chakkour K, Gouny P, Nussaume O, and Vayssairat M. [Medical treatment of aortic aneurysms using beta-blockers]. *J Mal Vasc.* 1995;20(4):288-9.
57. Wheat MW, Jr., Palmer RF, Bartley TD, and Seelman RC. Treatment of Dissecting Aneurysms of the Aorta without Surgery. *J Thorac Cardiovasc Surg.* 1965;50:364-73.
58. Shores J, Berger KR, Murphy EA, and Pyeritz RE. Progression of aortic dilatation and the benefit of long-term beta-adrenergic blockade in Marfan's syndrome. *N Engl J Med.* 1994;330(19):1335-41.
59. Selamet Tierney ES, Feingold B, Printz BF, Park SC, Graham D, Kleinman CS, et al. Beta-blocker therapy does not alter the rate of aortic root dilation in pediatric patients with Marfan syndrome. *J Pediatr.* 2007;150(1):77-82.
60. Yetman AT, Bornemeier RA, and McCrindle BW. Usefulness of enalapril versus propranolol or atenolol for prevention of aortic dilation in patients with the Marfan syndrome. *Am J Cardiol.* 2005;95(9):1125-7.
61. Gersony DR, McClaughlin MA, Jin Z, and Gersony WM. The effect of beta-blocker therapy on clinical outcome in patients with Marfan's syndrome: a meta-analysis. *Int J Cardiol.* 2007;114(3):303-8.
62. Bonser RS, Pagano D, Lewis ME, Rooney SJ, Guest P, Davies P, et al. Clinical and patho-anatomical factors affecting expansion of thoracic aortic aneurysms. *Heart.* 2000;84(3):277-83.
63. Coady MA, Rizzo JA, Goldstein LJ, and Elefteriades JA. Natural history, pathogenesis, and etiology of thoracic aortic aneurysms and dissections. *Cardiology clinics.* 1999;17(4):615-35; vii.
64. Lohse F, Lang N, Schiller W, Roell W, Dewald O, Preusse CJ, et al. Quality of life after replacement of the ascending aorta in patients with true aneurysms. *Tex Heart Inst J.* 2009;36(2):104-10.
65. Crawford ES, Hess KR, Cohen ES, Coselli JS, and Safi HJ. Ruptured aneurysm of the descending thoracic and thoracoabdominal aorta. Analysis according to size and treatment. *Ann Surg.* 1991;213(5):417-25; discussion 25-6.
66. Kouchoukos NT, and Dougenis D. Surgery of the thoracic aorta. *N Engl J Med.* 1997;336(26):1876-88.
67. Estrera AL, Rubenstein FS, Miller CC, 3rd, Huynh TT, Letsou GV, and Safi HJ. Descending thoracic aortic aneurysm: surgical approach and treatment using the adjuncts cerebrospinal fluid drainage and distal aortic perfusion. *Ann Thorac Surg.* 2001;72(2):481-6.

68. Coselli JS, LeMaire SA, Conklin LD, and Adams GJ. Left heart bypass during descending thoracic aortic aneurysm repair does not reduce the incidence of paraplegia. *Ann Thorac Surg.* 2004;77(4):1298-303; discussion 303.
69. Karthikesalingam A, Bahia SS, Patterson BO, Peach G, Vidal-Diez A, Ray KK, et al. The shortfall in long-term survival of patients with repaired thoracic or abdominal aortic aneurysms: retrospective case-control analysis of hospital episode statistics. *Eur J Vasc Endovasc Surg.* 2013;46(5):533-41.
70. Coady MA, Ikonomidis JS, Cheung AT, Matsumoto AH, Dake MD, Chaikof EL, et al. Surgical management of descending thoracic aortic disease: open and endovascular approaches: a scientific statement from the American Heart Association. *Circulation.* 2010;121(25):2780-804.
71. Mitchell RS. Presented at the 85th Annual Meeting of the American Association for Thoracic Surgery, San Francisco, California.; 2005.
72. Stone DH, Brewster DC, Kwolek CJ, Lamuraglia GM, Conrad MF, Chung TK, et al. Stent-graft versus open-surgical repair of the thoracic aorta: mid-term results. *J Vasc Surg.* 2006;44(6):1188-97.
73. Goodney PP, Travis L, Lucas FL, Fillinger MF, Goodman DC, Cronenwett JL, et al. Survival after open versus endovascular thoracic aortic aneurysm repair in an observational study of the Medicare population. *Circulation.* 2011;124(24):2661-9.
74. von Allmen RS, Anjum A, and Powell JT. Outcomes after endovascular or open repair for degenerative descending thoracic aortic aneurysm using linked hospital data. *Br J Surg.* 2014;101(10):1244-51.
75. Daugherty A, and Cassis LA. Mouse models of abdominal aortic aneurysms. *Arterioscler Thromb Vasc Biol.* 2004;24(3):429-34.
76. Dobrin PB. Animal models of aneurysms. *Ann Vasc Surg.* 1999;13(6):641-8.
77. Anidjar S, Salzmann JL, Gentric D, Lagneau P, Camilleri JP, and Michel JB. Elastase-induced experimental aneurysms in rats. *Circulation.* 1990;82(3):973-81.
78. Pyo R, Lee JK, Shipley JM, Curci JA, Mao D, Ziporin SJ, et al. Targeted gene disruption of matrix metalloproteinase-9 (gelatinase B) suppresses development of experimental abdominal aortic aneurysms. *J Clin Invest.* 2000;105(11):1641-9.
79. Daugherty A, and Cassis L. Chronic angiotensin II infusion promotes atherogenesis in low density lipoprotein receptor -/- mice. *Ann N Y Acad Sci.* 1999;892:108-18.
80. Lu H, Howatt DA, Balakrishnan A, Moorleghen JJ, Rateri DL, Cassis LA, et al. Subcutaneous Angiotensin II Infusion using Osmotic Pumps Induces Aortic Aneurysms in Mice. *J Vis Exp.* 2015(103).
81. Chiou AC, Chiu B, and Pearce WH. Murine aortic aneurysm produced by periarterial application of calcium chloride. *J Surg Res.* 2001;99(2):371-6.
82. Ikonomidis JS, Gibson WC, Gardner J, Sweterlitsch S, Thompson RP, Mukherjee R, et al. A murine model of thoracic aortic aneurysms. *J Surg Res.* 2003;115(1):157-63.
83. Bhamidipati CM, Mehta GS, Lu G, Moehle CW, Barbery C, DiMusto PD, et al. Development of a novel murine model of aortic aneurysms using peri-adventitial elastase. *Surgery.* 2012;152(2):238-46.
84. Crowley SD, Gurley SB, Herrera MJ, Ruiz P, Griffiths R, Kumar AP, et al. Angiotensin II causes hypertension and cardiac hypertrophy through its receptors in the kidney. *Proceedings of the National Academy of Sciences of the United States of America.* 2006;103(47):17985-90.

85. Qin Z. Newly developed angiotensin II-infused experimental models in vascular biology. *Regul Pept.* 2008;150(1-3):1-6.
86. Weiss D, Sorescu D, and Taylor WR. Angiotensin II and atherosclerosis. *Am J Cardiol.* 2001;87(8A):25C-32C.
87. Daugherty A, Manning MW, and Cassis LA. Angiotensin II promotes atherosclerotic lesions and aneurysms in apolipoprotein E-deficient mice. *J Clin Invest.* 2000;105(11):1605-12.
88. Daugherty A, Rateri DL, Charo IF, Owens AP, Howatt DA, and Cassis LA. Angiotensin II infusion promotes ascending aortic aneurysms: attenuation by CCR2 deficiency in apoE-/- mice. *Clin Sci (Lond).* 2010;118(11):681-9.
89. Deng GG, Martin-McNulty B, Sukovich DA, Freay A, Halks-Miller M, Thinnes T, et al. Urokinase-type plasminogen activator plays a critical role in angiotensin II-induced abdominal aortic aneurysm. *Circ Res.* 2003;92(5):510-7.
90. Uchida HA, Sugiyama H, Takiue K, Kikumoto Y, Inoue T, and Makino H. Development of angiotensin II-induced abdominal aortic aneurysms is independent of catalase in mice. *Journal of cardiovascular pharmacology.* 2011;58(6):633-8.
91. Gertz SD, Kurgan A, and Eisenberg D. Aneurysm of the rabbit common carotid artery induced by periarterial application of calcium chloride in vivo. *J Clin Invest.* 1988;81(3):649-56.
92. Longo GM, Xiong W, Greiner TC, Zhao Y, Fiotti N, and Baxter BT. Matrix metalloproteinases 2 and 9 work in concert to produce aortic aneurysms. *J Clin Invest.* 2002;110(5):625-32.
93. Freestone T, Turner RJ, Coady A, Higman DJ, Greenhalgh RM, and Powell JT. Inflammation and matrix metalloproteinases in the enlarging abdominal aortic aneurysm. *Arterioscler Thromb Vasc Biol.* 1995;15(8):1145-51.
94. Jones JA, Beck C, Barbour JR, Zavadzkas JA, Mukherjee R, Spinale FG, et al. Alterations in aortic cellular constituents during thoracic aortic aneurysm development: myofibroblast-mediated vascular remodeling. *Am J Pathol.* 2009;175(4):1746-56.
95. Goldsmith EC, Hoffman A, Morales MO, Potts JD, Price RL, McFadden A, et al. Organization of fibroblasts in the heart. *Dev Dyn.* 2004;230(4):787-94.
96. Osborn M, and Weber K. Tumor diagnosis by intermediate filament typing: a novel tool for surgical pathology. *Lab Invest.* 1983;48(4):372-94.
97. Rungger-Brandle E, and Gabbiani G. The role of cytoskeletal and cytocontractile elements in pathologic processes. *Am J Pathol.* 1983;110(3):361-92.
98. Skalli O, Schurch W, Seemayer T, Lagace R, Montandon D, Pittet B, et al. Myofibroblasts from diverse pathologic settings are heterogeneous in their content of actin isoforms and intermediate filament proteins. *Lab Invest.* 1989;60(2):275-85.
99. Salvesen GS. Caspases: opening the boxes and interpreting the arrows. *Cell Death Differ.* 2002;9(1):3-5.
100. Xiong W, Knispel R, MacTaggart J, Greiner TC, Weiss SJ, and Baxter BT. Membrane-type 1 matrix metalloproteinase regulates macrophage-dependent elastolytic activity and aneurysm formation in vivo. *J Biol Chem.* 2009;284(3):1765-71.
101. Della Corte A, Quarto C, Bancone C, Castaldo C, Di Meglio F, Nurzynska D, et al. Spatiotemporal patterns of smooth muscle cell changes in ascending aortic dilatation with bicuspid and tricuspid aortic valve stenosis: focus on cell-matrix signaling. *J Thorac Cardiovasc Surg.* 2008;135(1):8-18, e1-2.

102. Mugge A. The role of reactive oxygen species in atherosclerosis. *Z Kardiol.* 1998;87(11):851-64.
103. Miller FJ, Jr., Sharp WJ, Fang X, Oberley LW, Oberley TD, and Weintraub NL. Oxidative stress in human abdominal aortic aneurysms: a potential mediator of aneurysmal remodeling. *Arterioscler Thromb Vasc Biol.* 2002;22(4):560-5.
104. Ejiri J, Inoue N, Tsukube T, Munezane T, Hino Y, Kobayashi S, et al. Oxidative stress in the pathogenesis of thoracic aortic aneurysm: protective role of statin and angiotensin II type 1 receptor blocker. *Cardiovascular research.* 2003;59(4):988-96.
105. Griendling KK, and FitzGerald GA. Oxidative stress and cardiovascular injury: Part I: basic mechanisms and in vivo monitoring of ROS. *Circulation.* 2003;108(16):1912-6.
106. Rajagopalan S, Meng XP, Ramasamy S, Harrison DG, and Galis ZS. Reactive oxygen species produced by macrophage-derived foam cells regulate the activity of vascular matrix metalloproteinases in vitro. Implications for atherosclerotic plaque stability. *J Clin Invest.* 1996;98(11):2572-9.
107. Li PF, Dietz R, and von Harsdorf R. Reactive oxygen species induce apoptosis of vascular smooth muscle cell. *FEBS Lett.* 1997;404(2-3):249-52.
108. Thomas M, Gavrila D, McCormick ML, Miller FJ, Jr., Daugherty A, Cassis LA, et al. Deletion of p47phox attenuates angiotensin II-induced abdominal aortic aneurysm formation in apolipoprotein E-deficient mice. *Circulation.* 2006;114(5):404-13.
109. Xiong W, Mactaggart J, Knispel R, Worth J, Zhu Z, Li Y, et al. Inhibition of reactive oxygen species attenuates aneurysm formation in a murine model. *Atherosclerosis.* 2009;202(1):128-34.
110. Gabbiani G. The biology of the myofibroblast. *Kidney Int.* 1992;41(3):530-2.
111. Hinz B. Formation and function of the myofibroblast during tissue repair. *J Invest Dermatol.* 2007;127(3):526-37.
112. Desmouliere A, Darby IA, and Gabbiani G. Normal and pathologic soft tissue remodeling: role of the myofibroblast, with special emphasis on liver and kidney fibrosis. *Lab Invest.* 2003;83(12):1689-707.
113. Kessler D, Dethlefsen S, Haase I, Plomann M, Hirche F, Krieg T, et al. Fibroblasts in mechanically stressed collagen lattices assume a "synthetic" phenotype. *J Biol Chem.* 2001;276(39):36575-85.
114. Gabbiani G. Some historical and philosophical reflections on the myofibroblast concept. *Curr Top Pathol.* 1999;93:1-5.
115. Jones JA, Barbour JR, Lowry AS, Bouges S, Beck C, McClister DM, Jr., et al. Spatiotemporal expression and localization of matrix metalloproteinas-9 in a murine model of thoracic aortic aneurysm. *J Vasc Surg.* 2006;44(6):1314-21.
116. Irizarry E, Newman KM, Gandhi RH, Nackman GB, Halpern V, Wishner S, et al. Demonstration of interstitial collagenase in abdominal aortic aneurysm disease. *J Surg Res.* 1993;54(6):571-4.
117. Raffetto JD, and Khalil RA. Matrix metalloproteinases and their inhibitors in vascular remodeling and vascular disease. *Biochem Pharmacol.* 2008;75(2):346-59.
118. Hynes RO. The extracellular matrix: not just pretty fibrils. *Science.* 2009;326(5957):1216-9.
119. Annes JP, Munger JS, and Rifkin DB. Making sense of latent TGFbeta activation. *J Cell Sci.* 2003;116(Pt 2):217-24.

120. Verrecchia F, and Mauviel A. Transforming growth factor-beta and fibrosis. *World J Gastroenterol.* 2007;13(22):3056-62.
121. Bobik A, Agrotis A, Kanellakis P, Dilley R, Krushinsky A, Smirnov V, et al. Distinct patterns of transforming growth factor-beta isoform and receptor expression in human atherosclerotic lesions. Colocalization implicates TGF-beta in fibrofatty lesion development. *Circulation.* 1999;99(22):2883-91.
122. Gaine SP, and Rubin LJ. Primary pulmonary hypertension. *Lancet.* 1998;352(9129):719-25.
123. Jones JA, Spinale FG, and Ikonomidis JS. Transforming growth factor-beta signaling in thoracic aortic aneurysm development: a paradox in pathogenesis. *J Vasc Res.* 2009;46(2):119-37.
124. Shi Y, and Massague J. Mechanisms of TGF-beta signaling from cell membrane to the nucleus. *Cell.* 2003;113(6):685-700.
125. Ihn H. Pathogenesis of fibrosis: role of TGF-beta and CTGF. *Curr Opin Rheumatol.* 2002;14(6):681-5.
126. Moussad EE, and Brigstock DR. Connective tissue growth factor: what's in a name? *Mol Genet Metab.* 2000;71(1-2):276-92.
127. Pan X, Chen Z, Huang R, Yao Y, and Ma G. Transforming growth factor beta1 induces the expression of collagen type I by DNA methylation in cardiac fibroblasts. *PLoS One.* 2013;8(4):e60335.
128. Feng XH, and Derynck R. Specificity and versatility in tgf-beta signaling through Smads. *Annu Rev Cell Dev Biol.* 2005;21:659-93.
129. Moustakas A, Souchelnytskyi S, and Heldin CH. Smad regulation in TGF-beta signal transduction. *J Cell Sci.* 2001;114(Pt 24):4359-69.
130. Chen YG, and Massague J. Smad1 recognition and activation by the ALK1 group of transforming growth factor-beta family receptors. *J Biol Chem.* 1999;274(6):3672-7.
131. Oh SP, Seki T, Goss KA, Imamura T, Yi Y, Donahoe PK, et al. Activin receptor-like kinase 1 modulates transforming growth factor-beta 1 signaling in the regulation of angiogenesis. *Proceedings of the National Academy of Sciences of the United States of America.* 2000;97(6):2626-31.
132. Goumans MJ, Lebrin F, and Valdimarsdottir G. Controlling the angiogenic switch: a balance between two distinct TGF-b receptor signaling pathways. *Trends Cardiovasc Med.* 2003;13(7):301-7.
133. Goumans MJ, Valdimarsdottir G, Itoh S, Rosendahl A, Sideras P, and ten Dijke P. Balancing the activation state of the endothelium via two distinct TGF-beta type I receptors. *EMBO J.* 2002;21(7):1743-53.
134. Jones JA, Barbour JR, Stroud RE, Bouges S, Stephens SL, Spinale FG, et al. Altered transforming growth factor-beta signaling in a murine model of thoracic aortic aneurysm. *J Vasc Res.* 2008;45(6):457-68.
135. Fukui D, Miyagawa S, Soeda J, Tanaka K, Urayama H, and Kawasaki S. Overexpression of transforming growth factor beta1 in smooth muscle cells of human abdominal aortic aneurysm. *Eur J Vasc Endovasc Surg.* 2003;25(6):540-5.
136. Willis BC, and Borok Z. TGF-beta-induced EMT: mechanisms and implications for fibrotic lung disease. *Am J Physiol Lung Cell Mol Physiol.* 2007;293(3):L525-34.

137. Shi Y, O'Brien JE, Jr., Fard A, and Zalewski A. Transforming growth factor-beta 1 expression and myofibroblast formation during arterial repair. *Arterioscler Thromb Vasc Biol.* 1996;16(10):1298-305.
138. Vaughan MB, Howard EW, and Tomasek JJ. Transforming growth factor-beta1 promotes the morphological and functional differentiation of the myofibroblast. *Exp Cell Res.* 2000;257(1):180-9.
139. Daugherty A, Manning MW, and Cassis LA. Antagonism of AT2 receptors augments angiotensin II-induced abdominal aortic aneurysms and atherosclerosis. *Br J Pharmacol.* 2001;134(4):865-70.
140. Detaint D, Aegerter P, Tubach F, Hoffman I, Plauchu H, Dulac Y, et al. Rationale and design of a randomized clinical trial (Marfan Sartan) of angiotensin II receptor blocker therapy versus placebo in individuals with Marfan syndrome. *Arch Cardiovasc Dis.* 2010;103(5):317-25.
141. Lareyre F, Clement M, Raffort J, Pohlod S, Patel M, Esposito B, et al. TGFbeta (Transforming Growth Factor-beta) Blockade Induces a Human-Like Disease in a Nondissecting Mouse Model of Abdominal Aortic Aneurysm. *Arterioscler Thromb Vasc Biol.* 2017;37(11):2171-81.
142. Lindsey ML, Mann DL, Entman ML, and Spinale FG. Extracellular matrix remodeling following myocardial injury. *Annals of medicine.* 2003;35(5):316-26.
143. Brinckerhoff CE, and Matrisian LM. Matrix metalloproteinases: a tail of a frog that became a prince. *Nat Rev Mol Cell Biol.* 2002;3(3):207-14.
144. Galis ZS, and Khatri JJ. Matrix metalloproteinases in vascular remodeling and atherogenesis: the good, the bad, and the ugly. *Circ Res.* 2002;90(3):251-62.
145. Visse R, and Nagase H. Matrix metalloproteinases and tissue inhibitors of metalloproteinases: structure, function, and biochemistry. *Circ Res.* 2003;92(8):827-39.
146. Allan JA, Docherty AJ, Barker PJ, Huskisson NS, Reynolds JJ, and Murphy G. Binding of gelatinases A and B to type-I collagen and other matrix components. *Biochem J.* 1995;309 (Pt 1):299-306.
147. Bini A, Itoh Y, Kudryk BJ, and Nagase H. Degradation of cross-linked fibrin by matrix metalloproteinase 3 (stromelysin 1): hydrolysis of the gamma Gly 404-Ala 405 peptide bond. *Biochemistry.* 1996;35(40):13056-63.
148. Nagase H, Visse R, and Murphy G. Structure and function of matrix metalloproteinases and TIMPs. *Cardiovascular research.* 2006;69(3):562-73.
149. Lee Y, Kim M, Han J, Yeom KH, Lee S, Baek SH, et al. MicroRNA genes are transcribed by RNA polymerase II. *EMBO J.* 2004;23(20):4051-60.
150. Nagase H, and Woessner JF, Jr. Matrix metalloproteinases. *J Biol Chem.* 1999;274(31):21491-4.
151. Matrisian LM. Matrix metalloproteinase gene expression. *Ann N Y Acad Sci.* 1994;732:42-50.
152. Kozak M. Initiation of translation in prokaryotes and eukaryotes. *Gene.* 1999;234(2):187-208.
153. Humphreys DT, Westman BJ, Martin DI, and Preiss T. MicroRNAs control translation initiation by inhibiting eukaryotic initiation factor 4E/cap and poly(A) tail function. *Proceedings of the National Academy of Sciences of the United States of America.* 2005;102(47):16961-6.

154. Iwakawa HO, and Tomari Y. The Functions of MicroRNAs: mRNA Decay and Translational Repression. *Trends Cell Biol.* 2015;25(11):651-65.
155. Pei D, and Weiss SJ. Furin-dependent intracellular activation of the human stromelysin-3 zymogen. *Nature.* 1995;375(6528):244-7.
156. George SJ. Therapeutic potential of matrix metalloproteinase inhibitors in atherosclerosis. *Expert Opin Investig Drugs.* 2000;9(5):993-1007.
157. Becher N, Hein M, Uldbjerg N, and Danielsen CC. Balance between matrix metalloproteinases (MMP) and tissue inhibitors of metalloproteinases (TIMP) in the cervical mucus plug estimated by determination of free non-complexed TIMP. *Reprod Biol Endocrinol.* 2008;6:45.
158. Baker AH, Edwards DR, and Murphy G. Metalloproteinase inhibitors: biological actions and therapeutic opportunities. *J Cell Sci.* 2002;115(Pt 19):3719-27.
159. Goldberg GI, Marmer BL, Grant GA, Eisen AZ, Wilhelm S, and He CS. Human 72-kilodalton type IV collagenase forms a complex with a tissue inhibitor of metalloproteases designated TIMP-2. *Proceedings of the National Academy of Sciences of the United States of America.* 1989;86(21):8207-11.
160. Baker AH, Zaltsman AB, George SJ, and Newby AC. Divergent effects of tissue inhibitor of metalloproteinase-1, -2, or -3 overexpression on rat vascular smooth muscle cell invasion, proliferation, and death in vitro. TIMP-3 promotes apoptosis. *J Clin Invest.* 1998;101(6):1478-87.
161. Yamashita K, Suzuki M, Iwata H, Koike T, Hamaguchi M, Shinagawa A, et al. Tyrosine phosphorylation is crucial for growth signaling by tissue inhibitors of metalloproteinases (TIMP-1 and TIMP-2). *FEBS Lett.* 1996;396(1):103-7.
162. Tamarina NA, McMillan WD, Shively VP, and Pearce WH. Expression of matrix metalloproteinases and their inhibitors in aneurysms and normal aorta. *Surgery.* 1997;122(2):264-71; discussion 71-2.
163. George SJ, Johnson JL, Angelini GD, Newby AC, and Baker AH. Adenovirus-mediated gene transfer of the human TIMP-1 gene inhibits smooth muscle cell migration and neointimal formation in human saphenous vein. *Hum Gene Ther.* 1998;9(6):867-77.
164. George SJ, Baker AH, Angelini GD, and Newby AC. Gene transfer of tissue inhibitor of metalloproteinase-2 inhibits metalloproteinase activity and neointima formation in human saphenous veins. *Gene Ther.* 1998;5(11):1552-60.
165. Allaire E, Forough R, Clowes M, Starcher B, and Clowes AW. Local overexpression of TIMP-1 prevents aortic aneurysm degeneration and rupture in a rat model. *J Clin Invest.* 1998;102(7):1413-20.
166. Heagerty AM, Aalkjaer C, Bund SJ, Korsgaard N, and Mulvany MJ. Small artery structure in hypertension. Dual processes of remodeling and growth. *Hypertension.* 1993;21(4):391-7.
167. Sartore S, Chiavegato A, Faggin E, Franch R, Puato M, Ausoni S, et al. Contribution of adventitial fibroblasts to neointima formation and vascular remodeling: from innocent bystander to active participant. *Circ Res.* 2001;89(12):1111-21.
168. Isselbacher EM. Thoracic and abdominal aortic aneurysms. *Circulation.* 2005;111(6):816-28.
169. Ikonomidis JS, Barbour JR, Amani Z, Stroud RE, Herron AR, McClister DM, Jr., et al. Effects of deletion of the matrix metalloproteinase 9 gene on development of murine thoracic aortic aneurysms. *Circulation.* 2005;112(9 Suppl):I242-8.

170. Sinha I, Bethi S, Cronin P, Williams DM, Roelofs K, Ailawadi G, et al. A biologic basis for asymmetric growth in descending thoracic aortic aneurysms: a role for matrix metalloproteinase 9 and 2. *J Vasc Surg.* 2006;43(2):342-8.
171. Rizzoni D, Rodella L, Porteri E, Rezzani R, Sleiman I, Paiardi S, et al. Effects of losartan and enalapril at different doses on cardiac and renal interstitial matrix in spontaneously hypertensive rats. *Clin Exp Hypertens.* 2003;25(7):427-41.
172. Hackam DG, Thiruchelvam D, and Redelmeier DA. Angiotensin-converting enzyme inhibitors and aortic rupture: a population-based case-control study. *Lancet.* 2006;368(9536):659-65.
173. Sweeting MJ, Thompson SG, Brown LC, Greenhalgh RM, and Powell JT. Use of angiotensin converting enzyme inhibitors is associated with increased growth rate of abdominal aortic aneurysms. *J Vasc Surg.* 2010;52(1):1-4.
174. Zhang X, Shen YH, and LeMaire SA. Thoracic aortic dissection: are matrix metalloproteinases involved? *Vascular.* 2009;17(3):147-57.
175. Curci JA, Mao D, Bohner DG, Allen BT, Rubin BG, Reilly JM, et al. Preoperative treatment with doxycycline reduces aortic wall expression and activation of matrix metalloproteinases in patients with abdominal aortic aneurysms. *J Vasc Surg.* 2000;31(2):325-42.
176. Thompson RW, Liao S, and Curci JA. Therapeutic potential of tetracycline derivatives to suppress the growth of abdominal aortic aneurysms. *Adv Dent Res.* 1998;12(2):159-65.
177. Mosorin M, Juvonen J, Biancari F, Satta J, Surcel HM, Leinonen M, et al. Use of doxycycline to decrease the growth rate of abdominal aortic aneurysms: a randomized, double-blind, placebo-controlled pilot study. *J Vasc Surg.* 2001;34(4):606-10.
178. Baxter BT, Pearce WH, Waltke EA, Littooy FN, Hallett JW, Jr., Kent KC, et al. Prolonged administration of doxycycline in patients with small asymptomatic abdominal aortic aneurysms: report of a prospective (Phase II) multicenter study. *J Vasc Surg.* 2002;36(1):1-12.
179. Chung AW, Yang HH, Radomski MW, and van Breemen C. Long-term doxycycline is more effective than atenolol to prevent thoracic aortic aneurysm in marfan syndrome through the inhibition of matrix metalloproteinase-2 and -9. *Circ Res.* 2008;102(8):e73-85.
180. Mendes O, Kim HT, and Stoica G. Expression of MMP2, MMP9 and MMP3 in breast cancer brain metastasis in a rat model. *Clin Exp Metastasis.* 2005;22(3):237-46.
181. Beaudeux JL, Giral P, Bruckert E, Foglietti MJ, and Chapman MJ. Matrix metalloproteinases, inflammation and atherosclerosis: therapeutic perspectives. *Clin Chem Lab Med.* 2004;42(2):121-31.
182. Treharne GD, Boyle JR, Goodall S, Loftus IM, Bell PR, and Thompson MM. Marimastat inhibits elastin degradation and matrix metalloproteinase 2 activity in a model of aneurysm disease. *Br J Surg.* 1999;86(8):1053-8.
183. Peterson JT. Matrix metalloproteinase inhibitor development and the remodeling of drug discovery. *Heart Fail Rev.* 2004;9(1):63-79.
184. Peterson JT. The importance of estimating the therapeutic index in the development of matrix metalloproteinase inhibitors. *Cardiovascular research.* 2006;69(3):677-87.
185. Annabi B, Shedid D, Ghosn P, Kenigsberg RL, Desrosiers RR, Bojanowski MW, et al. Differential regulation of matrix metalloproteinase activities in abdominal aortic aneurysms. *J Vasc Surg.* 2002;35(3):539-46.

186. Ikonomidis JS, Jones JA, Barbour JR, Stroud RE, Clark LL, Kaplan BS, et al. Expression of matrix metalloproteinases and endogenous inhibitors within ascending aortic aneurysms of patients with Marfan syndrome. *Circulation.* 2006;114(1 Suppl):I365-70.
187. Nollendorfs A, Greiner TC, Nagase H, and Baxter BT. The expression and localization of membrane type-1 matrix metalloproteinase in human abdominal aortic aneurysms. *J Vasc Surg.* 2001;34(2):316-22.
188. Jones JA, Ruddy JM, Bouges S, Zavadzkas JA, Brinsa TA, Stroud RE, et al. Alterations in membrane type-1 matrix metalloproteinase abundance after the induction of thoracic aortic aneurysm in a murine model. *Am J Physiol Heart Circ Physiol.* 2010;299(1):H114-24.
189. Itoh Y, and Seiki M. MT1-MMP: a potent modifier of pericellular microenvironment. *J Cell Physiol.* 2006;206(1):1-8.
190. Imai K, Ohuchi E, Aoki T, Nomura H, Fujii Y, Sato H, et al. Membrane-type matrix metalloproteinase 1 is a gelatinolytic enzyme and is secreted in a complex with tissue inhibitor of metalloproteinases 2. *Cancer Res.* 1996;56(12):2707-10.
191. Sato H, Takino T, Kinoshita T, Imai K, Okada Y, Stetler Stevenson WG, et al. Cell surface binding and activation of gelatinase A induced by expression of membrane-type-1-matrix metalloproteinase (MT1-MMP). *FEBS Lett.* 1996;385(3):238-40.
192. Ikonomidis JS, Nadeau EK, Akerman AW, Stroud RE, Mukherjee R, and Jones JA. Regulation of membrane type-1 matrix metalloproteinase activity and intracellular localization in clinical thoracic aortic aneurysms. *J Thorac Cardiovasc Surg.* 2017;153(3):537-46.
193. Ashworth JL, Murphy G, Rock MJ, Sherratt MJ, Shapiro SD, Shuttleworth CA, et al. Fibrillin degradation by matrix metalloproteinases: implications for connective tissue remodelling. *Biochem J.* 1999;340 (Pt 1):171-81.
194. Tatti O, Vehvilainen P, Lehti K, and Keski-Oja J. MT1-MMP releases latent TGF-beta1 from endothelial cell extracellular matrix via proteolytic processing of LTBP-1. *Exp Cell Res.* 2008;314(13):2501-14.
195. Jones JA, Zavadzkas JA, Chang EI, Sheats N, Koval C, Stroud RE, et al. Cellular phenotype transformation occurs during thoracic aortic aneurysm development. *J Thorac Cardiovasc Surg.* 2010;140(3):653-9.
196. Bartel DP. MicroRNAs: genomics, biogenesis, mechanism, and function. *Cell.* 2004;116(2):281-97.
197. Krek A, Grun D, Poy MN, Wolf R, Rosenberg L, Epstein EJ, et al. Combinatorial microRNA target predictions. *Nat Genet.* 2005;37(5):495-500.
198. Small EM, Frost RJ, and Olson EN. MicroRNAs add a new dimension to cardiovascular disease. *Circulation.* 2010;121(8):1022-32.
199. Budak H, Bulut R, Kantar M, and Alptekin B. MicroRNA nomenclature and the need for a revised naming prescription. *Brief Funct Genomics.* 2016;15(1):65-71.
200. Schanen BC, and Li X. Transcriptional regulation of mammalian miRNA genes. *Genomics.* 2011;97(1):1-6.
201. Ozsolak F, Poling LL, Wang Z, Liu H, Liu XS, Roeder RG, et al. Chromatin structure analyses identify miRNA promoters. *Genes & development.* 2008;22(22):3172-83.
202. Corcoran DL, Pandit KV, Gordon B, Bhattacharjee A, Kaminski N, and Benos PV. Features of mammalian microRNA promoters emerge from polymerase II chromatin immunoprecipitation data. *PLoS One.* 2009;4(4):e5279.

203. Lee Y, Jeon K, Lee JT, Kim S, and Kim VN. MicroRNA maturation: stepwise processing and subcellular localization. *EMBO J.* 2002;21(17):4663-70.
204. Lee Y, Ahn C, Han J, Choi H, Kim J, Yim J, et al. The nuclear RNase III Drosha initiates microRNA processing. *Nature.* 2003;425(6956):415-9.
205. Bohnsack MT, Czaplinski K, and Gorlich D. Exportin 5 is a RanGTP-dependent dsRNA-binding protein that mediates nuclear export of pre-miRNAs. *RNA.* 2004;10(2):185-91.
206. Lund E, Guttinger S, Calado A, Dahlberg JE, and Kutay U. Nuclear export of microRNA precursors. *Science.* 2004;303(5654):95-8.
207. Hutvagner G, McLachlan J, Pasquinelli AE, Balint E, Tuschl T, and Zamore PD. A cellular function for the RNA-interference enzyme Dicer in the maturation of the let-7 small temporal RNA. *Science.* 2001;293(5531):834-8.
208. Kawamata T, and Tomari Y. Making RISC. *Trends Biochem Sci.* 2010;35(7):368-76.
209. Ha M, and Kim VN. Regulation of microRNA biogenesis. *Nat Rev Mol Cell Biol.* 2014;15(8):509-24.
210. Guo L, and Lu Z. The fate of miRNA* strand through evolutionary analysis: implication for degradation as merely carrier strand or potential regulatory molecule? *PLoS One.* 2010;5(6):e11387.
211. Liu J, Rivas FV, Wohlschlegel J, Yates JR, 3rd, Parker R, and Hannon GJ. A role for the P-body component GW182 in microRNA function. *Nature cell biology.* 2005;7(12):1261-6.
212. Jones JA, Stroud RE, O'Quinn EC, Black LE, Barth JL, Elefteriades JA, et al. Selective microRNA suppression in human thoracic aneurysms: relationship of miR-29a to aortic size and proteolytic induction. *Circ Cardiovasc Genet.* 2011;4(6):605-13.
213. Ikonomidis JS, Ivey CR, Wheeler JB, Akerman AW, Rice A, Patel RK, et al. Plasma biomarkers for distinguishing etiologic subtypes of thoracic aortic aneurysm disease. *J Thorac Cardiovasc Surg.* 2013;145(5):1326-33.
214. Torella D, Iaconetti C, Catalucci D, Ellison GM, Leone A, Waring CD, et al. MicroRNA-133 controls vascular smooth muscle cell phenotypic switch in vitro and vascular remodeling in vivo. *Circ Res.* 2011;109(8):880-93.
215. Bostjancic E, Zidar N, Stajer D, and Glavac D. MicroRNAs miR-1, miR-133a, miR-133b and miR-208 are dysregulated in human myocardial infarction. *Cardiology.* 2010;115(3):163-9.
216. Care A, Catalucci D, Felicetti F, Bonci D, Addario A, Gallo P, et al. MicroRNA-133 controls cardiac hypertrophy. *Nat Med.* 2007;13(5):613-8.
217. Shan H, Zhang Y, Lu Y, Pan Z, Cai B, Wang N, et al. Downregulation of miR-133 and miR-590 contributes to nicotine-induced atrial remodelling in canines. *Cardiovascular research.* 2009;83(3):465-72.
218. Renaud L, Harris LG, Mani SK, Kasiganesan H, Chou JC, Baicu CF, et al. HDACs Regulate miR-133a Expression in Pressure Overload-Induced Cardiac Fibrosis. *Circulation Heart failure.* 2015;8(6):1094-104.
219. Shan H, Zhang Y, Lu Y, Zhang Y, Pan Z, Cai B, et al. Downregulation of miR-133 and miR-590 contributes to nicotine-induced atrial remodelling in canines. *Cardiovascular research.* 2009;83(3):465-72.
220. Duisters RF, Tijsen AJ, Schroen B, Leenders JJ, Lentink V, van der Made I, et al. miR-133 and miR-30 regulate connective tissue growth factor: implications for a role of microRNAs in myocardial matrix remodeling. *Circ Res.* 2009;104(2):170-8, 6p following 8.

221. Castoldi G, Di Gioia CR, Bombardi C, Catalucci D, Corradi B, Gualazzi MG, et al. MiR-133a regulates collagen 1A1: potential role of miR-133a in myocardial fibrosis in angiotensin II-dependent hypertension. *J Cell Physiol.* 2012;227(2):850-6.
222. Xu M, and Wang YZ. miR133a suppresses cell proliferation, migration and invasion in human lung cancer by targeting MMP14. *Oncol Rep.* 2013;30(3):1398-404.
223. Chapman GB, Durante W, Hellums JD, and Schafer AI. Physiological cyclic stretch causes cell cycle arrest in cultured vascular smooth muscle cells. *Am J Physiol Heart Circ Physiol.* 2000;278(3):H748-54.
224. Guo F, Carter DE, and Leask A. Mechanical tension increases CCN2/CTGF expression and proliferation in gingival fibroblasts via a TGFbeta-dependent mechanism. *PLoS One.* 2011;6(5):e19756.
225. Rouillard AD, and Holmes JW. Mechanical boundary conditions bias fibroblast invasion in a collagen-fibrin wound model. *Biophysical journal.* 2014;106(4):932-43.
226. Eckes B, Zweers MC, Zhang ZG, Hallinger R, Mauch C, Aumailley M, et al. Mechanical tension and integrin alpha 2 beta 1 regulate fibroblast functions. *The journal of investigative dermatology Symposium proceedings / the Society for Investigative Dermatology, Inc [and] European Society for Dermatological Research.* 2006;11(1):66-72.
227. Atance J, Yost MJ, and Carver W. Influence of the extracellular matrix on the regulation of cardiac fibroblast behavior by mechanical stretch. *J Cell Physiol.* 2004;200(3):377-86.
228. Butcher JT, Barrett BC, and Nerem RM. Equibiaxial strain stimulates fibroblastic phenotype shift in smooth muscle cells in an engineered tissue model of the aortic wall. *Biomaterials.* 2006;27(30):5252-8.
229. van Rooij E, and Olson EN. MicroRNA therapeutics for cardiovascular disease: opportunities and obstacles. *Nature reviews Drug discovery.* 2012;11(11):860-72.
230. Song J, Hu B, Qu H, Bi C, Huang X, and Zhang M. Mechanical stretch modulates microRNA 21 expression, participating in proliferation and apoptosis in cultured human aortic smooth muscle cells. *PLoS One.* 2012;7(10):e47657.
231. Hu B, Song JT, Qu HY, Bi CL, Huang XZ, Liu XX, et al. Mechanical stretch suppresses microRNA-145 expression by activating extracellular signal-regulated kinase 1/2 and upregulating angiotensin-converting enzyme to alter vascular smooth muscle cell phenotype. *PLoS One.* 2014;9(5):e96338.
232. Lloyd-Jones D, Adams RJ, Brown TM, Carnethon M, Dai S, De Simone G, et al. Executive summary: heart disease and stroke statistics--2010 update: a report from the American Heart Association. *Circulation.* 2010;121(7):948-54.
233. Laurent S, Boutouyrie P, Asmar R, Gautier I, Laloux B, Guize L, et al. Aortic stiffness is an independent predictor of all-cause and cardiovascular mortality in hypertensive patients. *Hypertension.* 2001;37(5):1236-41.
234. Ruddy JM, Jones JA, Stroud RE, Mukherjee R, Spinale FG, and Ikonomidis JS. Differential effects of mechanical and biological stimuli on matrix metalloproteinase promoter activation in the thoracic aorta. *Circulation.* 2009;120(11 Suppl):S262-8.
235. Ruddy JM, Jones JA, Stroud RE, Mukherjee R, Spinale FG, and Ikonomidis JS. Differential effect of wall tension on matrix metalloproteinase promoter activation in the thoracic aorta. *J Surg Res.* 2010;160(2):333-9.

236. Ruddy JM, Akerman AW, Kimbrough D, Nadeau EK, Stroud RE, Mukherjee R, et al. Differential hypertensive protease expression in the thoracic versus abdominal aorta. *J Vasc Surg.* 2016.
237. Bartel DP. MicroRNAs: target recognition and regulatory functions. *Cell.* 2009;136(2):215-33.
238. Friedman RC, Farh KK, Burge CB, and Bartel DP. Most mammalian mRNAs are conserved targets of microRNAs. *Genome Res.* 2009;19(1):92-105.
239. Humphrey JD, Dufresne ER, and Schwartz MA. Mechanotransduction and extracellular matrix homeostasis. *Nat Rev Mol Cell Biol.* 2014;15(12):802-12.
240. Alenghat FJ, and Ingber DE. Mechanotransduction: all signals point to cytoskeleton, matrix, and integrins. *Sci STKE.* 2002;2002(119):pe6.
241. Duscher D, Maan ZN, Wong VW, Rennert RC, Januszyk M, Rodrigues M, et al. Mechanotransduction and fibrosis. *J Biomech.* 2014;47(9):1997-2005.
242. Anstadt MP, Franga DL, Portik-Dobos V, Pennathur A, Bannan M, Mawulawde K, et al. Native matrix metalloproteinase characteristics may influence early stenosis of venous versus arterial coronary artery bypass grafting conduits. *Chest.* 2004;125(5):1853-8.
243. Eckhouse SR, Akerman AW, Logdon CB, Oelsen JM, O'Quinn EC, Nadeau EK, et al. Differential membrane type 1 matrix metalloproteinase substrate processing with ischemia-reperfusion: relationship to interstitial microRNA dynamics and myocardial function. *J Thorac Cardiovasc Surg.* 2013;145(1):267-75, 77 e1-4; discussion 75-7.
244. Mohamed JS, Hajira A, Lopez MA, and Boriek AM. Genome-wide Mechanosensitive MicroRNA (MechanomiR) Screen Uncovers Dysregulation of Their Regulatory Networks in the mdm Mouse Model of Muscular Dystrophy. *J Biol Chem.* 2015;290(41):24986-5011.
245. Catt KJ, Cain MD, Zimmet PZ, and Cran E. Blood angiotensin II levels of normal and hypertensive subjects. *Br Med J.* 1969;1(5647):819-21.
246. Catt KJ, Cran E, Zimmet PZ, Best JB, Cain MD, and Coghlan JP. Angiotensin II blood-levels in human hypertension. *Lancet.* 1971;1(7697):459-64.
247. Jiang M, Qiu J, Zhang L, Lu D, Long M, Chen L, et al. Changes in tension regulates proliferation and migration of fibroblasts by remodeling expression of ECM proteins. *Exp Ther Med.* 2016;12(3):1542-50.
248. Boddy AM, Lenk GM, Lillvis JH, Nischan J, Kyo Y, and Kuivaniemi H. Basic research studies to understand aneurysm disease. *Drug news & perspectives.* 2008;21(3):142-8.
249. Chen F, Kook H, Milewski R, Gitler AD, Lu MM, Li J, et al. Hop is an unusual homeobox gene that modulates cardiac development. *Cell.* 2002;110(6):713-23.
250. Zhao Y, Samal E, and Srivastava D. Serum response factor regulates a muscle-specific microRNA that targets Hand2 during cardiogenesis. *Nature.* 2005;436(7048):214-20.
251. Pillai RS. MicroRNA function: multiple mechanisms for a tiny RNA? *RNA.* 2005;11(12):1753-61.
252. Min PK, and Chan SY. The biology of circulating microRNAs in cardiovascular disease. *European journal of clinical investigation.* 2015;45(8):860-74.
253. Zhang Z, Qin YW, Brewer G, and Jing Q. MicroRNA degradation and turnover: regulating the regulators. *Wiley interdisciplinary reviews RNA.* 2012;3(4):593-600.
254. Gantier MP, McCoy CE, Rusinova I, Saulep D, Wang D, Xu D, et al. Analysis of microRNA turnover in mammalian cells following Dicer1 ablation. *Nucleic acids research.* 2011;39(13):5692-703.

255. Ruegger S, and Grosshans H. MicroRNA turnover: when, how, and why. *Trends Biochem Sci.* 2012;37(10):436-46.
256. Bail S, Swerdel M, Liu H, Jiao X, Goff LA, Hart RP, et al. Differential regulation of microRNA stability. *RNA.* 2010;16(5):1032-9.
257. Chatterjee S, and Grosshans H. Active turnover modulates mature microRNA activity in Caenorhabditis elegans. *Nature.* 2009;461(7263):546-9.
258. Chatterjee S, Fasler M, Bussing I, and Grosshans H. Target-mediated protection of endogenous microRNAs in C. elegans. *Developmental cell.* 2011;20(3):388-96.
259. Boon RA, and Vickers KC. Intercellular transport of microRNAs. *Arterioscler Thromb Vasc Biol.* 2013;33(2):186-92.
260. Hunter MP, Ismail N, Zhang X, Aguda BD, Lee EJ, Yu L, et al. Detection of microRNA expression in human peripheral blood microvesicles. *PLoS One.* 2008;3(11):e3694.
261. Kosaka N, Iguchi H, Yoshioka Y, Takeshita F, Matsuki Y, and Ochiya T. Secretory mechanisms and intercellular transfer of microRNAs in living cells. *J Biol Chem.* 2010;285(23):17442-52.
262. Kosaka N, Iguchi H, Hagiwara K, Yoshioka Y, Takeshita F, and Ochiya T. Neutral sphingomyelinase 2 (nSMase2)-dependent exosomal transfer of angiogenic microRNAs regulate cancer cell metastasis. *J Biol Chem.* 2013;288(15):10849-59.
263. Zhang J, Li S, Li L, Li M, Guo C, Yao J, et al. Exosome and exosomal microRNA: trafficking, sorting, and function. *Genomics, proteomics & bioinformatics.* 2015;13(1):17-24.
264. Aryani A, and Denecke B. In vitro application of ribonucleases: comparison of the effects on mRNA and miRNA stability. *BMC Res Notes.* 2015;8:164.
265. Frazier JL, Caskey JH, Yoffe M, and Seligman PA. Studies of the transferrin receptor on both human reticulocytes and nucleated human cells in culture: comparison of factors regulating receptor density. *J Clin Invest.* 1982;69(4):853-65.
266. Pan BT, Blostein R, and Johnstone RM. Loss of the transferrin receptor during the maturation of sheep reticulocytes in vitro. An immunological approach. *Biochem J.* 1983;210(1):37-47.
267. Pan BT, and Johnstone RM. Fate of the transferrin receptor during maturation of sheep reticulocytes in vitro: selective externalization of the receptor. *Cell.* 1983;33(3):967-78.
268. Pan BT, Teng K, Wu C, Adam M, and Johnstone RM. Electron microscopic evidence for externalization of the transferrin receptor in vesicular form in sheep reticulocytes. *The Journal of cell biology.* 1985;101(3):942-8.
269. Johnstone RM, Bianchini A, and Teng K. Reticulocyte maturation and exosome release: transferrin receptor containing exosomes shows multiple plasma membrane functions. *Blood.* 1989;74(5):1844-51.
270. Barres C, Blanc L, Bette-Bobillo P, Andre S, Mamoun R, Gabius HJ, et al. Galectin-5 is bound onto the surface of rat reticulocyte exosomes and modulates vesicle uptake by macrophages. *Blood.* 2010;115(3):696-705.
271. Muralidharan-Chari V, Clancy J, Plou C, Romao M, Chavrier P, Raposo G, et al. ARF6-regulated shedding of tumor cell-derived plasma membrane microvesicles. *Current biology : CB.* 2009;19(22):1875-85.
272. Muralidharan-Chari V, Clancy JW, Sedgwick A, and D'Souza-Schorey C. Microvesicles: mediators of extracellular communication during cancer progression. *J Cell Sci.* 2010;123(Pt 10):1603-11.

273. Properzi F, Logozzi M, and Fais S. Exosomes: the future of biomarkers in medicine. *Biomarkers in medicine.* 2013;7(5):769-78.
274. Ostrowski M, Carmo NB, Krumeich S, Fanget I, Raposo G, Savina A, et al. Rab27a and Rab27b control different steps of the exosome secretion pathway. *Nature cell biology.* 2010;12(1):19-30; sup pp 1-13.
275. Savina A, Vidal M, and Colombo MI. The exosome pathway in K562 cells is regulated by Rab11. *J Cell Sci.* 2002;115(Pt 12):2505-15.
276. Khan S, Jutzy JM, Aspe JR, McGregor DW, Neidigh JW, and Wall NR. Survivin is released from cancer cells via exosomes. *Apoptosis.* 2011;16(1):1-12.
277. Gupta S, and Knowlton AA. HSP60 trafficking in adult cardiac myocytes: role of the exosomal pathway. *Am J Physiol Heart Circ Physiol.* 2007;292(6):H3052-6.
278. Trajkovic K, Hsu C, Chiantia S, Rajendran L, Wenzel D, Wieland F, et al. Ceramide triggers budding of exosome vesicles into multivesicular endosomes. *Science.* 2008;319(5867):1244-7.
279. Colombo M, Raposo G, and Thery C. Biogenesis, secretion, and intercellular interactions of exosomes and other extracellular vesicles. *Annu Rev Cell Dev Biol.* 2014;30:255-89.
280. Wang X, Huang W, Liu G, Cai W, Millard RW, Wang Y, et al. Cardiomyocytes mediate anti-angiogenesis in type 2 diabetic rats through the exosomal transfer of miR-320 into endothelial cells. *J Mol Cell Cardiol.* 2014;74:139-50.
281. Kulshreshtha A, Ahmad T, Agrawal A, and Ghosh B. Proinflammatory role of epithelial cell-derived exosomes in allergic airway inflammation. *J Allergy Clin Immunol.* 2013;131(4):1194-203, 203 e1-14.
282. Li J, Liu K, Liu Y, Xu Y, Zhang F, Yang H, et al. Exosomes mediate the cell-to-cell transmission of IFN-alpha-induced antiviral activity. *Nat Immunol.* 2013;14(8):793-803.
283. Valadi H, Ekstrom K, Bossios A, Sjostrand M, Lee JJ, and Lotvall JO. Exosome-mediated transfer of mRNAs and microRNAs is a novel mechanism of genetic exchange between cells. *Nature cell biology.* 2007;9(6):654-9.
284. Huang X, Yuan T, Tschannen M, Sun Z, Jacob H, Du M, et al. Characterization of human plasma-derived exosomal RNAs by deep sequencing. *BMC genomics.* 2013;14:319.
285. Liao J, Liu R, Yin L, and Pu Y. Expression profiling of exosomal miRNAs derived from human esophageal cancer cells by Solexa high-throughput sequencing. *International journal of molecular sciences.* 2014;15(9):15530-51.
286. Guduric-Fuchs J, O'Connor A, Camp B, O'Neill CL, Medina RJ, and Simpson DA. Selective extracellular vesicle-mediated export of an overlapping set of microRNAs from multiple cell types. *BMC genomics.* 2012;13:357.
287. Skog J, Wurdinger T, van Rijn S, Meijer DH, Gainche L, Sena-Esteves M, et al. Glioblastoma microvesicles transport RNA and proteins that promote tumour growth and provide diagnostic biomarkers. *Nature cell biology.* 2008;10(12):1470-6.
288. Mammoto A, Mammoto T, and Ingber DE. Mechanosensitive mechanisms in transcriptional regulation. *J Cell Sci.* 2012;125(Pt 13):3061-73.
289. Anderson AA, Ushakov DS, Ferenczi MA, Mori R, Martin P, and Saffell JL. Morphoregulation by acetylcholinesterase in fibroblasts and astrocytes. *J Cell Physiol.* 2008;215(1):82-100.
290. Danielson KM, and Das S. Extracellular Vesicles in Heart Disease: Excitement for the Future ? *Exosomes Microvesicles.* 2014;2(1).

291. Thery C, Zitvogel L, and Amigorena S. Exosomes: composition, biogenesis and function. *Nat Rev Immunol.* 2002;2(8):569-79.
292. Goldie BJ, Dun MD, Lin M, Smith ND, Verrills NM, Dayas CV, et al. Activity-associated miRNA are packaged in Map1b-enriched exosomes released from depolarized neurons. *Nucleic acids research.* 2014;42(14):9195-208.
293. Villarroya-Beltri C, Gutierrez-Vazquez C, Sanchez-Cabo F, Perez-Hernandez D, Vazquez J, Martin-Cofreces N, et al. Sumoylated hnRNPA2B1 controls the sorting of miRNAs into exosomes through binding to specific motifs. *Nat Commun.* 2013;4:2980.
294. Koppers-Lalic D, Hackenberg M, Bijnsdorp IV, van Eijndhoven MAJ, Sadek P, Sie D, et al. Nontemplated nucleotide additions distinguish the small RNA composition in cells from exosomes. *Cell Rep.* 2014;8(6):1649-58.
295. Gibbings DJ, Ciaudo C, Erhardt M, and Voinnet O. Multivesicular bodies associate with components of miRNA effector complexes and modulate miRNA activity. *Nature cell biology.* 2009;11(9):1143-9.
296. Shurtleff MJ, Temoche-Diaz MM, Karfilis KV, Ri S, and Schekman R. Y-box protein 1 is required to sort microRNAs into exosomes in cells and in a cell-free reaction. *Elife.* 2016;5.
297. Ikeda K, Satoh M, Pauley KM, Fritzler MJ, Reeves WH, and Chan EK. Detection of the argonaute protein Ago2 and microRNAs in the RNA induced silencing complex (RISC) using a monoclonal antibody. *J Immunol Methods.* 2006;317(1-2):38-44.
298. Fan J, and Bertino JR. K-ras modulates the cell cycle via both positive and negative regulatory pathways. *Oncogene.* 1997;14(21):2595-607.
299. McKenzie AJ, Hoshino D, Hong NH, Cha DJ, Franklin JL, Coffey RJ, et al. KRAS-MEK Signaling Controls Ago2 Sorting into Exosomes. *Cell Rep.* 2016;15(5):978-87.
300. Melo SA, Sugimoto H, O'Connell JT, Kato N, Villanueva A, Vidal A, et al. Cancer exosomes perform cell-independent microRNA biogenesis and promote tumorigenesis. *Cancer Cell.* 2014;26(5):707-21.
301. Squadrito ML, Baer C, Burdet F, Maderna C, Gilfillan GD, Lyle R, et al. Endogenous RNAs modulate microRNA sorting to exosomes and transfer to acceptor cells. *Cell Rep.* 2014;8(5):1432-46.
302. Ramanath VS, Oh JK, Sundt TM, 3rd, and Eagle KA. Acute aortic syndromes and thoracic aortic aneurysm. *Mayo Clin Proc.* 2009;84(5):465-81.
303. Chim SS, Shing TK, Hung EC, Leung TY, Lau TK, Chiu RW, et al. Detection and characterization of placental microRNAs in maternal plasma. *Clinical chemistry.* 2008;54(3):482-90.
304. Muthalif MM, Karzoun NA, Gaber L, Khandekar Z, Benter IF, Saeed AE, et al. Angiotensin II-induced hypertension: contribution of Ras GTPase/Mitogen-activated protein kinase and cytochrome P450 metabolites. *Hypertension.* 2000;36(4):604-9.
305. Wang YX, Martin-McNulty B, Freay AD, Sukovich DA, Halks-Miller M, Li WW, et al. Angiotensin II increases urokinase-type plasminogen activator expression and induces aneurysm in the abdominal aorta of apolipoprotein E-deficient mice. *Am J Pathol.* 2001;159(4):1455-64.
306. Elias MF, Sorrentino RN, Pentz CA, 3rd, and Florini JR. "Spontaneously" hypertensive mice: a potential genetic model for the study of the relationship between heart size and blood pressure. *Experimental aging research.* 1975;1(2):251-65.

307. Uddin M, and Harris-Nelson N. Renin activity and angiotensin I concentration in genetically selective inbred line of hypertensive mice. *Biochem Biophys Res Commun.* 2004;316(3):842-4.
308. Schlager G, and Sides J. Characterization of hypertensive and hypotensive inbred strains of mice. *Lab Anim Sci.* 1997;47(3):288-92.
309. Kuwabara Y, Ono K, Horie T, Nishi H, Nagao K, Kinoshita M, et al. Increased microRNA-1 and microRNA-133a levels in serum of patients with cardiovascular disease indicate myocardial damage. *Circ Cardiovasc Genet.* 2011;4(4):446-54.
310. Hammond SM, Boettcher S, Caudy AA, Kobayashi R, and Hannon GJ. Argonaute2, a link between genetic and biochemical analyses of RNAi. *Science.* 2001;293(5532):1146-50.
311. Sakr M, Takino T, Sabit H, Nakada M, Li Z, and Sato H. miR-150-5p and miR-133a suppress glioma cell proliferation and migration through targeting membrane-type-1 matrix metalloproteinase. *Gene.* 2016;587(2):155-62.
312. Spinale FG, Escobar GP, Mukherjee R, Zavadzkas JA, Saunders SM, Jeffords LB, et al. Cardiac-restricted overexpression of membrane type-1 matrix metalloproteinase in mice: effects on myocardial remodeling with aging. *Circulation Heart failure.* 2009;2(4):351-60.
313. Krege JH, Hodgin JB, Hagaman JR, and Smithies O. A noninvasive computerized tail-cuff system for measuring blood pressure in mice. *Hypertension.* 1995;25(5):1111-5.
314. Rateri DL, Davis FM, Balakrishnan A, Howatt DA, Moorleghen JJ, O'Connor WN, et al. Angiotensin II induces region-specific medial disruption during evolution of ascending aortic aneurysms. *Am J Pathol.* 2014;184(9):2586-95.
315. Wang BW, Wu GJ, Cheng WP, and Shyu KG. Mechanical stretch via transforming growth factor-beta1 activates microRNA-208a to regulate hypertrophy in cultured rat cardiac myocytes. *Journal of the Formosan Medical Association = Taiwan yi zhi.* 2013;112(10):635-43.
316. Barbour JR, Stroud RE, Lowry AS, Clark LL, Leone AM, Jones JA, et al. Temporal disparity in the induction of matrix metalloproteinases and tissue inhibitors of metalloproteinases after thoracic aortic aneurysm formation. *J Thorac Cardiovasc Surg.* 2006;132(4):788-95.
317. Ikonomidis JS, Gibson WC, Butler JE, McClister DM, Sweterlitsch SE, Thompson RP, et al. Effects of deletion of the tissue inhibitor of matrix metalloproteinases-1 gene on the progression of murine thoracic aortic aneurysms. *Circulation.* 2004;110(11 Suppl 1):II268-73.
318. Liu WF. Mechanical regulation of cellular phenotype: implications for vascular tissue regeneration. *Cardiovasc Res.* 2012;95(2):215-22.
319. Spruill LS, Lowry AS, Stroud RE, Squires CE, Mains IM, Flack EC, et al. Membrane-type-1 matrix metalloproteinase transcription and translation in myocardial fibroblasts from patients with normal left ventricular function and from patients with cardiomyopathy. *American journal of physiology Cell physiology.* 2007;293(4):C1362-73.
320. Flack EC, Lindsey ML, Squires CE, Kaplan BS, Stroud RE, Clark LL, et al. Alterations in cultured myocardial fibroblast function following the development of left ventricular failure. *J Mol Cell Cardiol.* 2006;40(4):474-83.
321. Woessner JF, Jr. MMPs and TIMPs. An historical perspective. *Methods Mol Biol.* 2001;151:1-23.

322. Manso AM, Elsherif L, Kang SM, and Ross RS. Integrins, membrane-type matrix metalloproteinases and ADAMs: potential implications for cardiac remodeling. *Cardiovascular research.* 2006;69(3):574-84.
323. Czarny M, Liu J, Oh P, and Schnitzer JE. Transient mechanoactivation of neutral sphingomyelinase in caveolae to generate ceramide. *J Biol Chem.* 2003;278(7):4424-30.
324. Czarny M, and Schnitzer JE. Neutral sphingomyelinase inhibitor scyphostatin prevents and ceramide mimics mechanotransduction in vascular endothelium. *Am J Physiol Heart Circ Physiol.* 2004;287(3):H1344-52.
325. Cogolludo A, Moreno L, Frazziano G, Moral-Sanz J, Menendez C, Castaneda J, et al. Activation of neutral sphingomyelinase is involved in acute hypoxic pulmonary vasoconstriction. *Cardiovascular research.* 2009;82(2):296-302.
326. Essandoh K, Yang L, Wang X, Huang W, Qin D, Hao J, et al. Blockade of exosome generation with GW4869 dampens the sepsis-induced inflammation and cardiac dysfunction. *Biochimica et biophysica acta.* 2015;1852(11):2362-71.
327. Ray JL, Leach R, Herbert JM, and Benson M. Isolation of vascular smooth muscle cells from a single murine aorta. *Methods Cell Sci.* 2001;23(4):185-8.
328. Livak KJ, and Schmittgen TD. Analysis of relative gene expression data using real-time quantitative PCR and the 2(-Delta Delta C(T)) Method. *Methods.* 2001;25(4):402-8.
329. Ho IK, and Ellman GL. Triton solubilized acetylcholinesterase of brain. *Journal of neurochemistry.* 1969;16(11):1505-13.
330. Zile MR, Baicu CF, Ikonomidis JS, Stroud RE, Nietert PJ, Bradshaw AD, et al. Myocardial stiffness in patients with heart failure and a preserved ejection fraction: contributions of collagen and titin. *Circulation.* 2015;131(14):1247-59.
331. Paulus WJ, Tschope C, Sanderson JE, Rusconi C, Flachskampf FA, Rademakers FE, et al. How to diagnose diastolic heart failure: a consensus statement on the diagnosis of heart failure with normal left ventricular ejection fraction by the Heart Failure and Echocardiography Associations of the European Society of Cardiology. *Eur Heart J.* 2007;28(20):2539-50.
332. Lindenfeld J, Albert NM, Boehmer JP, Collins SP, Ezekowitz JA, Givertz MM, et al. HFSA 2010 Comprehensive Heart Failure Practice Guideline. *Journal of cardiac failure.* 2010;16(6):e1-194.